Spatializing Net Ecosystem Exchange in the Brazilian Amazon biome using the JULES model and vegetation properties

Amauri C. Prudente Junior[1], Luiz A.T. Machado[1,5], Felipe S. Silva[1], Tercio Ambrizzi [2], Paulo Artaxo[1], Santiago Botia[3], Luan P. Cordeiro[1], Cleo Q. Dias Junior[4], Edmilson Freitas[2], Demerval S. Moreira[6], Christopher Pöhlker[5], Ivan M. C. Toro[1], Xiyan Xu[7], and Luciana V. Rizzo[1]

[1] Physics Institute, University of São Paulo, São Paulo, Brazil

[2] Institute of Astronomy, Geophysics and Atmosphere Science, University of São Paulo, São Paulo, Brazil

[3] Max Planck Institute for Biogeochemistry, Jena, Germany

[4] Federal Institute of Education, Science, and Technology of Pará, Belém, Brazil

[5] Max Planck Institute for Chemistry, Mainz, Germany

[6] Department of Physics and Meteorology, State University of São Paulo, Bauru, Brazil

[7] Chinese Academy of Sciences, Beijing, China

Corresponding to: Amauri Cassio Prudente Junior (email: amauri.cassio@usp.br)

Abstract. The large extension and diversity of the Brazilian Amazon biome hampers the assessment of the regional-scale carbon budget based solely on local observations. Considering the shortage of observations, this study aims to examine the carbon fluxes throughout the Brazilian Amazon biome using a process-based model (JULES, Joint UK land environment simulator). A sensitivity analysis detected five critical model parameters for the Amazon tropical broadleaf evergreen forest, optimized using carbon flux and meteorological data from four forest sites. The simulations with the new parametrization were compared with JULES default parameter values and with simulations of the Vegetation Photosynthesis and Respiration Model (VPRM). Net ecosystem exchange (NEE) and gross primary production (GPP) estimates were improved at all sites, reaching a Root Mean Squared Error (RMSE) about 30% lower in comparison to the default version. The optimized parameter values varied among the four sites, indicating that a single parameterization for the whole Amazonia may not be adequate. JULES model parameters were spatializedestimated for the Brazilian Amazonia, based on canopy height and leaf area index gridded data. Applying JULES with spatially dependent parameterization for the year of 2021 resulted in a carbon sink of -1.34 Pg C year^{-1}. Regional differences were observed in the carbon fluxes, with a carbon source of 0.75 Kg C m^{-2} year^{-1} in the southwest and north, likely explained by increased ecosystem respiration in older and taller forests.

1. Introduction

The Amazon forest is one of the largest carbon reservoirs in the world, being relevant to the global environment, biodiversity, and climate regulation (Brienen et al., 2015). Amazon forests are responsible for 16% of the gross primary production in terrestrial ecosystems, storing approximately 90 Pg C in above- and below-ground vegetation biomass (Saatchi et al., 2011; Malhi et al., 2021). The region's critical role in the global carbon budget is at risk, as carbon dynamics are being significantly impacted by climate change, including rising air temperatures and increased hydric stress (Liu et al., 2017; Gatti et al., 2021). These effects can lead to a decrease in the leaf area index (LAI) and an increase in plant respiration (Meir et al., 2008) and hence influence the sign of the net carbon exchange, shifting areas from a sink to a source of carbon.

Accurate estimates of carbon fluxes are crucial for understanding how the Amazon will evolve under the impacts of climate change. Because the Amazon forest is ecologically and structurally heterogeneous, carbon fluxes between the biosphere and the atmosphere vary markedly across the region, making site-specific estimates essential for capturing this spatial diversity~~The diverse vegetation of the Amazon biome and the strategies used to estimate carbon fluxes across different sites are essential for identifying the region's different behaviors~~ (Restrepo-Coupe et al., 2013). The traditional method of carbon flux measurement is the Eddy-~~c~~Covariance (Baldochi, 2003), which quantifies the Net Ecosystem Exchange (NEE)~~,~~ by measuring the CO_2 turbulent ~~CO_2~~ exchange and correcting for canopy storage. NEE represents the difference between the gross primary production (GPP) of ~~the vegetation~~vegetation and emissions from the ecosystem respiration (Reco) (Hayek et al., 2018). However, E~~e~~ddy-~~-~~covariance measurements are insufficient to represent the vast diversity of ecosystems and vegetation in the Brazilian Amazon biome (Aguirre-Gutierrez et al., 2025). This limitation arises due to logistical challenges, the substantial investment required for installation and equipment, and the need for highly skilled labor to ensure proper maintenance (Andreae et al., 2015). Considering the limitation of expanding flux towers throughout the Amazon biome, process-based and data-driven models have been applied in different studies to estimate NEE in different parts of the Amazon, such as the Vegetation Photosynthesis and Respiration Model (VPRM) (Mahadevan et al., 2008)~~(Botia et al., 2022 and 2024)~~, FluxCom (Nelson et al., 2024; Chen et al., 2024), and the Organizing Carbon and Hydrology in Dynamic Ecosystems (ORCHIDEE model) (Verbeeck et al., 2011).

One of the comprehensive land surface models used to simulate ~~the~~ biophysical processes is the Joint UK Land Environment Simulator (JULES; Best et al., 2011). JULES is a community land surface model used both as a standalone system and as the land surface component of the Met Office Unified Model. It is considered the state-of-the-art for large-scale simulations (Moreira et al., 2013~~,~~; Harper et al., 2018). JULES has a tiled model of sub-grid heterogeneity able to reproduce energy, water, carbon, and momentum fluxes (Best et al., 2011~~,~~; Clark et al., 2011). The model was progressively updated, enhancing the number of plant functional types (PFT): ~~-~~five PFTs (HadGEM3, Clark et al., 2012), nine PFTs (Harper et al., 2016), more recently 13 PFTs (UKESM1, Harper et al., 2018), and additionally four non-vegetation land cover types. Currently, JULES is used to simulate carbon fluxes in different ~~biomes~~ biome types, as applied for agriculture (Osborne et al., 2015; Williams et al., 2017) and ~~in~~ tropical forests (Moreira et al., 2013; Restrepo-Coupe et al., 2017; Caen et al., 2022).

Although JULES has been widely used in various studies to estimate carbon fluxes in tropical regions, a lack of specific parameterizations remains a challenge to simulate plant-soil-atmosphere interactions. Harper et al. (2016) introduced a PFT specific to tropical forests, but this parameterization has not been thoroughly tested or validated across different regions of the Amazon. Additionally, the most sensitive parameters in this region have not been deeply evaluated. In general, studies to estimate NEE using process-based models have not accounted for the large differences of vegetation characteristics across this territory (Ometto et al., 2023). Based on these aspects, this study aims to characterize the seasonal and spatial variability of carbon fluxes between the biosphere and atmosphere in the Brazilian Amazon biome. Here, we present an improvement of the JULES parameterization specifically for the Brazilian Amazon, performing a sensitivity analysis of the model parameters using as reference to Eddy-covariance towerstower sites in different regions of the Brazilian Amazon biome as references. Model parameters were spatialized using two ancillary datasets— canopy height and LAI—to estimate regional differences in NEE in the Brazilian Amazon biome.

2.Material and Methods

The current study combined observational datasets and modeling. Section 2.1 describes the study area and the tower flux sites in the Brazilian Amazon Basin. Section 2.2 describes the main features of the JULES model. Section 2.3 describes the meteorological and edaphological datasets used as input for the JULES run and Eddy covariancethe Eddy covariance dataset used to validate the model optimization. Section 2.4 describes the gridded data used for simulations in the Brazilian Amazon biome. Section 2.5 describes the JULES model procedures adopted in this study — including the sensitivity analyses and calibration steps—as well as the remote sensing data and the regression approach as sensitivity analyses and calibration procedures and the description of the remote sensing data and the regression method used to extrapolate the JULES model parameters across the Amazon Basin. Section 2.6 describes the VPRM model that was used to compare with the JULES model at the tower sites.

2.1. Study area

The study area corresponds to the Brazilian Amazon biome, covering 4,212,472 km^2. We compiled carbon flux data from five Eddy-covariance towers to represent carbon fluxes and evaluate JULES simulations (Figure 1). From east to west and north to south, these sites are: The Amazon Tall Tower Observatory (ATTO), the Tapajos National Forest (K67, K83), the Reserva Jarú (RJA), and the Reserva Cuieiras near Manaus (K34). The equatorial forest was represented by 4 towers (ATTO, K34, K67, K83), and RJA represented the southern Amazonia (Restrepo-Coupe et al., 2021). The K34 tower is located 60 km north of the city of Manaus (Araujo et al., 2002; Restrepo-Coupe et al., 2013) (Table 1). The Santarem moist tropical forest (sites K67 and K83) is located at the confluence of the Amazon and Tapajós rivers, in the northeast Brazilian Amazon. The ATTO tower is the most recent tower built in the Amazon region, based 150 km northeast of the city of Manaus (Andreae et

al., 2015). In the southern Amazon region, the RJA tower is located in a forest reserve in the state of Rondônia, characterized as Aw: Tropical savanna climate with dry season in the Köppen-Geiger climate classification (Peel et al., 2007). Some of these flux towers are still operational, while others have been discontinued. As such, observations from each tower are available for different periods ranging from 2001 to 2021, sometimes with intermittent measurements. For the current study, data from different years were used in the JULES model calibration (see Table 1). A complete year of data ~~,~~was ~~with one complete year being~~ selected for each site, comprising ~~that had~~ the most reliable set of observations in terms of both data coverage and quality assurance. Using a single year of data for each site provided similar conditions for model parameter optimisation at the different sites. To minimise the influence of atypical atmospheric conditions ~~reflected in the variability of carbon fluxes~~, years with extreme dryness or wetness were avoided during the model optimi~~z~~sation process. The towers K34, K67, RJA, and ATTO were used in model calibration. The K83 tower was used as an independent reference point to validate the spatialization model. This tower was selected as independent data based on the availability and quality of observational data over a period of one year.

All the Eddy-covariance flux towers are located in upland (*terra firme*) forest sites, with canopy heights in the range 27-36 m and LAI in the range 3.26-5.46 m^2 m^{-2} (Table 1), respectively comprising 61% and 85% of the distribution of values in the study area (Figure 1). The five flux towers considered in this study represent upland forests in regions with subtle differences in climate regime and in the level of stress associated with deforestation and climate change pressures. While the K34 and ATTO towers are located in pristine forest reserves in the Western Amazonia, the RJA tower sits in a forest reserve surrounded by agricultural areas in Southwestern Amazonia. The K67 and K83 towers sit in a forest reserve near the deforestation frontier in the Eastern Amazonia. Therefore, this set of flux towers spans diverse upland forest communities, which cover more than 80% of the Amazon biome (Moraes et al., 2021). ~~Therefore, this set of flux towers includes multiple kinds of upland forests communities, which extend through more than 80% of the Amazon biome (Moraes et al., 2021).~~ However, it is important to acknowledge that this set of flux towers is not representative of all Amazonian ecosystems, like seasonally flooded, swamp, or white sand forests.

Table 1: Description of five different eddy covariance towers based on Amazon region (Restrepo-Coupe et al., 2021). LAI data is from ERA5 and Canopy Height data is from the Global Canopy Forest (Simardi et al., 2011).

ID	Site location	Canopy height (m)	Year evaluated	Annual total rainfall (mm)	Average air temperature (°C)	LAI (m^2 m^{-2})
	Lat/Lon					
K34	2.614°S/60.12°W	27	2005	196~~54.81~~	2~~6~~5.0~~98~~	4.79
K67	2.85°S/54.97°W	36	2003	128~~43.72~~	28.2~~19~~	3.26
RJA	10.08°S/61.93°W	35	2001	251~~32.58~~	25.1~~5~~	4.05
K83	3.01°S/54.88°W	28	2001	1658~~.29~~	26.4~~37~~	3.78
ATTO	2.15°S/59.03°W	30	2018	219~~32.87~~	26.0~~3~~	5.46

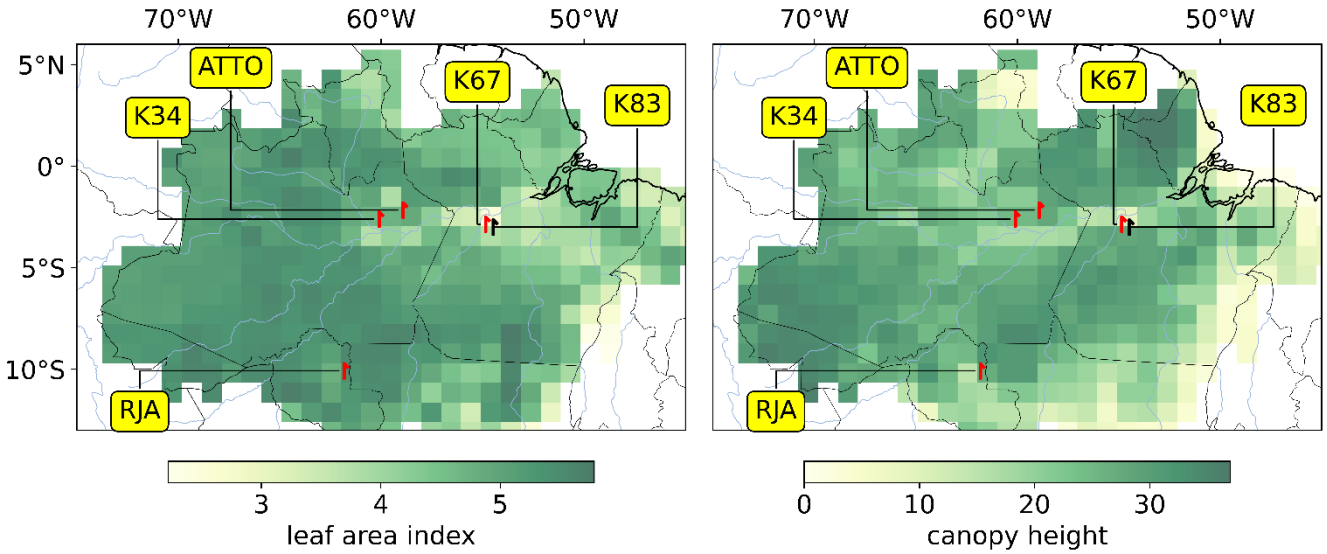

Figure 1: Eddy-covariance towers across the Brazilian Amazon biome (red symbols) used to validate JULES simulation. Gridded background colors denote the spatial distribution of leaf area index (m^2 m^{-2}) on the left panel and canopy height (m) on the right panel (refer to section 2.4). The black symbol indicates the tower used to validate the spatialization of JULES parameters. LAI data is from ERA5, and canopy height data is from the Global Canopy Forest (Simardi et al., 2011).

2.2. JULES model description

JULES is a land surface model that can simulate carbon fluxes punctually or in a grid with a temporal resolution of one hour. The JULES version utilized in this study was 7.0, based on nine plant functional types (PFT), including tropical forests (Harper et al., 2016). JULES requires hourly meteorological data as input, as described in section 2.3. Also, it requires an edaphic dataset, which is also described in section 2.3. JULES estimates GPP and Reco based on the limitation factor of three potential photosynthesis rates (Collatz et al., 1991, 1992). This topic presents the main equations to estimate GPP and Reco, defining the most relevant parameters to quantify~~for the calculation of~~ carbon fluxes. A more detailed description of ~~equations used by JULES to estimate carbon fluxes is demonstrated in the Supplementary material~~the equations used by JULES to estimate carbon fluxes is provided in the Supplementary Material S1.

The model considers three potentially-limiting photosynthesis rates: Light limitation rate (W_l); Rubisco limitation rate (W_c); and transport of photosynthetic products for C3 and PEP Carboxylase limitation for C4 plants (W_e). W_l and W_c depend on the maximum rate of carboxylation of Rubisco (V_{cmax}), which is calculated using an optimal temperature range for each plant functional type (T$_{upp}$~~upp~~ and T$_{low}$~~low~~), as described by Clark et al.~~,~~ (2011) (Equation 1):

$$V_{c\,max} = \frac{V_{c\,max25} f_t(T_c)}{\left[1+e^{0.3(T_c - T_{upp})}\right]\left[1+e^{0.3(T_{low} - T_c)}\right]} \quad (1)$$

where T_c is the canopy (leaf) temperature in degrees Celsius, f_t is the standard Q_{10} temperature dependence (see equation S2 in the Supplementary material), and V_{cmax} at ~~25°C~~ 25 °C is calculated based on leaf nitrogen content (kg N kg C^{-1}) in each canopy layer (i) (see equation S3 in the Supplementary material).

With V_{cmax} it is possible to calculate two potential photosynthesis rates: W_c and W_e:

$$Wc = \begin{cases} V_{c\,max}\left(\frac{c_i - \Gamma}{c_i + K_c(1+\frac{O_a}{K_o})}\right), & for\ C3\ plants, \\ V_{c\,max}, & for\ C4\ plants. \end{cases} \quad (2)$$

where V_{cmax} (mol CO_2 m^{-2} s^{-1}) is the maximum rate carboxylation of Rubisco, c_i is the leaf internal carbon dioxide partial pressure (Pa), Γ is the CO_2 compensation point in the absence of mitochondrial respiration (Pa), O_a is the partial pressure of atmospheric oxygen, and K_c and K_o are the Michaelis-Menten parameters for CO_2 and O_2, respectively.

$$We = \begin{cases} 0.5 \cdot V_{c\,max}, & for\ C3\ plants, \\ 2 \cdot 10^{4} \cdot V_{c\,max}\frac{c_i}{P*}, & for\ C4\ plants. \end{cases} \quad (3)$$

where P* is the surface air pressure.

The light-limited rate (W_l) relies on the quantum efficiency for photosynthesis (α, in mol CO_2 mol^{-1} PAR):

$$W_l = \begin{cases} \alpha(1-\omega)I_{PAR}\left(\frac{c_i - \Gamma}{c_i + 2\Gamma}\right), & for\ C3\ plants, \\ \alpha(1-\omega)I_{PAR}, & for\ C4\ plants. \end{cases} \quad (4)$$

where ω is the leaf scattering coefficient for PAR, and I_{PAR} is the incident photosynthetically active radiation (PAR, mol m^{-2} s^{-1}).

The three potentially limiting rates are essential to calculate the rate of gross photosynthesis, which is the smoothed minimum of the three limited rates previously calculated, as described in the Supplementary section (Equation S7). GPP is calculated based on the integration of leaf photosynthesis (*Al*, see the ~~Suplementary~~supplementary material~~s~~ equation S11), taking into account every canopy level adopted by Harper et al.~~,~~ (2016), assuming a multi-layer canopy with sunlit and shaded leaves in each layer.

The CO_2 concentration at the leaf surface or within the leaf is determined from the leaf humidity deficit, calculated using the leaf-surface vapor pressure deficit (D), together with two parameters characteristic of each plant functional type~~The leaf CO_2 concentration on the surface or internal is defined based on the leaf humidity deficit estimated by the vapor deficit in the leaf surface (D) and on two parameters related to specific plant function types~~ (f_0 and D*crit*) (Equation 5):

$$\frac{C_i-\Gamma}{C_s-\Gamma} = f_0\left(1-\frac{D}{Dcrit}\right) \quad (5)$$

where C_s is the leaf surface CO_2 concentration.

T~~o calculate~~he total ecosystem respiration, -Reco, is calculated as the sum of different respiration components. L~~first aspect l~~eaf dark respiration (R_d) is defined as a proportion of V_{cmax}.(Equation 6)

$$R_d = f_d V_{cmax} \quad (6)$$

-where f_d is the dark respiration coefficient. To calculate the total plant respiration, JULES considers the sum of two processes: maintenance and growth respiration (R_{pm} and R_{pg}, Equations 7 and 12, respectively)

$$R_{pm} = 0.012 \cdot R_d\left(\beta + \frac{N_r+N_s}{N_l}\right) \quad (7)$$

where N_l, N_s, and N_r are the nitrogen contents of leaf, stem, and root, respectively, and β is the soil moisture stress factor based on Cox et al.~~,~~ 1998 (see ~~equation~~ equations S9 and S10 ~~on~~ in the Supplementary materials). To calculate the nitrogen contents of leaves, ~~stem~~ stems, and roots, LAI and canopy height are important elements (Equations 8-10):

$$N_l = n_m \sigma_l L \quad (8)$$

$$N_s = \mu_{sl} n_m S \quad (9)$$

$$N_r = \mu_{rl} n_m R \quad (10)$$

where n_m is the mean leaf nitrogen concentration (kg N (kg C)$^{-1}$), R and S are the quantity of carbon present in roots and respiring stem, L is the leaf area index (m^2 m^{-2}), and σl ~~(kg C m^{-2} per unit of LAI)~~ is the specific leaf density (kg C m^{-2} per unit of LAI). ~~-~~The nitrogen contents of roots and stems are assumed to be multiples, μ_{rl} and μ_{sl}, of the mean leaf nitrogen concentration, assuming: μ_{rl} = 1.0 for all PFTs, μ_{sl} = 0.1 for woody plants (trees and shrubs), and μ_{sl} = 1.0 for grasses. To calculate the respiring stemwood, the pipe model of Shinozaki et al. (1964) was utilized, taking into account canopy height and LAI (Equation 11):

$$S = n_{sl} h L \quad (11)$$

Where n_{sl} is a constant of proportionality from Friend~~s~~ et al (1993), and h is the canopy height.

To calculate the growth respiration, it is necessary to consider the maintenance respiration and also the estimated GPP (Equation 12)

$$R_{pg} = r_g(GPP - R_{pm}) \quad (12)$$

Where r_g is the growth respiration coefficient, set as 0.25 for all plant functional types (Clark et al., 2011, and Harper et al., 2016).

Finally, NEE is calculated by JULES as the difference between GPP and total ecosystem respiration (plant and soil respiration, $R_{eco,}$ Equation 13):

$$NEE = R_{eco} - \text{GPP} \quad (13)$$

2.3. Ancillary environmental data

The JULES model requires the meteorological variables listed in Table 2 as input. In-situ meteorological forcing data from each flux tower (Restrepo-Coupe et al., 2021; Andreae et al., 2015) were used for model calibration (Section 2.4.2) and cross-validation using K83 tower data. For the spatializ~~s~~ation of carbon fluxes, meteorological data from reanalysis ~~was~~ were applied, as will be described in Section 2.4. Soil information required by JULES was obtained from the EMBRAPA database (Reatto et al., 2004), which provides soil texture data (silt, sand, and clay content) at a 30 m ~~of~~ resolution down to a depth of 120 cm below the surface. To convert soil texture into the parameters required to run JULES (Table 3), we applied equations from Marthews et al. (2014). The edaphological parameters in the model are static.

Table 2: Meteorological variables required by JULES ~~an~~ and their respective definitions and units.

Variable	Definition
sw_down	Downward flux of short-wave radiation, W m^{-2}
lw_down	Downward flux of long-wave radiation, W m^{-2}
Precip	Rainfall, kg m^{-2} s^{-1}
T	Air temperature, ˚C
Wind	Wind speed, m s^{-1}
Pstar	Air pressure, Pa
Q	Specific humidity, kg kg^{-1}

Table 3: Soil physical parameters required for JULES with their respective definitions and units for five different sites in the Amazon region.

Parameter	Definition	ATTO	K67	RJA	K34	K83
b	Brooks-Corey exponential for hydraulic soil characteristics (dimensionless)	15.65	11.19	6.52	11.19	11.19
hcap	Dry heat capacity, J m^{-3} k^{-1}	1236203	1228469	1272748	1228469	1228469
sm_wilt	Soil moisture at the point of permanent wilt, m^3 m^{-3}	0.12	0.26	0.14	0.26	0.26
hcon	Dry thermal conductivity, W m^{-1} k^{-1}	0.20	0.22	0.27	0.22	0.22
sm_crit	Soil moisture at the critical point, m^3 m^{-3}	0.21	0.37	0.25	0.37	0.37
satcon	Saturation hydraulic conductivity, kg m^{-2} s^{-1}	0.00063	0.00152	0.0065	0.00152	0.00152
sathh	Soil matrix suction at saturation, m	0.39	0.32	0.14	0.32	0.32
sm_sat	Soil moisture at saturation, m^3 m^{-3}	0.39	0.46	0.42	0.46	0.46
albsoil	Soil albedo (dimensionless)	0.13	0.17	0.13	0.17	0.17

Concerning the carbon fluxes, the variables utilized to calibrate and evaluate JULES simulations were NEE, GPP, and Reco. It is important to mention that the direct observation from the Eddy-covariance tower measurement is NEE. NEE was partitioned following Botía et al. (2022) and~~, who followed a similar approach as~~ Restrepo-Coupe et al.~~,~~ (2017), assuming that nighttime NEE corresponds to nighttime Reco. Nighttime Reco was used as the daytime respiration, while daytime GPP

was calculated from the difference between GPP and NEE (NEE=Reco-GPP). NEE data was available every 60 minutes for all flux towers, except for the ATTO tower, available every 30 minutes.

2.4. Gridded data

In addition to the in situ observational data, gridded datasets were used in JULES model simulations and as benchmarks ~~to~~ for the simulated carbon fluxes. Meteorological data from the ERA5 reanalysis (Hersbach et al., 2020) were used to force ~~ce~~ the JULES model in spatialized runs (refer to Section 2.5.3). ERA5 has hourly temporal resolution and a spatial resolution of 0.25ºx0.25º, which was resampled to 1ºx1º, providing data for the variables listed in Table 2. This resolution was proposed in view of the computational ~~limitation~~ limitations to run JULES for the Brazilian Amazon biome.

Gridded data of vegetation properties and land use were also used in the spatialized model runs, extrapolating model parameters across the Brazilian Amazon biome. Canopy height was collected in the Global Forest Canopy dataset (Simard et al., 2011). This dataset represents the tree canopy heights with a resolution of 927 m based on a fusion of spaceborne-lidar data (2005) from the Geoscience Laser Altimeter System (GLAS) and ancillary geospatial data. Canopy heights retrieved from the gridded product were similar to local observations at the 5 tower fluxes considered in this study. LAI data from the ERA5 Land monthly reanalysis ~~was~~ were used, with a resolution of 11132 m. In ERA5, LAI is calculated using the land surface model of the European Centre for Medium-Range Weather Forecasts, known as CTESSEL (Boussetta et al., 2013), with the assimilation of a 9-year monthly climatology derived from satellite-based data from MODIS (Moderate Resolution Imaging Spectroradiometer). Therefore, the LAI product from ERA5 describes a fixed vegetation state. Land use and land cover data ~~was~~ were provided by MapBiomas, collection 9, with a spatial resolution of 30 m (Souza Jr. et al., 2020). The percentage of PFTs type in each grid cell was based on the MapBiomas land cover dataset ~~MapBiomas data was the reference to run JULES for each PFT represented in each grid~~ (refer to the Supplementary material, Section 3.1, Table S3.1). All data ~~was~~ were resampled to the 1ºx1º resolution and utilized in different versions of models approached in this study, as described in Section 2.5.3

Two gridded datasets on carbon fluxes were used as benchmarks for the simulations conducted in this study: FluxCom-X (Nelson et al., 2024) and the European Carbon Tracker CT 2022 (Jacobson et al., 2023). European Carbon Tracker provided hourly NEE at a resolution of 0.1º in latitude by 0.2° in longitude, calculated by the Simple Biosphere model Version 4 (SiB4), which is driven by meteorology variables from the European Centre for Medium-Range Weather Forecasts (ECMWF) Reanalysis 5th Generation (ERA5) dataset. To retrieve ~~compare~~ NEE from the CT 2022 carbon fluxes ~~with JULES simulation~~, the optimized biological flux was used (i.e., excluding Carbon flux from fuel and fire), and lateral fluxes from rivers were removed, following Friedlingstein et al. (2022). FluxCom-X, providing estimates with 0.05° spatial and hourly temporal resolution, is produced using a data-driven approach using an ensemble of machine-learning methods, ~~-~~combining local observations from Eddy-covariance flux towers, satellite observations, and meteorological reanalysis data. In the Brazilian Amazon biome, FluxCom-X assimilates data from only two flux towers: K67 and K83. The scarcity of flux data in

the Amazon -hinders the model training, resulting in ~~a~~ decreased model performance in this region when compared to other terrestrial ecosystems worldwide. Overestimation of the carbon sink (strongly negative NEE) in tropical regions is a well-known bias of the FluxCom-X dataset (Nelson et al., 2024).

2.5 .JULES model procedures

In this section, we described the procedures necessary to optimize and spatialize NEE using JULES for the Brazilian Amazon biome. In the first topic, we describe~~approach~~ a local sensitivity analysis ~~the first step~~ to select the most sensitive parameters of JULES ~~in~~ at a specific point in the Brazilian Amazon biome. The second topic will present the calibration of ~~and evaluation to improve~~ the most ~~sensitivity~~ sensitive parameters ~~selected in the sensitivity analysis~~. The third topic will describe the method utilized to spatialize JULES in the Brazilian Amazon biome. Considering the large number of grid points required to simulate the Brazilian Amazon region, a spin-up procedure would be very computationally expensive, considering that many years of simulation would be necessary to reach the equilibrium in the soil carbon stocks and humidity ~~Attaining equilibrium between carbon stocks and humidity via the soil moisture spin-up procedure was a computationally expensive process. For this study, it was difficult to implement because of the large number of grid points required to simulate the Brazilian Amazon region~~. To initialize the JULES simulations, we adopted the strategy employed by Moreira et al. (2013), which consists ~~in~~ of initializing the model with soil moisture fields and carbon stocks as close as possible to observations. ~~We ran JULES from the start to the end of the simulation period.~~ The carbon pool was not altered during the simulation, and carbon levels varied in accordance with seasonal changes throughout the year. Also, we considered the soil texture obtained in the EMBRAPA database (described in ~~the~~ section 2.3) as a source that closely matches ~~with~~ the observed data, and this can reduce the uncertainties in the water balance.

2.5.1. Sensitivity analysis

The first step in process-based model calibration and local sensitivity analysis is to understand how the modulation of GPP and Reco is influenced by the model parameters ~~(with NEE calculated by the difference of GPP and Reco)~~. This study initially assessed the sensitivity of the 21 core parameters of the JULES model by varying their values within the minimum and maximum expected ranges (Table S1~~2.1~~). The underlying hypothesis was that the heterogeneity of the Amazon forest would lead to variation in these parameters. Understanding their impact on NEE helps ~~identifying~~ identify which parameters

are critical for parameterization and should not be treated as fixed values, as ~~it~~ is done in the default JULES model PFT parameterization.

The local sensitivity analysis was developed for 2018 using the location of the ATTO tower as a reference. Each JULES parameter was perturbed within its maximum and minimum expected range, as shown in Supplement Table S~~2.~~1. The effect of these changes on NEE calculations was quantified using the mean absolute deviation (MAD, g C m^{-2} day^{-1}) (Equation 14) and Δvar (%) (Equation 15). MAD and Δvar depend on the difference of NEE computed using the maximum and minimum value of a specific parameter (all others are maintained fixed with the default value). The calculation is computed considering each day of simulation~~for the simulation of each day~~ and averaged over the year. Δvar is computed by Equation 15 ~~as the sum of the square difference divided by the square root of the number of days analyzed~~. Since Δvar is based on square differences, this metric is sensitive to outliers. We ~~which can generate spurious values with significantly higher magnitudes. To mitigate the impact of these spurious values, we treated them as outliers and~~ applied the Grubbs' test (Grubbs, 1969) with a significance level of 95% to remove the NEE outliers~~, removing days with NEE considered outliers based on the absolute difference between maximum and minimum disturbed values, divided by the NEE before optimization (Harper et al., 2016)~~. After this procedure, each parameter was classified by relevance ~~level~~ based on the largest Δvar values, identifying the most sensitive parameters. Supplement ~~Figures~~ Figure S~~2.~~1 ~~present~~ presents the NEE monthly simulations for 2018, considering the impact of changes in the most relevant parameters compared to observed data (retrieved from the Eddy-covariance towers). The simulations were performed by varying each relevant parameter individually, using different values within the specified minimum and maximum range.

$$\mathrm{MAD} = \frac{\sqrt{\sum_{i=1}^{N}(ymax_i - ymin_i)}}{N} \quad (14)$$

$$\Delta\mathrm{var}\ (\%) = \frac{100}{N} \cdot \sqrt{\sum_{i=1}^{N} \frac{(ymax_i - ymin_i)^2}{(ydefault_i)^2}} \quad (15)$$

Where ymax is the NEE daily value simulated with the maximum parameter; ymin is the NEE daily value simulated with the minimum parameter ~~the minimum~~; ydefault is the daily value simulated using the default version of JULES default (Figure S2~~.2~~), and N is the number of observations, removing days with outliers (352 days).

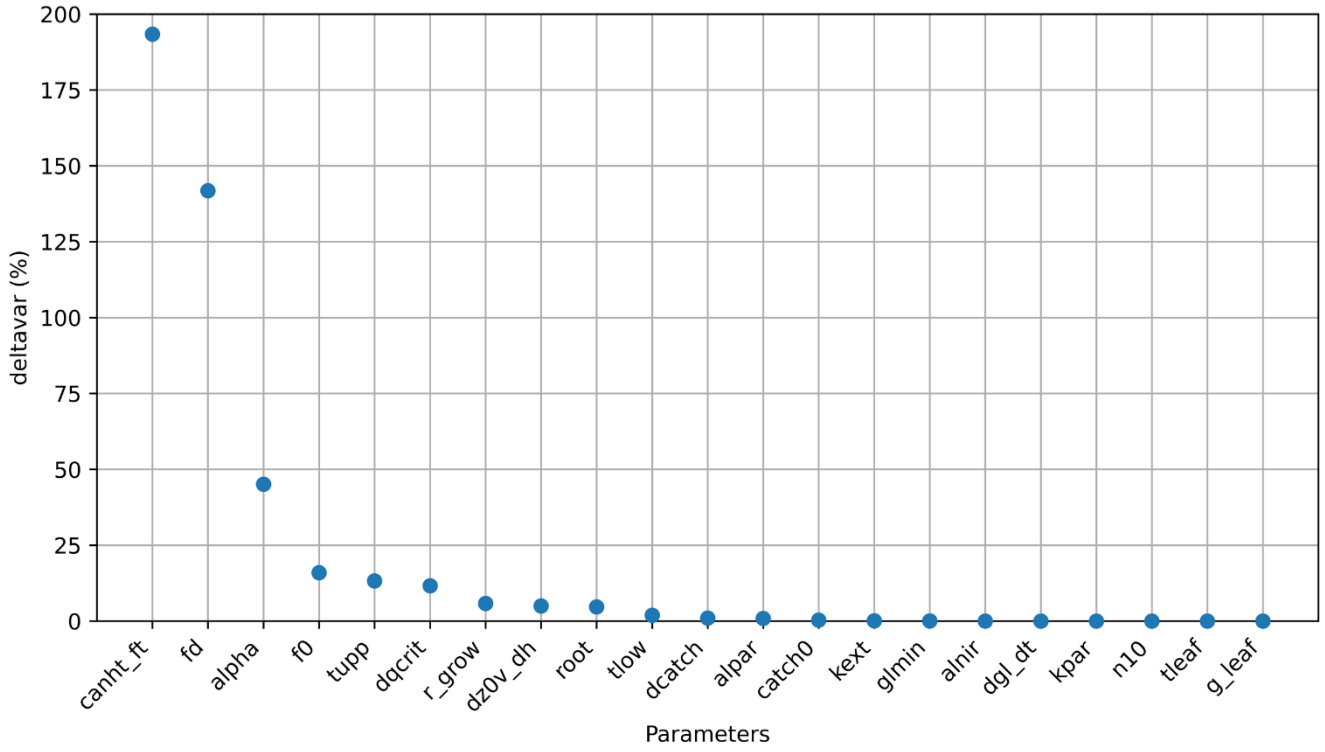

Figure 2: Variation in (%) (Δvar) of JULES parameters relative to the default version of JULES at the ATTO tower, representing the Amazon biome during 2018. The abbreviations were defined in Supplement Table S~~2.~~1.

We considered the five most sensitive parameters (Figure 2): canopy height (canht); scale factor for dark respiration (fd), which is a coefficient between 0 and 1 associated with leaf dark respiration (Equation 6); quantum efficiency for photosynthesis (alpha, mol CO_2 mol^{-1} PAR) (Equation 4); the maximum ratio of internal to external CO_2 (f0), necessary to simulate leaf CO_2 concentration based on leaf humidity deficit, and the upper-temperature threshold for photosynthesis (tupp, Equation 1). The sensitivity analysis has shown that variations in canopy height between 19 m and 50 m can lead to variations of almost 200% in NEE. The variation of the dark respiration scaling factor, for potential values found in Amazonia, can also lead to differences in NEE of the order of 140%. The quantum efficiency, the maximum ratio of internal to external CO_2, and the upper temperature for photosynthesis can lead to variations in NEE of 45%, 16%, and 13%, respectively (refer to Table S2.~~2~~).

The set of parameters selected in the sensitivity analysis ~~were~~ was similar ~~compared~~ to Raoult et al. (2016), ~~which~~ who calibrated JULES for different plant functional types using GPP to evaluate the new parameterization. The reason behind the high sensitivity of NEE towards the parameter canht can be explained by its influence on calculating Maintenance Respiration (Equation 11, section 2.2), as canht is necessary to estimate stem wood respiration (Clark et al., 2011). -Another factor behind the high sensitivity of canht is its linear relationship with roughness length (Best et al., 2011), which strongly

influences mechanically driven turbulence and the efficiency of CO_2 exchange between the land surface and the atmosphere (Khanna and Medvigy, 2014).~~Another relevant aspect that explains the high sensitivity of canht is the linear relation with roughness length (Best et al., 2011), which is important for carbon fluxes estimated by the mechanical turbulence and the capacity to enhance the mixing of air and to facilitate the transfer of gases, including CO_2, between the land and the atmosphere (Khanna and Medvigy, 2014).~~ The parameter fd is ~~also~~ relevant for~~to~~ estimating~~e~~ the dark respiration coefficient (Equation 6, section 2.2) and is associated with the content of nitrogen in the estimation of the maintenance respiration (Equation 11, section 2.2) ~~related to the Reco estimation~~. Alpha is a parameter associated~~that is related~~ to estimating the rate of light-limited photosynthesis (Equation 3, section 2.2), f0 is a relevant parameter for estimating~~to estimate~~ hydric stress and the ~~the~~ stomata regulation (Equation 5, section 2.2), and tupp is required to estimate V_{cmax} for different temperatures (Equation 1, section 2.2). The parameters alpha, tupp, and f0 were also found to be important for modeling GPP by Raoult et al. (2016) and Li et al. (2016) in their work on~~to optimize~~ GPP optimization~~estimation~~ using JULES. Parameters related to~~with~~ light-limitation of photosynthesis, such as the ~~case of~~ alpha were also sensitive in other Dynamic Vegetation models~~, such as ORCHIDEE model.~~, ~~demonstrated by~~ Zhu et al.~~,~~ (2025), working with~~-~~ the ORCHIDEE model in the Amazon region~~a spatialization procedure of the carbon cycle in the Amazon region~~, demonstrated high sensitivity in the parameter alpha self-thinning, which controls tree mortality induced by light competition. Another relevant parameter observed by Zhu et al.~~,~~ (2025) was related to the nitrogen use of photosynthesis, which, in the JULES model, is the fd parameter. In this study, following ~~directly related to the content of nitrogen to estimate maintenance respiration (Equation 11, section 2.2). After~~ canopy height, the fd parameter is the most sensitive parameter of JULES, followed by alpha ~~in the Brazilian Amazon biome~~. Although JULES and ORCHIDEE models differ in their parametrization, the convergence of certain parameters highlights the importance of nitrogen and radiation in simulating carbon fluxes in tropical trees. Consequently, optimizing these parameters improves the spatial representation of carbon fluxes across the Brazilian Amazon biome, accounting for its vegetation heterogeneity.

~~Despite the difference in parametrization of these two different models, similarities of the parameters indicate relevance of nitrogen and radiation to reproduce carbon fluxes in tropical trees. Thus, optimizing this set of parameters makes it possible to spatialize the carbon fluxes in the Brazilian Amazon biome and their vegetation heterogeneity.~~

2.5.2. Calibration and validation

After the local sensitivity analysis, which defined the most important parameters for GPP and Reco, JULES was optimized by comparing simulations with observed data at each site described in section 2.2. For this attempt, we ~~used the Nelder-Mead method (Nelder and Mead, 1965) for the optimization, using the SciPy implementation (Harris, et al., 2020) and NumPy to process data (Virtanen et al., 2020)~~employed the Nelder-Mead method (Nelder and Mead, 1965) for optimization, utilizing the SciPy implementation (Harris et al., 2020) and NumPy (Virtanen et al., 2020) to process the data. The Nelder-Mead method is a numerical method used to find the minimum or maximum of an objective function in a multidimensional space (Dakhlaoui, 2014). This method was successfully applied in studies of calibration and evaluation of different models as

described by Jérôme et al.~~,~~ (2021). NEE was the control variable in the calibration process~~The JULES output utilized as a reference for calibration at each site was NEE~~, since it is directly retrieved from Eddy-covariance measurements without assumptions on flux partitioning. Canopy height was set to the corresponding values at each site (Table 1), and the four most sensitive parameters were adjusted within physiological limits to minimize daily model-observation error (Table S4). ~~Canopy height was fixed as the average canopy height of each site, while the next four most sensitive parameters were concomitantly modified within the physiological limits, looking for the combination of values that minimized the error between model and observation on a daily scale (Table S4.1).~~ The statistical index adopted to evaluate the error in this study was the root mean square error (RMSE) (Loague and Green, 1991, equation 16).

$$RMSE = \sqrt{\frac{1}{n}\sum_{i=1}^{n}(y_i - p_i)^2} \quad (16)$$

Where y_i is the predicted value of NEE~~,~~, pi ~~is~~ the observed value of NEE, and n is the number of observations.

Another statistical ~~matric~~ metric used to analyze the accuracy of the simulations during the year was the index of agreement (*d*) proposed by Wilmott et al. (2012), given by

$$d = 1 - \left|\frac{\sum_{i=1}^{n}(yi-pi)^2}{\sum_{i=1}^{n}(|yi-P|+|pi-P|)^2}\right|, \quad (17)$$

where P is the average value of NEE ~~of standard observations of NEE~~. When d is close to 1, this indicates a high accuracy level.

It was necessary to delimit maximum and minimum values for each parameter according to the physiological characteristics of tropical species (Table S4~~.1~~). Within the delimited values of reference, the optimization was developed starting from the JULES parameter default value~~s of each JULES parameter adopted by~~ (Harper et al., ~~(~~2016). Important to mention that the Nelder-Mead method does not generate uncertainties for fitted parameters at a confidence level.~~e level, being limited to one value in a physiological range that will be our reference to the calibration procedure~~

2.5.3. Spatializing JULES in the Amazon biome

The optimization of the JULES model parameters for different forest sites in Amazonia showed significant differences, reflecting the heterogeneity of vegetation characteristics categorized in the PFT Broadleaf Evergreen Trees - tropical (BET-TR). This motivated the spatial extrapolation of JULES model parameters across the Amazon Basin using remote sensing data as predictors.

Following the calibration of sensitive parameters for each flux tower~~After the sensitive parameters were adjusted for each tower~~, it was possible to spatialize the parameter values across the Amazon biome. As such, we developed a spatially dependent parameterization of the BET-TR PFT in JULES. The spatialization model was based on linear regressions, having each sensible parameter as the target variable, and two remote-sensed vegetation properties as predictors: canopy height and LAI. The reasons behind the choice of these variables include: data availability and expected correlations between these

properties and the 5 most sensitive parameters (Li et al., 2018; Moudry et al., 2024). Also, canopy height and LAI can be considered constant in the short term, describing a fixed vegetation state. Moreover, these two variables are required as input for JULES simulations~~,~~: canopy height as a plant functional type parameter, and LAI as an initial condition for simulations.

With independent linear regressions on canopy height and LAI, it was possible to extrapolate the model parameters to the whole Brazilian Amazon biome. Different configurations for linear regression models were tested for each JULES parameter, following one of the general formats of Equation 18a and 18 b:

$$P(x,y,LAI) = a + b \cdot LAI(x,y) \quad (18a)$$

$$P(x,y,height) = a + b \cdot height(x,y) \quad (18b)$$

~~$$\begin{matrix} P(x,y,LAI) = a + b \cdot LAI(x,y) \\ P(x,y,height) = a + b \cdot height(x,y) \end{matrix} \quad (18)$$~~

where P represents JULES model parameters (tupp, alpha, f0_io, and fd); x, y are the coordinates of each model grid cell; a, b, are regression coefficients to be determined. The regression models were fitted to the parameters optimized at four forest sites described in section 2.1 (K34, ATTO, K67, and RJA), using the maximum likelihood method. The choice of the regression model configuration for each JULES parameter was based on a compromise between the regression model residuals and the physical consistency of the extrapolated values. Section 3 in the Supplementary material shows the reasoning behind the choice of each regression model. A leave-one-out cross-validation was applied to evaluate calibration across regions of the Brazilian Amazon biome (Wallach et al., 2018), using predictions from spatialized linear models based on canopy height and LAI.~~After that, a leave-one-out cross-validation method was used to validate the calibration in different parts of the Brazilian Amazon biome (Wallach et al., 2018), utilizing the predict values obtained by the spatialization linear equations from canopy height and LAI.~~

To represent variations in carbon fluxes throughout the year, simulations were performed with one-degree resolution across the Brazilian Amazon biome. The months selected were ~~during~~ April and September 2021~~2~~, representing a wet and a dry season month in the Amazon Region, respectively. The meteorological dataset required for JULES to simulate GPP, respiration, and NEE (Section 2.1, Table 2) was provided by ERA5 reanalysis data at an hourly scale and resampled to~~with~~ a 1°x1° resolution.

It is important to highlight that the spatially dependent parameterization was used only for the BET-TR PFT, representing 71% of the Brazilian Amazon biome. For other PFTs present in the Amazon Basin, the default values were used for all parameters (Harper et al., 2016). The canopy height for BET-TR was provided by the Global Forest Canopy dataset (section 2.4), while for the other types of vegetation, we used the default values by Clark et al. (2011) and Harper et al. (2016). In the case of C4 grass that has relevance in the arc of deforestation, ~~-~~we utilized a canopy height of 15 cm, which is typical for cattle farms in this region (Fernandes et al., 2015). In the case of soybean, a relevant crop cultivated in the northern region of the state of Mato Grosso, we considered the sowing date in September and the harvest in February, as described by the Mato

Grosso Institution of Agricultural Economics (De Lima Filho, 2021). To assign a PFT for each model grid, a correspondence was established between JULES landland functional types and land use data from MapBiomas collection 9 (Souza Jr et al., 2020) (see supplementary material, Section 3.1, Table S3.1). Since MapBiomas data have a resolution of 30 m, it was necessary to calculate the percent contribution of each land use class present in each 1° model cell grid (Figure S3.1). To run the model, it was necessary to introduce the fraction of each land functional type as a tile to represent each vegetation type present in the grid for JULES simulations. A description of all procedures utilized to spatialize JULES is described in Figure S164.5 (see ssupplementary materials section S.4).

2.6 VPRM model

The Vegetation Photosynthesis and Respiration Model (VPRM) (Mahadevan et al., 2008) is a satellite data-driven empirical model designed to estimate NEE by integrating GPP and ecosystem respiration. GPP is calculated using a light-use efficiency method that combines meteorological inputs (e.g., temperature and photosynthetically active radiation) with remote sensing indices such as the Enhanced Vegetation Index (EVI) and the Land Surface Water Index (LSWI). These indices are derived from the MODIS Surface Reflectance 8-Day L3 Global 500 m (MOD09A1) product, which wasis collected within a ±0.1° area around each tower evaluated in this study (ATTO, K34, K67, K83, RJA; see Table 1 for descriptions). MODIS data was interpolated to the daily frequency These data are interpolated to daily intervals using a curve smoothing technique (LOWESS filter). Ecosystem respiration is modeled ussing a linear function of temperature to capture the temperature dependence of carbon release. VPRM's key parameters include $\lambda 0$ (maximum light-use efficiency), PAR0 (light saturation constant), α and β (coefficients controlling Reco temperature dependence), as well as the temperature thresholds Tmin, Tmax , Topt, and Tlow. In this study, the parameter values employed were those calibrated by Botía et al. (2022) for the Amazon forest.

3.Results

3.1. Calibration and evaluation of JULES

After the identification of the model parameters with the highest sensitivity in the ATTO tower, utilized as reference for the local sensitive analysis for the Brazilian Amazon biome, the JULES model was calibrated for each flux tower, following the methods described in Section 2.5.2. Table 4 shows the JULES default values for the BET-TR PFT parameters (Harper et al., 2016) along with the optimized values considering local measurements in the Amazon. The optimized values showed a strong variability, even among the equatorial forest sites. This explains the motivation for the spatialization of JULES parameters for the BET-TR plant functional type.

Table 4: New parameterization of JULES optimized by Nelder-Mead in each simulated site in this study. Four parameters were optimized: upper-temperature threshold for photosynthesis (tupp), quantum efficiency (alpha), scale factor for dark respiration (fd), and maximum ratio of internal to external CO_2 (f0). Canopy height (canht) was ~~retrived~~ retrieved from observations at each site.

Parameter	unit	Default	ATTO	K67	K34	RJA
tupp	ºC	43	42.18	36	42.77	36
alpha	mol CO_2 per mol PAR photons	0.08	0.05	0.066	0.061	0.05
fd	dimensionless	0.01	0.011	0.0066	0.01	0.007
f0	dimensionless	0.875	0.95	0.713	0.93	0.875
canht	m	30	30	36	27	35

Figure 3 shows the simulated fluxes for GPP, Reco, and NEE using optimized JULES parameters, JULES default parameters, and simulations with the VPRM model. Observations are also depicted~~,~~ as a reference. The statistical metrics RMSE and *d* (Equations 16 and 17) were calculated in each case~~,~~ to assess the performance of each model setup in reproducing the observations. The new parameterization reduced RMSE for GPP and NEE in all flux towers, in comparison to the default parameter values and to the VPRM results. However, the optimized parameter values did not improve the Reco simulations. It is important to note that NEE was the control variable in the calibration process so that the GPP and Reco partitioned fluxes

were indirectly optimized. NEE was used as the control variable because it is directly measured in the flux towers, without assumptions regarding ~~to~~ the partition into GPP and ~~respirations~~respiration.

The seasonality of the carbon fluxes was also improved using the JULES optimized parameters~~better represented by JULES optimized utilizing the Nelder-Mead method~~ (Figure 3). Although the JULES~~JULES~~ optimized version did not capture the ~~increase in~~ GPP increase during the~~in the~~ dry-to-wet ~~season~~ transition (Oct-Dec), it reduced ~~the new version of JULES reduced the error in~~ GPP errors compared~~P in relation~~ to the default version and VPRM in each season of the year. Model limitations in representing dry-season effects were also noted by Restrepo-Coupe et al. (2013), who reported distinct dynamics at the RJA tower, located near pasture and under a rainfall regime unlike the equatorial sites ATTO, K67, and K34.~~The difficult in representing the dry season effects by the models was also described by Restrepo Coupe et al. (2013) who observed a different dynamic during the dry season in RJA tower, which is a region near to pasture and with a rainfall regime different from the equatorial region represented by ATTO, K67 and K34.~~ In most process-based vegetation models, GPP is strongly associated with hydric stress, which may not be adequate for some Amazonian regions where leaf phenology and litter fall dynamics could play an important role (Restrepo-Coupe et al., 2017; Botia et al., 2022). JULES optimized was the version that better represented the observed carbon sink (NEE<0) between September and January at the K67 tower. Reco was overestimated in November and December, due to the direct relation between the dark respiration coefficient (fd) and Vc_{max} (Clark et al., 2011, equation 1). Despite the limitations in the reproduction of the carbon seasonality, the optimization of JULES parameters resulted in improved estimates for annual means in NEE, reducing the bias in comparison to the default parameter values.

VPRM demonstrated weaknesses in simulating GPP seasonality, and the error magnitude in NEE was higher than in the optimized JULES model and, in some regions (K67 and K34), even higher than its default version. Botia et al. (2022), comparing different models at the ATTO tower, reported that VPRM demonstrated low efficiency in capturing carbon seasonality in this region. This was attributed to the lack of model representation of hydric stress, as the only water scaling source was the Water Scale Index, derived from remotely sensed Land Surface Water Index using MODIS reflectance data (Chandrasekar et al., 2010, and Gourdji et al., 2022).

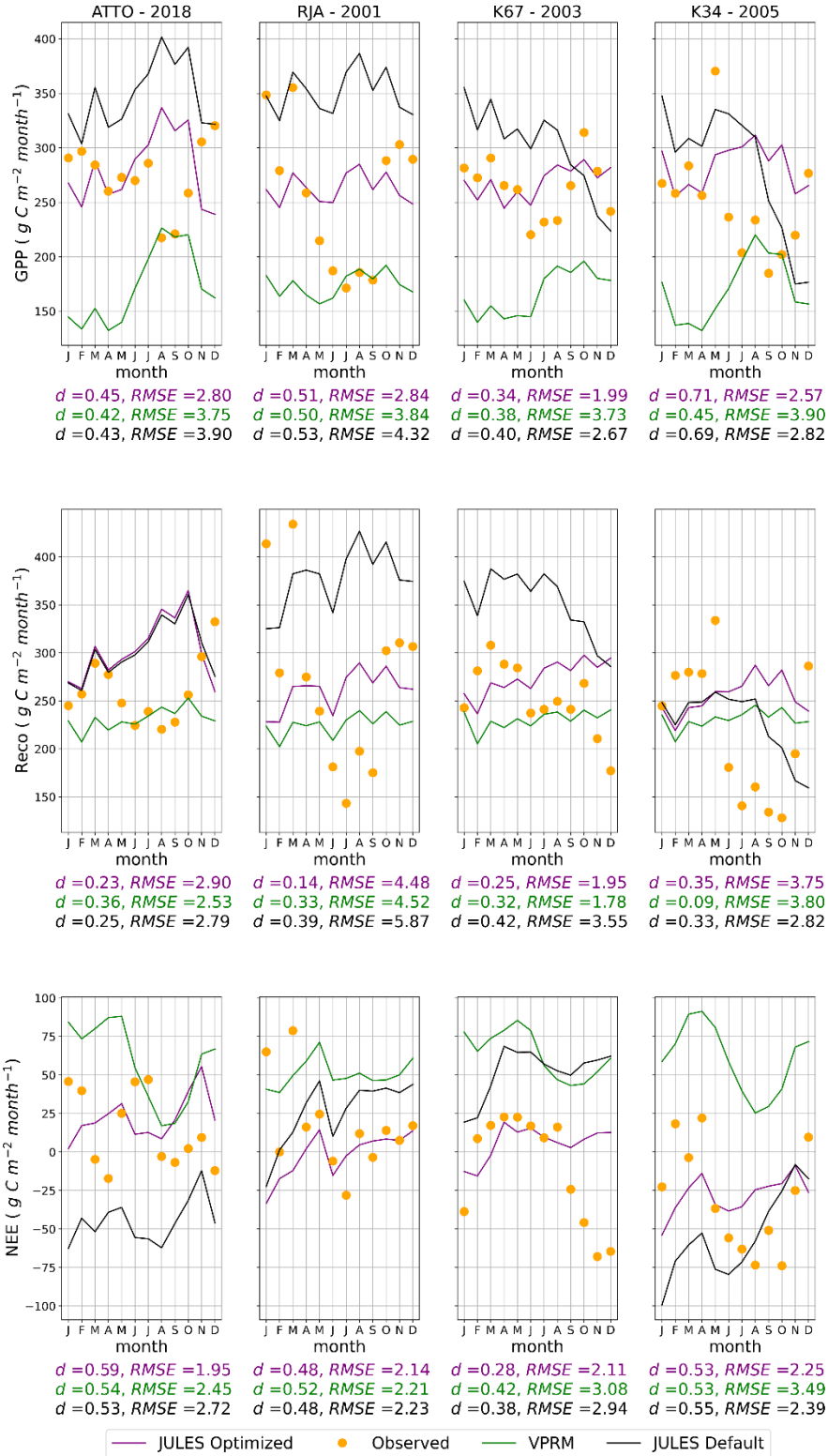
ATTO - 2018
RJA - 2001
K67 - 2003
K34 - 2005
GPP (g C m−2 month−1)
Reco (g C m−2 month−1)
NEE (g C m−2 month−1)
month
J F M A M J J A S O N D
d =0.45, RMSE =2.80
d =0.42, RMSE =3.75
d =0.43, RMSE =3.90
d =0.51, RMSE =2.84
d =0.50, RMSE =3.84
d =0.53, RMSE =4.32
d =0.34, RMSE =1.99
d =0.38, RMSE =3.73
d =0.40, RMSE =2.67
d =0.71, RMSE =2.57
d =0.45, RMSE =3.90
d =0.69, RMSE =2.82
d =0.23, RMSE =2.90
d =0.36, RMSE =2.53
d =0.25, RMSE =2.79
d =0.14, RMSE =4.48
d =0.33, RMSE =4.52
d =0.39, RMSE =5.87
d =0.25, RMSE =1.95
d =0.32, RMSE =1.78
d =0.42, RMSE =3.55
d =0.35, RMSE =3.75
d =0.09, RMSE =3.80
d =0.33, RMSE =2.82
d =0.59, RMSE =1.95
d =0.54, RMSE =2.45
d =0.53, RMSE =2.72
d =0.48, RMSE =2.14
d =0.52, RMSE =2.21
d =0.48, RMSE =2.23
d =0.28, RMSE =2.11
d =0.42, RMSE =3.08
d =0.38, RMSE =2.94
d =0.53, RMSE =2.25
d =0.53, RMSE =3.49
d =0.55, RMSE =2.39
JULES Optimized
Observed
VPRM
JULES Default

Figure 3: GPP, Reco, and NEE simulations using different model setups and observations at each flux tower in Amazonia. The observed data in the plots is the aggregate value for each month of the year, and the RMSE error described is the daily average during the year in g C m^{-2} day^{-1}.

3.2. Spatialization of JULES parameters

Considering the variability of the optimized parameters for different sites of the Brazilian Amazon biome (Table 5), simple linear regression models were developed to extrapolate the parameter values for the whole Brazilian Amazon. As predictors, vegetation characteristics described in Section 2.5.3, namely LAI and canopy height, were used. Table 5 shows the linear regression models developed for the JULES parameters with the highest sensitivity. Section 3 of the supplementary materials details the rationale for each regression model and includes maps of spatialized JULES parameters and their relationships with vegetation characteristics. ~~The reasoning behind each regression model is available in section 3 of the supplementary material, where maps showing the spatialized values for the JULES parameters and the relationship of each parameter with the respective vegetation index are also provided.~~

The relationship between each parameter and the selected predictor is shown in Figure 4. Canopy height was selected for tupp and alpha, while LAI was selected for f0 and fd. Tupp showed an inversely proportional relationship with the canopy height (Figure S~~.5~~3.2.2), which is consistent with ~~that~~ the fact that low-canopy plants like C4 grasses typically have higher temperature thresholds for photosynthesis. The parameter alpha did not show a clear relationship with any of the predictors, resulting in a rather constant behavior against canopy height (Figure S7~~.3.3.2~~). Canopy height was chosen as a predictor for alpha to obtain the expected lower quantum yields for C3 and C4 plants (0.055 mol^{1} mol^{-1}, Skilman 2008) (Figure S6~~3.3.1~~). The correlation between~~of~~ alpha and~~with~~ canopy height is weak~~small~~; however, given the narrow variation of alpha in the Amazon (0.05-0.06 mol^{1} mol^{-1}~~as alpha in the Amazon has a small range of variation (between 0.05 and 0.06 mol mol^{-1} for C$_3$ species, in line with Skilman, 2008), this low correlation has a small impact on the final result~~ for C_3 species, consistent with Skilman, 2008), this low correlation exerts minimal influence on the final result. Parameter f0 was positively associated with LAI (Figure S9~~.3.4.2~~), consistent with the fact that f0 is expected to be lower in the arc of deforestation compared to forest sites. For the fd parameter, the selected predictor was LAI (Figure S11~~.3.5.2~~), which is expected to have a positive relationship with fd, given the greater photorespiration efficiency in C4 plants.

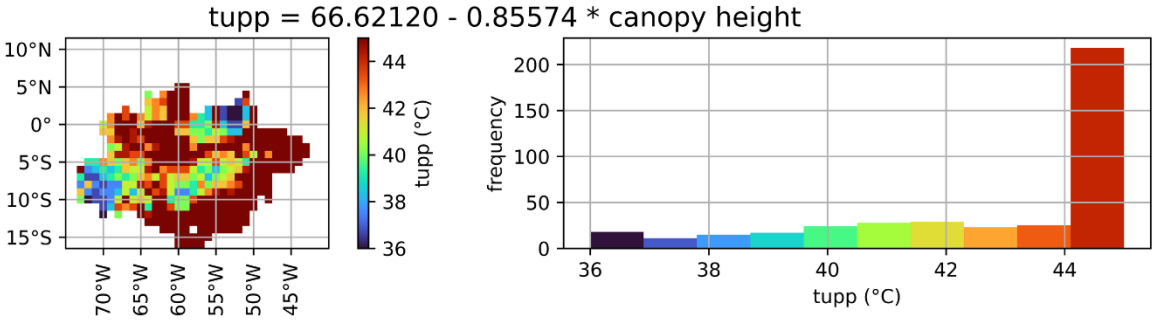
tupp = 66.62120 - 0.85574 * canopy height
10°N
5°N
0°
5°S
10°S
15°S
70°W
65°W
60°W
55°W
50°W
45°W
44
42
40
38
36
tupp (°C)
frequency
200
150
100
50
0
36
38
40
42
44
tupp (°C)

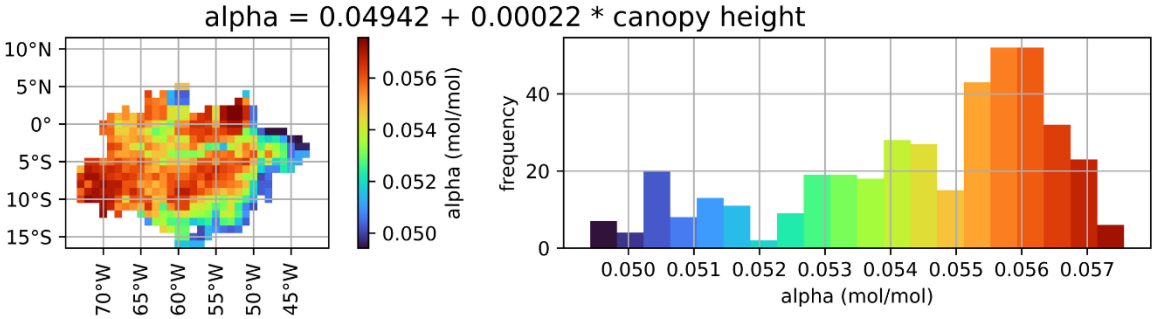
alpha = 0.04942 + 0.00022 * canopy height
10°N
5°N
0°
5°S
10°S
15°S
70°W
65°W
60°W
55°W
50°W
45°W
0.056
0.054
0.052
0.050
alpha (mol/mol)
frequency
40
20
0
0.050
0.051
0.052
0.053
0.054
0.055
0.056
0.057
alpha (mol/mol)

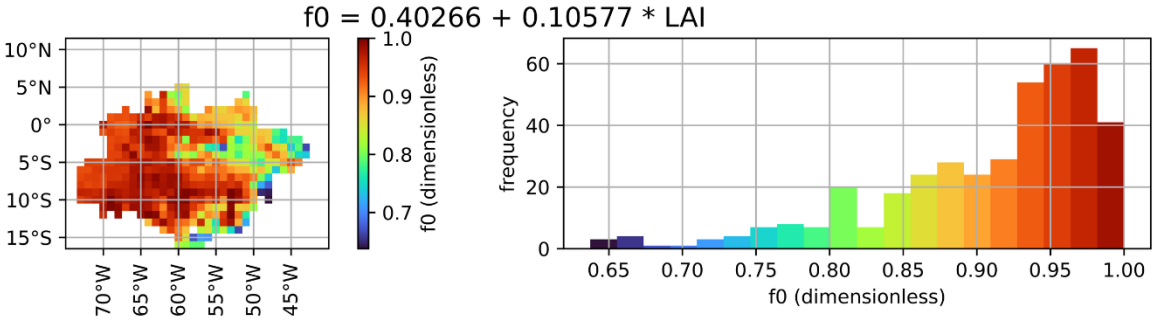
f0 = 0.40266 + 0.10577 * LAI
10°N
5°N
0°
5°S
10°S
15°S
70°W
65°W
60°W
55°W
50°W
45°W
1.0
0.9
0.8
0.7
f0 (dimensionless)
frequency
60
40
20
0
0.65
0.70
0.75
0.80
0.85
0.90
0.95
1.00
f0 (dimensionless)

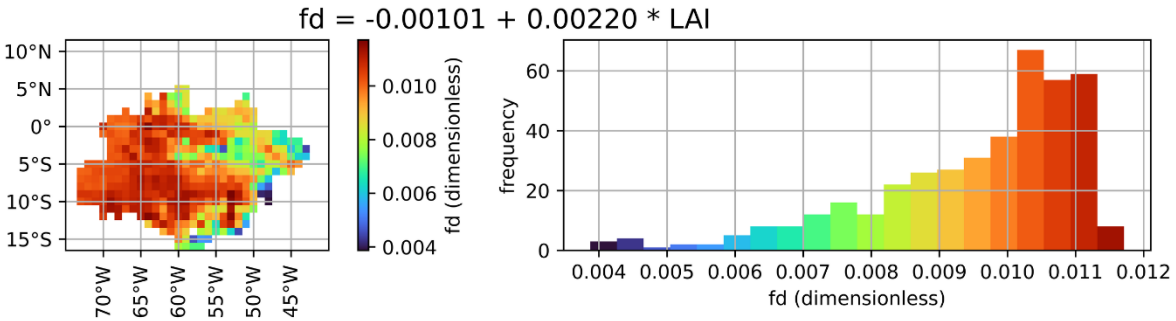
fd = -0.00101 + 0.00220 * LAI
10°N
5°N
0°
5°S
10°S
15°S
70°W
65°W
60°W
55°W
50°W
45°W
0.010
0.008
0.006
0.004
fd (dimensionless)
frequency
60
40
20
0
0.004
0.005
0.006
0.007
0.008
0.009
0.010
0.011
0.012
fd (dimensionless)

Figure 4: Spatialization of the parameters tupp (upper-temperature threshold for photosynthesis), alpha (quantum efficiency), f0 (maximum ratio of internal to external CO_2), and fd (scale factor for dark respiration) for the Amazon biome using linear regression models based on canopy height or LAI~~two different methods: based on canopy height and based on LAI~~.

The regression equations were used to obtain the parameter values at the K83 tower site, which was left aside during~~in~~ the spatialization ~~parametrization~~ process. Using a canopy height of 28 m and an average LAI value of 3.78, as described in section 2.4, the parameter values obtained for K83 were used in a JULES simulation for the year ~~of~~ 2001, predicting the GPP, Reco, ~~-~~and NEE fluxes depicted in Figure 5.

Table 5: Parameterization based on the spatialization in the Amazon region for four JULES parameters in Tower K83

Parameter	Equation	R^2	Value extrapolated to K83
Tupp (ºC)	66.6212-0.85574*Height	0.94	42.66
alpha (mol mol^{-1})	0.04942 + 0.00022*Height	0.01	0.056
f0	0.40266 + 0.10577*LAI	0.87	0.802
fd	-0.00101+0.0022*LAI	0.91	0.0073

The most relevant aspect was the improvement in GPP, reducing the RMSE in 37% in comparison to the default version of JULES and 39 % in comparison to the VPRM model. Observations at the K83 tower showed a weak annual cycle in the carbon fluxes, which was satisfactorily reproduced by the models. Overall, this validation process indicates that the method used for the spatialization of JULES parameters provided satisfactory estimates in a forest site that was left out of the regression models.

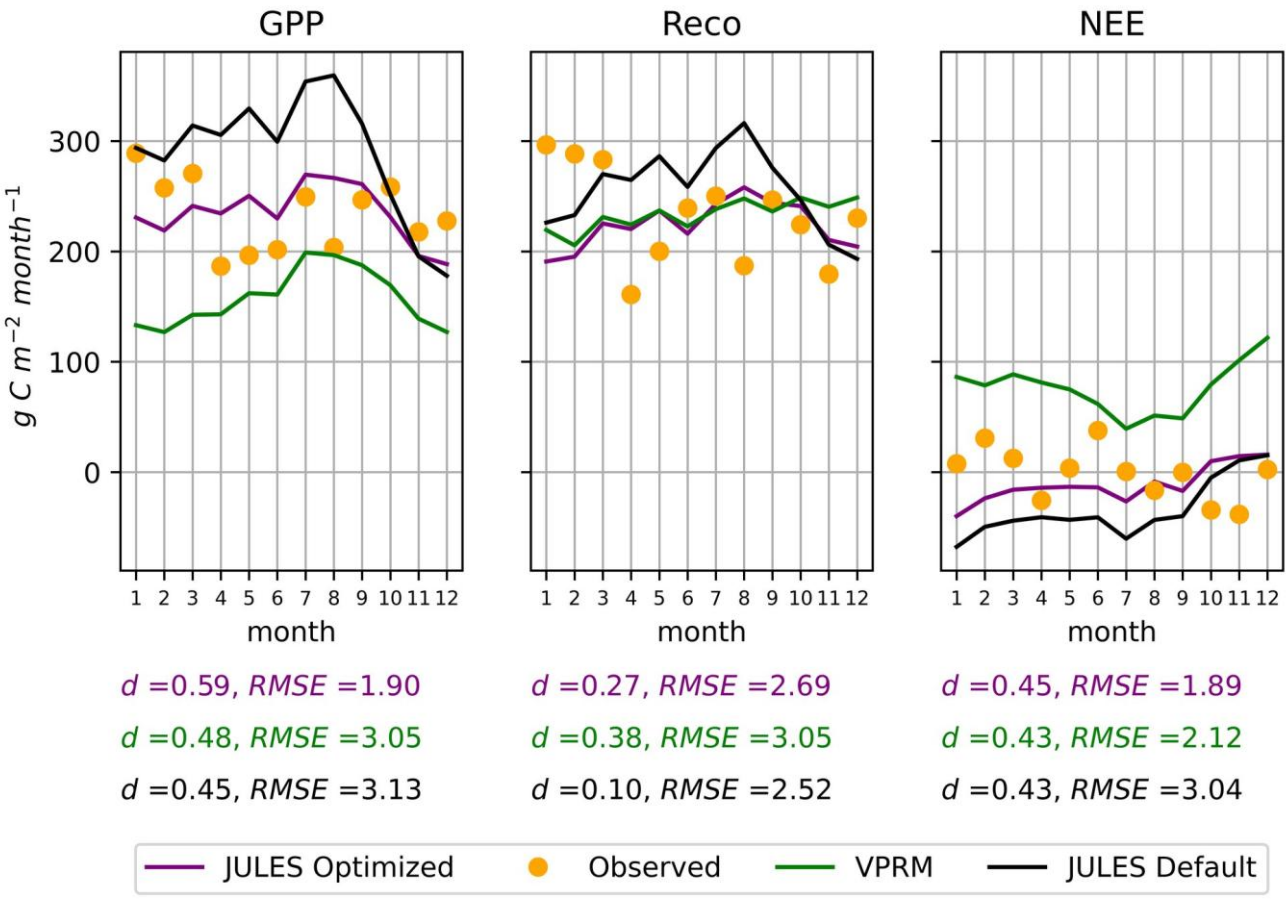

Figure 5: GPP, Reco, and NEE fluxes in the independent Tower of validation K83, for the year ~~of~~ 2001. The observed data in the plots is the accumulated during each month of the year, and the RMSE error described is the daily average during the year in g C m^{-2} day^{-1}.

580

3.3. Spatial variability of carbon fluxes in Amazonia

After validation with an independent tower (K83), we were confident in using JULES to estimate carbon fluxes across the entire Brazilian Amazon biome for the year 2021. This year was chosen to allow comparison of the simulated carbon fluxes
585 with recently released or updated global datasets. The simulations used the spatialized values of the 5 most sensitive parameters of the BET-TR JULES PFT (Figure~~.~~ 4). Default parameter values were used for other PFTs in the Amazon Basin. Although JULES did not accurately reproduce carbon flux seasonal cycles (Figure 3), assessing the spatial variability of NEE under contrasting meteorological conditions remains essential to evaluate model responses. ~~Despite the fact that the JULES model~~

~~was not able to reproduce precisely the carbon flux seasonal cycles (Fig. 3), it is important to assess the estimated spatial variability of NEE in months with contrasting meteorological conditions, investigating the model responses.~~ Figure 6 highlights the results from two representative months of the wet (April) and dry (September) seasons in Amazonia.

The mean GPP in April was 223 g C m^{-2} $month^{-1}$, while the mean Reco was 170 g C m^{-2} $month^{-1}$, characterizing a carbon sink (NEE) of -53 g C m^{-2} $month^{-1}$. During the dry season month (September), there was an increase in GPP, reaching a mean of 240 g C m^{-2} $month^{-1}$, and in Reco, with a mean of 182 g C m^{-2} $month^{-1}$, increasing the carbon sink to -58 g C m^{-2} $month^{-1}$. The fact that GPP was not reduced by water limitation during the dry season ~~also was~~was also observed by Restrepo-Coupe et al. (2013), who observed an increase in GPP during the dry season based on observations at the flux towers K34, K67, and K83.

The Reco value estimated by JULES ~~are~~ is underestimated in the wet season (April) when compared to Botia et al. (2022), which reported a mean value of 350 g C m^{-2} $month^{-1}$ for the wet season at the ATTO tower. In the dry season, however, Reco estimates were similar to the values reported by Botia et al. (2022) (200 g C m^{-2} $month^{-1}$) in the same region. This aspect ~~, which~~ suggests that further improvements are needed to better reproduce the seasonality of Reco, particularly~~,~~ in the Amazon basin.

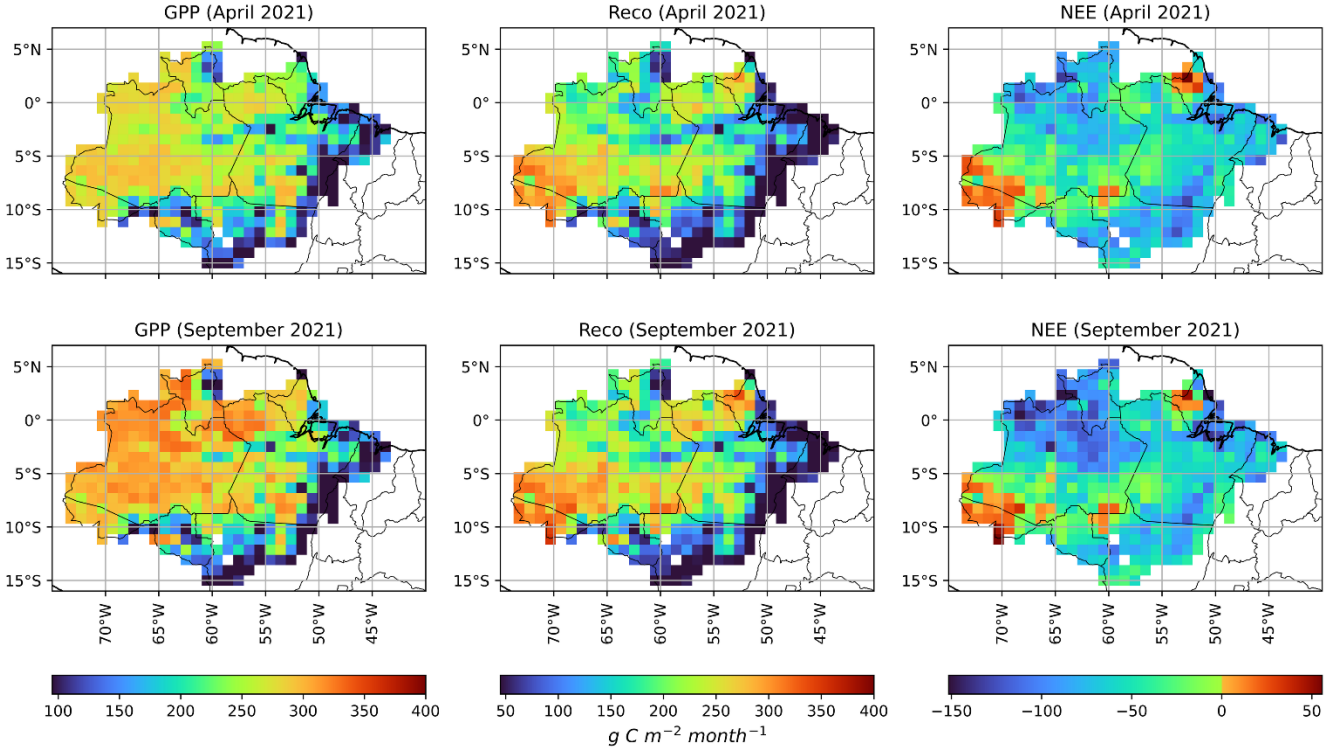

Figure 6: Monthly accumulated GPP, Reco, and NEE for April and September, representing the wet and dry ~~season~~ seasons in the Brazilian Amazon biome in 2021. The carbon fluxes were simulated by JULES, using spatially dependent vegetation parameters.

To further evaluate the spatialized model results, the simulated NEE fluxes for the year ~~of~~ 2021 were compared to the following estimates (Figure 7): i) European Carbon Tracker CT 2022 (Jacobson et al., 2023); ii) FluxCom-X (Nelson et al., 2024); iii) JULES simulation using fixed average values for the BET-TR parameters, considering the optimized values presented in Table 4; iv) JULES simulation using default parameter values (Harper et al., 2016).

Figure 7 clearly shows that ~~that~~ the three different modelling approaches using JULES (optimized, default, and spatially dependent~~fixed best adjusted~~ parameters) ~~-~~result in an increase in the estimated carbon sink in Amazonia (~~i. e.~~i.e., more negative NEE values) during both the wet and dry seasons, when compared to Carbon Tracker and FluxCom-X. It is worth noting that the carbon sink overestimation was smaller for the JULES run with spatialized parameters. The JULES run with spatialized vegetation parameters reveals spatial structures in the NEE fluxes, such as the less intense carbon sink observed in the far western Amazonian region (Acre state). Although direct carbon flux measurements are unavailable for this region, optimized Carbon Tracker estimates suggest a less intense carbon sink or even a carbon source (NEE > 0) during the wet season (Figure 7). ~~There are no carbon flux measurements in this region to be used as ground truth, but the optimized Carbon Tracker estimates also indicate less intense carbon sink in this area, or even a carbon source (NEE>0) in the wet season (Figure 7).~~ Another spatial pattern revealed in the JULES ~~simulation with~~ spatialized ~~vegetation parameters~~ was a reduced carbon sink in northern Amazonia (Amapa state and northern Para state), where the Carbon Tracker and the FluxCom-X datasets also detected reduced carbon sinks or even carbon sources.

The regions of Acre and Amapa demonstrated a high carbon source. What these regions have in common ~~are~~ is canopy heights above ~~the average~~average, with trees reaching above 35 m in Amapa (Figure 1). Compared to FluxCom-X, JULES simulated a stronger carbon sink across the Brazilian Amazon biome during both the wet and dry months, except in forests located in the states of Amapa and Acre (Figure 7). This feature was also observed in the ~~average~~ JULES run using average vegetation parameters for Amazonia ~~version and can be attributed to a modification of the tupp parameter in the BET-TR (43 °C)~~. The increased carbon sink simulated by JULES was driven by greater GPP estimates. The updated parametrization of tupp and f0 may explain the higher GPP values estimated by JULES. In this study, the tupp parameter ranged between 36 and 45 °C (Figure 4), while in previous studies using JULES version 2.1, tupp was set as 36 °C (Restrepo-Coupe et al., 2017). Greater tupp values softened the temperature controls of photosynthesis, resulting in higher GPP estimates, especially in the dry season. ~~Restrepo-Coupe et al. (2017) simulated a reduction of GPP during the dry season, however the version used in this study was 2.1, based on the parameterization of Clark et al. (2011), which considered a tupp of 36 °C in comparison with our study that utilized a tupp between 36 and 45°C as a limit in the calibration procedure.~~ Another factor that may have contributed to GPP increases in JULES simulations is the higher f0 values in calibrated regions such as ATTO (0.95) and K34 (0.93), compared to the default value of 0.875 (Harper et al., 2016). ~~Also, another relevant aspect that may have induced the GPP increases in JULES's simulations was the higher values of f0 observed in some regions calibrated in this study, such as ATTO and K34~~

~~(0.95 and 0.93, respectively), in comparison with the default value determined by Harper et al (2016) (0.875).~~ The modification of f0 led to a reduction in water stress, mainly in ~~areas of the Amazon associated with the Amazon basin and~~ the northern region of the State of Mato Grosso. Moreover, f0 may also help explain the simulated carbon source in the states of Amapá and Acre, as the calibration procedure indicated an f0 value near 0.7 in regions with more sparsely spaced trees (LAI <4.0), which can contribute to an increase of Reco, as shown in Figure 3.

Although JULES simulations overestimated ~~highly increase~~ the carbon sink, they showed a similar seasonal trend compared to the Carbon Tracker estimates, with an increase in magnitude of the carbon sink from April to September. The states of Acre and Amapa showed similar patterns to Carbon Tracker, both representing a reduced carbon sink in ~~this~~ these areas (less than 50 g C m^{-2} $month^{-1}$) (Figure 7). This similarity can be explained by the effects of the spatialization of JULES parameters, mainly in regions with tall trees, such as the case of forests of Amapa and Acre. In the wet month, Carbon Tracker indicated a broader carbon source across the Amazon compared to FluxCom-X, which showed sources mainly in April in Amapa, parts of the Amazon basin, Acre, and deforested areas of Roraima (Figure 7). ~~During the wet month, Carbon Tracker showed a larger carbon source area across the Amazon biome compared to FluxCom-X, which represented a carbon source mainly in April in Amapá, in some regions of Amazon basin, the state of Acre, and the deforested areas of Roraima. (Figure 7).~~ During September, Carbon Tracker was similar to FluxCom-X in representing a carbon sink across most of the Brazilian Amazon biome. However, FluxCom-X showed a carbon source in the arc of deforestation, which was not indicated by either JULES or Carbon Tracker. ~~Another important aspect was that the spatialized JULES model leads to a weaker sink of carbon in NEE in comparison to the default and mean versions (Figure 7).~~

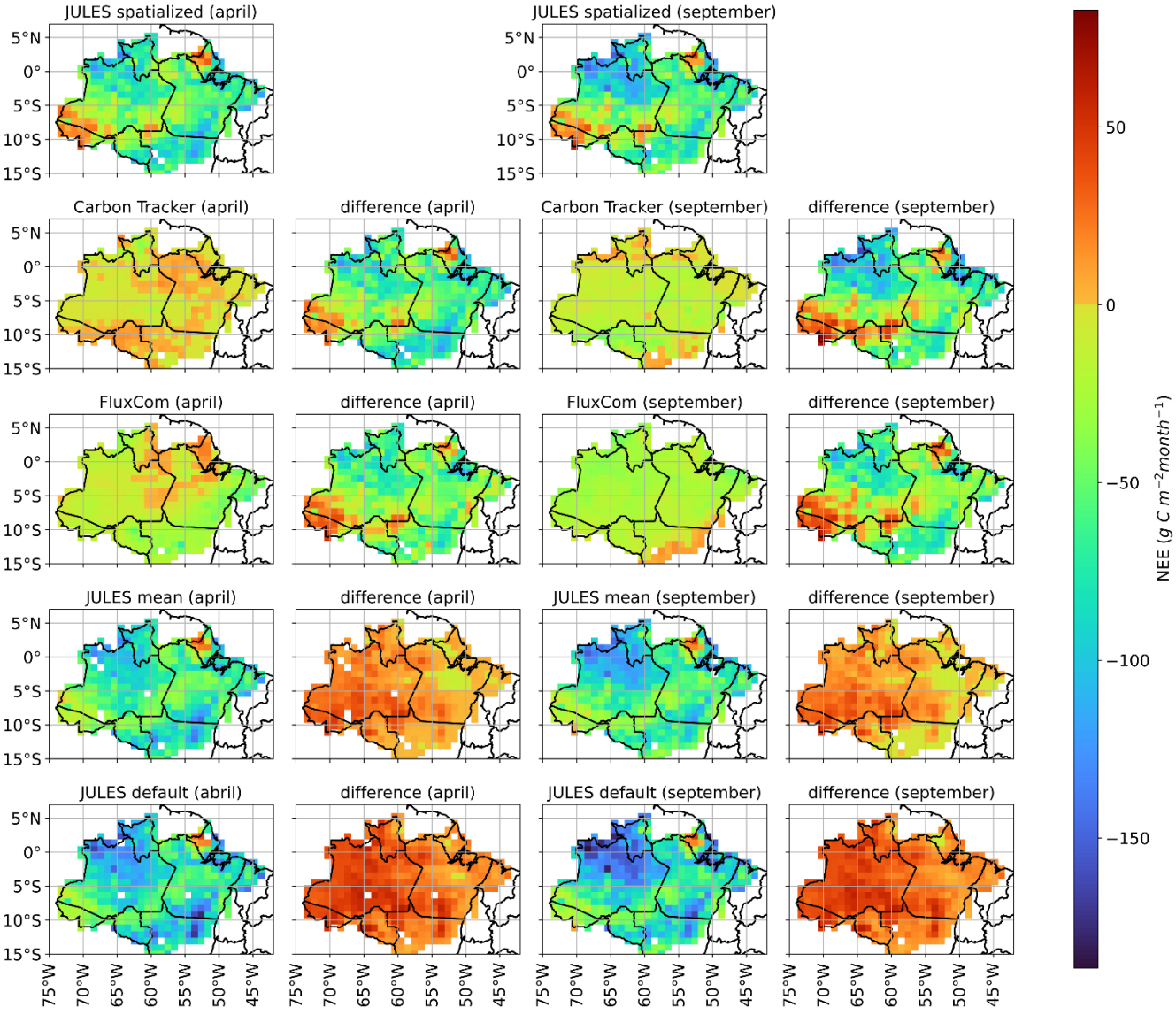

660 **Figure 7: Comparison of NEE fluxes for April (wet season) and September (dry season) of 2021 using different modeling approaches: JULES model with spatialized vegetation parameters (spatialized JULES); European Carbon Tracker, FluxCom-X, JULES model using the spatially constant mean values of optimized vegetation parameters (mean JULES), and JULES model using default vegetation parameter values (default JULES). Differences between spatialized JULES and the other estimates are also presented. Positive and negative differences indicate a stronger carbon source or sink, respectively.**

665

After applying the spatialization procedure and comparing with different models, the JULES model was run for the entire year ~~of~~ 2021. Monthly accumulated NEE values were summed up from each 1º x 1º pixel to estimate NEE for the

Brazilian Amazon biome, resulting in -1.34 Pg C year $^{-1}$. It is important to mention that this value represents the sum of different regions within the Amazon biome (Figure 8). The one-year accumulation revealed that the most concentrated carbon sources are located in the states of Amapa and Acre, with values exceeding 0.75 Kg C m^{-2} ~~year $^{-1}$~~year^{-1} of carbon released to the atmosphere. Some regions stood out as strong carbon sinks (below -1.0 Kg C m^{-2} ~~year $^{-1}$~~year^{-1}), such as the forest in the north of the State of Mato Grosso (longitude 53ºW and latitude 12ºS) and the forest of São Gabriel da Cachoeira (longitude 74ºW and latitude 0º N). The forests in the Amazon basin also demonstrated a high carbon sink (-0.25 to 1.0 Kg C m^{-2} year $^{-1}$) during 2021.

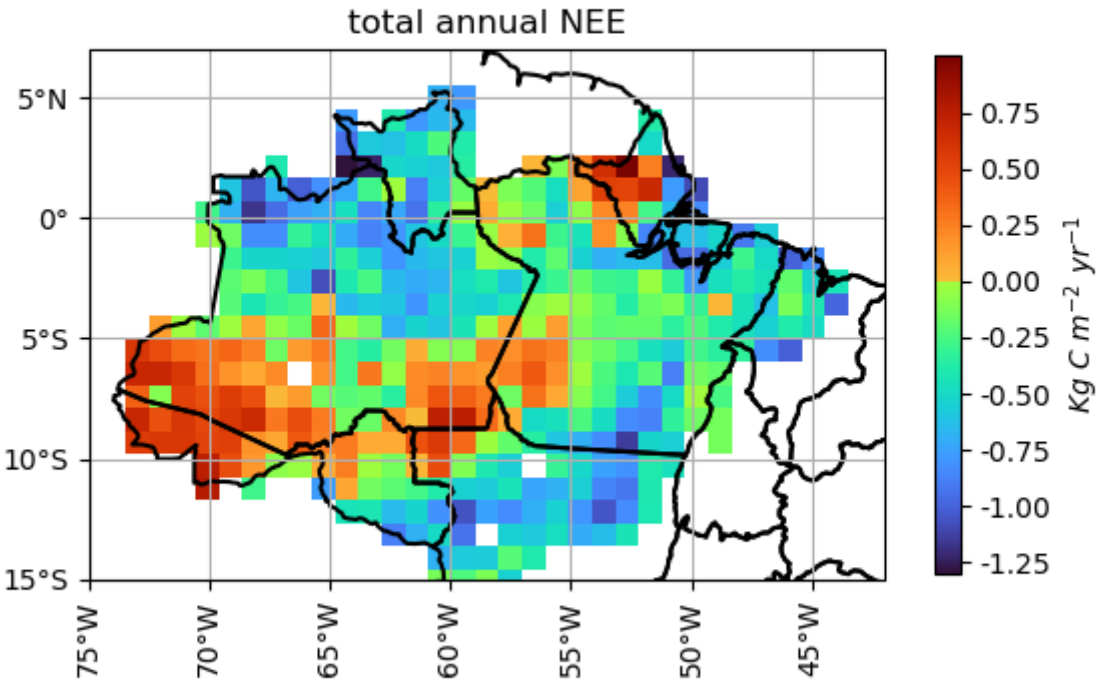

Figure 8: NEE accumulated in Kg C m^{-2} during 2021 in the Brazilian Amazon biome in the spatialized JULES model.

4. Discussion

This section will discuss some relevant results demonstrated in this study. The first aspect is related to the new parametrization of the JULES model in four different sites of the Brazilian Amazon biome, taking into account the adjustment of the most sensitive parameters of JULES. The Nelder-Mead method optimized~~was able to optimize~~ the JULES model, and the resulting~~new set of~~ parameters w~~ere~~as ~~spatialized~~applied to develop a method of spatialization u~~stiliz~~ing linear regressions ~~with the dependent variable as canopy height or LAI and independent variable the most sensitive parameters adjusted in the calibration procedure~~. ~~-~~The second aspect of the discussion is related to the NEE ~~estimative~~ estimation utilizing the JULES spatialized. In this aspect, JULES spatialized demonstrated a carbon sink of -1.34 Pg C m^{-2} in the year ~~of~~ 2021, showing~~being demonstrated~~ a strong carbon source in the states of Acre and Amapa, regions characterized by specific climatic and ~~vegetations~~ vegetation characteristics, respectively.

4.1. JULES optimization

The optimization of JULES for four parameters at the four flux tower sites in this study showed convergence in their values, consistent with the findings of Clark et al. (2011) for tupp value (36 ºC) for Santarém and Jarú, and the f0 value for Jarú (0.875). Additionally, the f0 value calibrated for Santarém in this study was close to that reported by Raoult et al. (2016), which was 0.765. The tupp values for ATTO and K34 were similar to those reported by Harper et al. (2016), who increased tupp to 43 ºC for tropical forests. The parameter fd was similar to the value reported by Harper et al. (2016) for ATTO and K34, however, it was lower than 0.01 for Santarém and Jarú, with values of 0.0066 and 0.007, respectively. The alpha parameter was lower than that in all previous JULES calibration studies for each of the towers. However, the results of this study for alpha parameter are in line with the values near 0.05 and 0.06 mol PAR mol CO_2^{-1} reported by Skillman~~n~~ (2008), who analyzed different types of C_3 plants, including Broadleaf Evergreen Trees. This could be explained by the way that the default version overestimated GPP in comparison to the calibrated version (Figure 4).

The cross-validation procedure also showed that the alpha parameter did not show a linear relationship with canopy height or LAI (Figure S13~~4.2~~). This may be explained by the fact that the values for each tower were nearly constant, with a difference of only 0.0018 mol PAR mol CO_2^{-1}, ~~-~~while the other parameters exhibited greater variability between sites. In practical terms, the spatialization of the alpha parameter was almost the same as using its mean value all over the study area. The spatialized JULES also showed lower RMSE for NEE compared to the VPRM model in every tower approached in this study, including the validation tower. This can be explained by the greater complexity of how JULES estimates GPP and, particularly, Reco. VPRM uses a simpler approach, relying on a linear regression in which air temperature is the sole independent variable (Gourdji et al., 2022). In contrast, JULES estimates GPP and Reco with more sophisticated equations that account for factors such as water stress, nitrogen content in different plant components (Best et al., 2011; Clark et al., 2011), photosynthesis light saturation (equation 3), and CO_2 leaf concentration (equation 5). The optimization of the parameters

alpha, tupp, f0, and fd ~~explain~~ explain the improvement in the performance compared to the default version and to the VPRM model.

4.2. NEE estimates using JULES spatialized

The first relevant aspect that spatialized JULES was able to reproduce was the increase of GPP during the dry season, showing that water may not be a limitation for carbon assimilation in the Amazonian dry season (~~Figure~~ Figures 3 and ~~Figure~~ 6). Restrepo-Coupe et al. (2013) also observed the same feature by comparing different Eddy-covariance towers spread in the Brazilian Amazon biome. One potential improvement to this methodology would be to consider parameters, primarily the leaf area index (LAI), which varies throughout the seasonal cycle. This is because the photosynthetic capacity of the canopy and leaf phenology are among the main seasonal drivers in this region (Restrepo-Coupe et al., 2013). Using different parameterizations throughout the year would provide a more accurate description of the effect of leaf phenology in different zones and seasons to cover the heterogeneity of trees. This is particularly important for the emergence of leaves, which open their stomata more frequently for photosynthesis than older leaves approaching senescence (Wu et al., 2016). The absence of phenology representation in some process-based models was noted by Restrepo-Coupe et al. (2017) and Botia et al. (2022), who observed a tendency for these models to underestimate GPP during the dry season. In contrast, the spatialization method used in this study, incorporating varying parameters based on LAI and canopy height, improved the model's ability to simulate GPP and Reco with greater diversity (Figure 6).

The spatialized JULES generated values of NEE between 0.75 and -1.25 Kg C m^{-2} $year^{-1}$. This range includes the mean value reported by Lian et al. (2023), which estimated an average value of NEE in the South ~~America~~ American Forest of -0.205 Kg C m^{-2} $year^{-1}$ using a ~~Random~~ Random Forest Model applied in a global system. The spatialized JULES also demonstrated that the major focus of carbon sources was located in the states of Amapa and Acre (Figure 7). The forest of Amapa has tall trees (> 35 m) and a low leaf area index (< 4.5 m^2 m^{-2}), considering that this region has the major above-ground biomass of the Amazon biome, reaching 518 Mg ha^{-1} (Ometto et al., 2023). The spatialization reduced the tupp and f0, which may lead to a reduction in GPP in relation to Reco, generating a carbon source in this region. A possible explanation is increased Reco in mature and tall forests, such as those found in the Amapa region. West (2020) observed in a review of studies with different tree species that the costs of respiration increase over the years while GPP remains constant, which could explain the net carbon source. The costs are based on adjustments in morphology and anatomy to construct new structures in the xylem, roots, and leaves to support the high amount of biomass. Concerning the state of Acre, there is a climatic condition that can explain the carbon source in this region, since annual rainfall is lower than 2000 mm (Silva et al., 2020), which can ~~, which can increase~~ increase the cost of maintenance and hence the respiration to avoid hydric stress. It is important to have Eddy-covariance measurements in this region~~,~~ to confirm the trend of the carbon source.

The total NEE estimated for the Brazilian Amazon biome demonstrated a carbon sink (NEE) ~~of~~ of -1.34 Pg C $year^{-1}$. The result obtained in this study fall~~s~~is between estimates~~the results obtained~~ by Chen et al. (2024), who reported~~hich~~

annual~~estimated the~~ NEE for~~in~~ the Amazon of~~region~~ -0.94 (~~using the~~ Trendy-v11 model~~)~~) ~~(-0.94 Pg C year^{-1})~~ and -3.46 Pg C year^{-1} (FluxCom-RS model) ~~(-3.46 Pg C year^{-1}) model~~for~~s on an annual basis between~~ 2001-2015. It is important to mention that the FluxCom version utilized to analyze the NEE across the Brazilian Amazon biome (Figure 7) is a new version with the X-BASE database (Nelson et al., 2024) in comparison to the FluxCom-RS utilized by Chen et al. (2024). The new version of FluxCom reduced the global NEE in relation to FluxCom-RS (-21 to -7 Pg C year^{-1}). Trendy v-11 is a dataset that provides global gridded carbon fluxes data from 16 different types of vegetation dynamics models (Sitch et al., 2024). Our result was closer to Trendy than to the FluxCom-RS, which can be favorable considering the uncertainties in the NEE partitioning in FluxCom-RS, with the Reco partitioned by the NEE instead of subtracting GPP to get NEE (Jung et al., 2020). Due to this reason, FluxCom-RS underestimated Reco and tends to estimate a higher carbon sink. JULES is included in Trendy v-11, however, the version utilized to simulate carbon fluxes was JULES 5.1 (Wiltshire et al., 2021). In this version, JULES has only five Plant Function Types, and the version we utilized to simulate carbon flux is v7.0. In this version, we use the parametrization specific ~~for~~ to Tropical Evergreen Broadleaf trees (Harper et al., 2016). One parameter modified in this version was tupp (~~36°C~~ 36 °C in Clark et al 2011 to 43°C in Harper et al., 2016). This could be a reason that the carbon sink in the Brazilian Amazon biome is larger than the JULES version in Trendy v-11, because this parameter is relevant for GPP. Due to this aspect~~reason~~, in section S.5 of the Supplementary material, we compared the default JULES, the spatialized version, and the Trendy v-11 configuration based on Clark et al. (2011). It was possible to observe that Harper et al. (2016) tend to overestimate the carbon sink, while the spatialized version aligns with ATTO observations for 2018 (Figure S17).~~with the spatialized version and the version utilized in Trendy v-11 based on Clark et al 2011 parametrization which demonstrates that the Harper et al., (2016) version tends to overestimate the carbon sink while the spatialized JULES version agrees with observed data in ATTO tower for 2018 (see Supplementary material, Figure S5.1).~~

In comparison with the annual value obtained by the mean and default versions of JULES (Harper et al., 2016), the default version obtained a carbon sink of -3.08 Pg C per year (see s~~S~~upplementary m~~M~~aterial, Figure S18~~5.2~~), while the mean version obtained a carbon sink of -2.06 Pg C per year (see s~~S~~upplementary m~~M~~aterial, Figure S19~~5.3~~). The default version of JULES presented a value similar to that obtained by FluxCom-RS (-3.46 Pg C per year). This can~~,~~ demonstrate~~ting~~ that the calibration procedure adopted in this study improved the carbon simulations by JULES despite the lack of FluxCom-RS equations to simulate Reco. Another piece of evidence demonstrating the improvements made by the calibration procedure is that the mean value of the optimi~~z~~ed parameters reduced the carbon sink in the Brazilian Amazon biome by 33.12% compared to the default value. The spatialised version of JULES reduced the carbon sink of the Brazilian Amazon biome by 56.49% compared to the default version. Also, reduced ~~and~~ by 34.96% in ~~compar~~comparison~~ed~~ to the mean version, reaching a value closest to that provided by Trendy-v11 (-0.94 Pg C year^{-1}) by Chen et al. (2024). This reduction in the carbon sink can mainly be explained by the regions of Acre, as shown in Figures S~~5~~18~~.2~~ and S~~5~~19~~.3~~ for the default and mean versions, respectively. This can be considered the effect of the method of spatiali~~z~~sing the sensitivity parameters f0 and fd, which are directly related to water stress (Clark et al., 2011), as characterised in this region. The same aspect can explain why the spatialised version of JULES demonstrated a high carbon source in the south of the Amazonian state (>0.50 kg C m^{-2} year^{-1}), which the default and

mean parametrizations did not capture (between 0 and 0.25 kg C m^{-2} $year^{-1}$). However, it is worth noting that the state of Amapá demonstrates a carbon source in all three versions of JULES, reaching 0.75 kg C m^{-2} $year^{-1}$. This suggests that the height of the tree canopy in this region contributes to the carbon source.

The result of -1.34 Pg C $year^{-1}$ was a stronger sink than found by other studies related to the Amazon region, as Botia et al (2024) (-0.33 Pg C $year^{-1}$) and Rosan et al. (2024) (-0.34 Pg C $year^{-1}$), however, some aspects need to be considered. The first aspect is related to the number of years evaluated in these studies in relation to our study. We have just evaluated the year 2021 instead of other studies that evaluated more than ten years, as the case of Chen et al. (2024), and nine years, as the case Botia et al. (2024). In order to assess uncertainties and the importance of interannual variability in NEE, future studies could perform simulations for additional years, using the spatialization of parameters developed here. The second aspect is that the carbon flux obtained by Botia et al. (2024) (Net Land Flux) is the sum ~~between~~ of river fluxes and NEE.~~;~~ ~~I~~n our simulation, we have just the NEE obtained by vegetation, similar ~~than~~ to the paper by Chen et al. (2024), which generated a NEE of -0.94 Pg C $year^{-1}$ using the Trendy-v11 and 3.46 Pg C $year^{-1}$ using the FluxCom-RS. The third aspect is related to the fire emissions that can contribute to reducing the carbon sink~~,~~; this value can vary from 0.09 Pg C $year^{-1}$ (Rosan et al., 2024) to 0.41 Pg C $year^{-1}$ (Gatti et al., 2021).

Another factor contributing to discrepancies among models is that some process-based models tend to overestimate the carbon sink in tropical forests, as reported by Restrepo-Coupe et al. (2017) and Botia et al. (2022). The distance between models particularly occurs when compared with process-based and inversion models, such as Carbon Tracker. ~~Another important aspect to be mentioned and that can contribute to this distance between other models is that some process-based models can overestimate the carbon sink in tropical forests, as previously related by Restrepo-Coupe et al., (2017) and also by Botia et al. (2022) mainly when compared with inversion models such as Carbon Tracker.~~ The reason can be explained by the incorrect assumption of water limitation and the lack of leaf phenology in model formulations (Gonçalves et al., 2020). Also, JULES demonstrated a higher sink in other types of vegetation presented in the Amazon biome as C4 grass (Harper et al., 2016) and C3 crops (Williams et al., 2017; Prudente Junior et al., 2022), in regions such as the states of Mato Grosso, Roraima, and east of Pará (Figure 8). In a region predominantly composed ~~by~~ of C4 grass (longitude 49.5°W, latitude 7.5°S), with 84.5 % of C4 grass (see supplementary material, Figure S3~~.1.1~~), JULES simulated a carbon sink of -250 g C m^{-2} $year^{-1}$ (Figure 8). ~~This~~ The~~value of~~ carbon sink value is stronger (more negative) than that reported by Bezerra et al.~~,~~ (2022), ~~which~~ who obtained an annual NEE of -215 g C m^{-2} $year^{-1}$ at an~~in~~ -Eddy-Covariance tower in ~~a NEE annual mean of -215 g C m^{-2} $year^{-1}$ in the~~ Brazil~~ian~~ Northeast, working with *Urochloa brizantha* cv Marandu, the main~~he most relevant~~ pasture ~~used~~ in the arc of deforestation. This indicates that tropical grassland can be considered a carbon sink mainly in regions with a latitude near ~~15°~~ 15 ° S to 0°, with similar radiation levels during different seasons of the year. However, it is important to point out that the improvement of grassland parameterization is out of the scope of the current study. One step that can improve the ~~estimat~~estimation~~e~~ of NEE in the arc of deforestation is the calibration and evaluation ~~in~~ of ~~agricultural~~ crops, which can reduce the carbon sink in the regions of Mato Grosso and Roraima. Another area for improvement in future studies would be

to use other canopy height databases, such as those based on airborne ~~lidat~~ lidar observations, to improve the spatializsation of plant physiological parameters

The spatialized JULES demonstrated a stronger carbon sink in comparison to FluxCom-X and the European Carbon Tracker in the Amazon basin, deforestation arc, and North of Mato Grosso, although it estimated a higher carbon source in the states of Acre and Amapá. However, the new optimization and the spatialization approach showed improvements over the version used by Harper et al. (2016), which applied ~~averaged~~average optimized parameters. Studies on spatializing carbon fluxes in the Amazon using process-based models are scarce; however, Zhu et al. (2025) reported similar sensitivities in ORCHIDEE model parameters. The similarities were related to light and nitrogen limitations and highlighted flux heterogeneity when accounting for vegetation differences. Despite some similar conclusions, the methodologies differed substantially. ~~. Studies regarding the spatialization carbon fluxes in the Amazon Forest utilizing process-based model are rare, however, Zhu et al., (2025) demonstrated some similarities with our work in the sensitive parameters in ORCHIDEE model, regarding to light and nitrogen limitation for photosynthesis and to demonstrate the heterogeneity of carbon fluxes when utilize a spatialization method taking into account the vegetation differences in a tropical forest, Although, these two studies reached the same conclusion, the methodologies employed were very different.~~ Our study uses Eddy-covariance towers and a statistical model to spatialize carbon fluxes based on sensitive, calibrated parameters and vegetation properties. By contrast, Zhu et al.'s (2025) study uses satellite observations of tree aboveground biomass and gross primary production (GPP) at a very different spatial scale. In addition to reducing the estimated carbon sink, it also highlighted the influence of vegetation heterogeneity on the spatial distribution of carbon budget across the Amazon biome, particularly in the states of Amapá and Acre.

5. Conclusions

This study presented a new method to estimate NEE from an optimized~~adjusted~~ land surface model, with parameters spatialized using two ~~relevant~~ vegetation properties: Canopy height and LAI. The first aspect presented in this study was to demonstrate the most sensitive parameters for NEE, which were canht, tupp, alpha, f0, and fd. The optimization of selected JULES parameters for the PFT BET-TR led to a reduction in both RMSE and the d-index across all four analyzed towers, when compared to the default parameter values and the VPRM model. Our ~~r attempt of~~ spatialization attempt was validated in an independent tower, resulting in ~~generating~~ a better performance compared to~~than~~ VPRM and to the default version of JULES. In general, the spatialized JULES model showed a stronger carbon sink in the northern Amazon region and across the Amazon basin compared to FluxCom-X and Carbon Tracker, particularly during the dry season. T~~However, t~~he spatialized version of JULES also indicated significant carbon source regions (> 75 g C m^{-2} $month^{-1}$) in Amapá and Acre. This highlights the importance of considering how forests with tall canopy height (>35m), such as those in Amapá, and the influence of climate conditions, as observed in Acre, contribute to the overall carbon budget. The spatialized JULES resulted in a NEE estimate of -1.34 Pg C in~~during~~ 2021, which is a value that approaches those of dynamic vegetation models for the Amazon biome.

Despite the advances presented in this study, some aspects still need more robust explanations. One ~~of these aspects~~ is related to the strong carbon source in the regions of Amapá and Acre, simulated by JULES in 2021. F~~However, the JULES spatialized simulation in 2021 gave~~ urther investigation of the carbon balance in these regions is needed~~a relevant aspect to better investigate the carbon balance in these regions~~. It is important to note that this study developed an optimization of JULES using a limited number of Eddy-covariance towers. While this approach improved model simulations, further improvements could be achieved by installing additional towers in different forest types across the Amazon region, especially in regions with tall canopy heights (> 35 m). Another aspect that could be improved is the simulation of regions dominated by agricultural land uses, such as soybean, maize, and pasture. These areas, particularly in northern Mato Grosso, are relevant because the model currently simulates them as carbon sinks. Despite the development of JULES-crop, this model is not coupled in the most recent version of JULES, a feature that could improve simulations in agricultural zones. Additionally, calibration and evaluation using Eddy-covariance towers in croplands and pastures could improve model performance in the deforestation arc. Despite these limitations, this study highlights the relevance of spatializing NEE using vegetation indices, demonstrating how this approach can improve the estimation of carbon fluxes in the Brazilian Amazon biome by identifying source and sink regions in relation to forest height and density.

Funding Information

Funding sources include the support of the RCGI – Research Centre for Greenhouse Gas Innovation hosted by the University of São Paulo and sponsored by FAPESP – São Paulo Research Foundation (process number 2020/15230-5). FAPESP also funds the projects 2023/06623-1, 2022/07974-0, 2023/04358-9 and 2024/12950-8. Also, the CNPq - National Council for Scientific and Technological Development, to fund the project 304819/2022-0.

Data and code availability

The dataset covering all simulations described in this report is available at this link:http://ftp.lfa.if.usp.br/ftp/public/LFA_Processed_Data/articles_database/Prudente_2025/.

Author contributions

ACPJ wrote the initial manuscript and ran the JULES model for the Brazilian Amazon biome. ACPJ, together with LATM, LVR, SB, and FSS, designed the methodology. DSM assisted in adapting JULES for the Amazon region. LPC ran VPRM model for different sites across the Brazilian Amazon biome. CQDJ provided meteorological data measured in the ATTO tower. LATM, LVR, PEAN, TA and EF provided Amanan's computers to run JULES. LATM, CP, SB and PEAN consolidated funding for the postdoctoral position and an exchange period at the Max Planck Institute for Biogeochemistry in Jena. LATM, LVR, XX, SB helped with the data curation and the interpretation of the results. IMCT helped to improve observed carbon fluxes at different sites in the Amazon region. FSS contributed to developing scripts to run JULES and to designed figures presented in the manuscript. LATM, LVRM, XX, SB, FSS, EF, CQDJ and IVCT contributed to review the manuscript.

Competing interests

The authors declare that they have no conflict to interest.

Acknowledgment

The authors acknowledge the use of the Amanan's Clusters, a collaborative facility supplied under the Institute of Astronomy, Geophysics and Atmosphere Science of the University of São Paulo. Also, the Max Planck Institute of Biogeochemistry for the ATTO towers data availability and the São Paulo Research Foundation to fund the project 2023/06623-1.

References

Aguirre-Gutiérrez, J., Rifai, S. W., Deng, X., Ter Steege, H., Thomson, E., Corral-Rivas, J. J., ... & Malhi, Y.: Canopy functional trait variation across Earth's tropical forests. Nature, 1-8.https://doi.org/10.5281/zenodo.14509493, 2025.

Andreae, M. O., Acevedo, O. C., Araùjo, A., Artaxo, P., Barbosa, C. G. G., Barbosa, H. M. J., Brito, J., Carbone, S., Chi, X., Cintra, B. B. L., da Silva, N. F., Dias, N. L., Dias-Júnior, C. Q., Ditas, F., Ditz, R., Godoi, A. F. L., Godoi, R. H. M., Heimann, M., Hoffmann, T., Kesselmeier, J., Könemann, T., Krüger, M. L., Lavric, J. V., Manzi, A. O., Lopes, A. P., Martins, D. L., Mikhailov, E. F., Moran-Zuloaga, D., Nelson, B. W., Nölscher, A. C., Santos Nogueira, D., Piedade, M. T. F., Pöhlker, C., Pöschl, U., Quesada, C. A., Rizzo, L. V., Ro, C.-U., Ruckteschler, N., Sá, L. D. A., de Oliveira Sá, M., Sales, C. B., dos Santos, R. M. N., Saturno, J., Schöngart, J., Sörgel, M., de Souza, C. M., de Souza, R. A. F., Su, H., Targhetta, N., Tóta, J., Trebs, I., Trumbore, S., van Eijck, A., Walter, D., Wang, Z., Weber, B., Williams, J., Winderlich, J., Wittmann, F., Wolff, S., and Yáñez-Serrano, A. M.: The Amazon Tall Tower Observatory (ATTO): overview of pilot measurements on ecosystem ecology, meteorology, trace gases, and aerosols. Atmospheric Chemistry and Physics, 15(18), 10723-10776. https://doi.org/10.5194/acp-15-10723-2015, 2015.

Best, M. J., Pryor, M., Clark, D. B., Rooney, G. G., Essery, R. L. H., Ménard, C. B., Edwards, J. M., Hendry, M. A., Porson, A., Gedney, N., Mercado, L. M., Sitch, S., Blyth, E., Boucher, O., Cox, P. M., Grimmond, C. S. B., and Harding, R. J. (2011). The Joint UK Land Environment Simulator (JULES), model description–Part 1: Energy and water fluxes. Geoscientific Model Development, 4(1), 677–699. https://doi.org/10.5194/gmd-4-677-2011, 2011.

Bezerra, B. G., e Silva, C. M. S., Mendes, K. R., Mutti, P. R., Fernandes, L. S., Marques, T. V., and Lucio, P. S.: CO2 exchanges and evapotranspiration of a grazed pasture under tropical climate conditions. Agricultural and Forest Meteorology, 323, 109088. https://doi.org/10.1016/j.agrformet.2022.109088, 2022.

Botía, S., Komiya, S., Marshall, J., Koch, T., Gałkowski, M., Lavric, J., and Gerbig, C.: The CO2 record at the Amazon Tall Tower Observatory: A new opportunity to study processes on seasonal and inter-annual scales. Global Change Biology, 28(2), 588-611. https://doi.org/10.1111/gcb.15905, 2022.

Botía, S., Munassar, S., Koch, T., Custodio, D., Basso, L. S., Komiya, S., and Gerbig, C.: Combined CO 2 measurement record indicates decreased Amazon forest carbon uptake, offset by Savannah carbon release. EGUsphere, 2024, 1-55. https://doi.org/10.5194/egusphere-2024-1735, 2024.

Boussetta, S., Balsamo, G., Beljaars, A., Kral, T., and Jarlan, L.: Impact of a satellite-derived leaf area index monthly climatology in a global numerical weather prediction model. International journal of remote sensing, 34(9-10), 3520-3542. https://doi.org/10.1080/01431161.2012.716543, 2013.

Brienen, R. J., Phillips, O. L., Feldpausch, T. R., Gloor, E., Baker, T. R., Lloyd, J., .Lopes-Gonzalez, G., Monteagudo-Mendoza, A., Malhi, Y., Lewis, L.S., Vasques Martinez, R., Alexiades, M., Alvarez Davila, E., Alvares Loyaza, P., Andrade, A., Aragão, L.E.O.C., Muramaki, A.A., Arets, E.J.M.M., Arroyo, L., Aymard, C.G.A., Banki, O.S., Baraloto, C., Barroso, J., Donal, D., Zagt, R. J. (2015). Long-term decline of the Amazon carbon sink. *Nature*, *519*(7543), 344-348. https://doi.org/10.1038/nature14283, 2015.

Caen, A., Smallman, T. L., de Castro, A. A., Robertson, E., von Randow, C., Cardoso, M., and Williams, M.: Evaluating two land surface models for Brazil using a full carbon cycle benchmark with uncertainties. Climate Resilience and Sustainability, 1(1), e10. https://doi.org/10.1002/cli2.10, 2022.

Chandrasekar, K., Sesha Sai, M. V. R., Roy, P. S., and Dwevedi, R. S.: Land Surface Water Index (LSWI) response to rainfall and NDVI using the MODIS Vegetation Index product. International Journal of Remote Sensing, 31(15), 3987-4005. https://doi.org/10.1080/01431160802575653, 2010.

Chen, B., Xu, X., Wang, S., Yang, T., Liu, Z., and Falk, S.: Carbon dioxide fertilization enhanced carbon sink offset by climate change and land use in Amazonia on a centennial scale. Science of The Total Environment, 955, 176903. https://doi.org/10.1016/j.scitotenv.2024.176903, 2024.

Clark, D. B., Mercado, L. M., Sitch, S., Jones, C. D., Gedney, N., Best, M. J., Pryor, M., Rooney, G. G., Essery, R. L. H., Blyth, E., Boucher, O., Harding, R. J., Huntingford, C., and Cox, P. M.: The Joint UK Land Environment Simulator (JULES), model description – Part 2: Carbon fluxes and vegetation dynamics, Geosci. Model Dev., 4, 701–722, https://doi.org/10.5194/gmd-4-701-2011, 2011.

Collatz, G. J., Ball, J. T., Grivet, C., & Berry, J. A.: Physiological and environmental regulation of stomatal conductance, photosynthesis and transpiration: a model that includes a laminar boundary layer. Agricultural and Forest meteorology, 54(2-4), 107-136. https://doi.org/10.1016/0168-1923(91)90002-8, (1991)

Collatz, G. J., Ribas-Carbo, M., & Berry, J. A. (1992). Coupled photosynthesis-stomatal conductance model for leaves of C4 plants. Functional Plant Biology, 19(5), 519-538. https://doi.org/10.1071/PP9920519

Dakhlaoui, H. (2014). Vers une procédure de calage automatique plus efficiente du modèle HBV (Doctoral dissertation, Thèse de Doctorat en Génie Hydraulique. Université de Tunis El Manar).

De Lima Filho, R. R. (2021). Produtor de soja deve ter um bom lucro na safra 2021/22. AgroANALYSIS, 41(9), 15-17.

Fernandes, L. D. O., Reis, R. D. A., Paes, J. M. V., Teixeira, R. M. A., Queiroz, D. S., Paschoal, J. J., and PASCHOAL, J. J.: Desempenho de bovinos da raça Gir em pastagem de Brachiaria brizantha submetidos a diferentes manejos. Revista Brasileira de Saúde e Produção Animal, 16(1), 36-46. https://doi.org/10.1590/S1519-99402015000100004, 2015.

Friedlingstein, P., O'Sullivan, M., Jones, M. W., Andrew, R. M., Gregor, L., Hauck, J., Le Quéré, C., Luijkx, I. T., Olsen, A., Peters, G. P., Peters, W., Pongratz, J., Schwingshackl, C., Sitch, S., Canadell, J. G., Ciais, P., Jackson, R. B., Alin, S. R., Alkama, R., Arneth, A., Arora, V. K., Bates, N. R., Becker, M., Bellouin, N., Bittig, H. C., Bopp, L., Chevallier, F., Chini, L. P., Cronin, M., Evans, W., Falk, S., Feely, R. A., Gasser, T., Gehlen, M., Gkritzalis, T., Gloege, L., Grassi, G., Gruber, N., Gürses, Ö., Harris, I., Hefner, M., Houghton, R. A., Hurtt, G. C., Iida, Y., Ilyina, T., Jain, A. K., Jersild, A., Kadono, K., Kato, E., Kennedy, D., Klein Goldewijk, K., Knauer, J., Korsbakken, J. I., Landschützer, P., Lefèvre, N., Lindsay, K., Liu, J., Liu, Z., Marland, G., Mayot, N., McGrath, M. J., Metzl, N., Monacci, N. M., Munro, D. R., Nakaoka, S.-I., Niwa, Y., O'Brien, K., Ono, T., Palmer, P. I., Pan, N., Pierrot, D., Pocock, K., Poulter, B., Resplandy, L., Robertson, E., Rödenbeck, C., Rodriguez, C., Rosan, T. M., Schwinger, J., Séférian, R., Shutler, J. D., Skjelvan, I., Steinhoff, T., Sun, Q., Sutton, A. J., Sweeney, C., Takao, S., Tanhua, T., Tans, P. P., Tian, X., Tian, H., Tilbrook, B., Tsujino, H., Tubiello, F., van der Werf, G. R., Walker, A. P., Wanninkhof, R., Whitehead, C., Willstrand Wranne, A., Wright, R., Yuan, W., Yue, C., Yue, X., Zaehle, S., Zeng, J., and Zheng, B.: Global Carbon Budget 2022, Earth Syst. Sci. Data, 14, 4811–4900, https://doi.org/10.5194/essd-14-4811-2022, 2022.

Friend, A. D., Schugart, H. H., & Running, S. W.: A physiology-based gap model of forest dynamics. Ecology, 74, 792-797, **https://doi.org/10.2307/1940806**, 1993.

Gatti, L. V., Basso, L. S., Miller, J. B., Gloor, M., Gatti Domingues, L., Cassol, H. L. G., Tejada, G., Aragão, L. E. O. C., Nobre, C., Peters, W., Marani, L., Arai, E., Sanches, A. H., CorralÃ~~l~~a, S. M., Anderson, L., Von Randow, C., Correia, C. S. C., Crispim, S. P., and Neves, R. A. L.: Amazonia as a carbon source linked to deforestation and climate change, Nature, 595, 388–393, https://doi.org/10.1038/s41586- 021-03629-6, 2021, 2021.

Gatti, L.V., Basso, L.S., Miller, J.B., Gloor, M., Gatti Domingues, L., Cassol, H.L.G., Tejada, G., Aragao, L.E.O.C., Nobre, C., Peters, W., Marani, L., Arai, E., Sanches, A. H., Correa, S.M., Anderson, L., Von Randow, C., Correia, C.S.C., Crispim, S.P., and Neves, R.A.L.: Amazonia as a carbon source linked to deforestation and climate change. Nature 595 (7867). https://doi.org/10.1038/s41586-021-03629-6, 2021.

Gonçalves, N. B., Lopes, A. P., Dalagnol, R., Wu, J., Pinho, D. M., and Nelson, B. W.: Both near-surface and satellite remote sensing con_rm drought legacy e_ect on tropical forest leaf phenology after 2015/2016 ENSO drought. Remote Sensing of Environment, 237, 111489. https://doi.org/10.1016/j.rse.2019.111489, 2020.

Gourdji, S. M., Karion, A., Lopez-Coto, I., Ghosh, S., Mueller, K. L., Zhou, Y., ... and Whetstone, J. R.: A modified Vegetation Photosynthesis and Respiration Model (VPRM) for the eastern USA and Canada, evaluated with comparison to atmospheric observations and other biospheric models. Journal of Geophysical Research: Biogeosciences, 127(1), e2021JG006290. https://doi.org/10.1029/2021JG006290, 2022.

Grubbs, F. E: Procedures for detecting outlying observations in samples. Technometrics, 11(1), 1-21. https://doi.org/10.1080/00401706.1969.10490657, 1969.

Harper, A. B., Cox, P. M., Friedlingstein, P., Wiltshire, A. J., Jones, C. D., Sitch, S., and Bodegom, P. V.: Improved representation of plant functional types and physiology in the Joint UK Land Environment Simulator (JULES v4. 2) using plant trait information. Geoscientific Model Development, 9(7), 2415-2440. https://doi.org/10.5194/gmd-9-2415-2016, 2015.

Harper, A. B., Wiltshire, A. J., Cox, P. M., Friedlingstein, P., Jones, C. D., Mercado, L. M., ... & Duran-Rojas, C. Vegetation distribution and terrestrial carbon cycle in a carbon cycle configuration of JULES4. 6 with new plant functional types. Geoscientific Model Development, 11(7), 2857-2873. https://doi.org/10.5194/gmd-11-2857-2018, 2018.

Harris, C. R., Millman, K. J., Van Der Walt, S. J., Gommers, R., Virtanen, P., Cournapeau, D., and Oliphant, T. E.:Array programming with NumPy. *Nature*, *585*(7825), 357-362, https://doi.org/10.1038/s41586-020-2649-2 , 2020.

Hayek, M. N., Wehr, R., Longo, M., Hutyra, L. R., Wiedemann, K., Munger, J. W., Bonal, D., Saleska, S. R., Fitzjarrald, D. R., and Wofsy, S. C.: A novel correction for biases in forest eddy covariance carbon balance, Agr. Forest Meteorol., 250–251, 90– 101, https://doi.org/10.1016/j.agrformet.2017.12.186, 2018.

Hersbach, H., Bell, B., Berrisford, P., Hirahara, S., Horányi, A., Muñoz-Sabater, J., ... & Thépaut, J. N.: The ERA5 global reanalysis. Quarterly Journal of the Royal Meteorological Society, 146(730), 1999-2049. https://doi.org/10.1002/qj.3803 , 2020.

Jacobson, A. R. et al. CarbonTracker CT2022. https://doi.org/10.25925/z1gj-3254 (2023).

Jérôme, Z. P., Eric, A. A., Ezéchiel, O., Eliézer, B. I., and Ezin, E. C.: An automatic optimization technique for the calibration of a physically based hydrological rainfall-runoff model. Journal of Geoscience and Environment Protection, 9(3), 1-20. https://doi.org/10.4236/gep.2021.93001, 2021.

Jung, M., Schwalm, C., Migliavacca, M., Walther, S., Camps-Valls, G., Koirala, S., Anthoni, P., Besnard, S., Bodesheim, P., Carvalhais, N., Chevallier, F., Gans, F., S Goll, D., Haverd, V., Kohler, ¨ P., Ichii, K., K Jain, A., Liu, J and Lombardozzi, D.. Scaling carbon fluxes from eddy covariance sites to globe: synthesis and evaluation of the FLUXCOM approach. Biogeosciences 17 (5), 1343–1365. https:// doi.org/10.5194/bg-17-1343-2020, 2020.

Khanna, J., & Medvigy, D. Strong control of surface roughness variations on the simulated dry season regional atmospheric response to contemporary deforestation in Rondônia, Brazil. Journal of Geophysical Research: Atmospheres, 119(23), 13-067, 2014. https://doi.org/10.1002/2014JD022278

Li, J., Wang, Y. P., Duan, Q., Lu, X., Pak, B., Wiltshire, A., and Ziehn, T.: Quantification and attribution of errors in the simulated annual gross primary production and latent heat fluxes by two global land surface models. Journal of Advances in Modeling Earth Systems, 8(3), 1270-1288. https://doi.org/10.1002/2015MS000583, 2016.

Li, L., Chen, S., Yang, C., Meng, F., and Sigrimis, N.: Prediction of plant transpiration from environmental parameters and relative leaf area index using the random forest regression algorithm. Journal of Cleaner Production, 261, 121136. https://doi.org/10.1016/j.jclepro.2020.121136, 2020.

Lian, Y., Li, H., Renyang, Q., Liu, L., Dong, J., Liu, X., and Zhang, H.: Mapping the net ecosystem exchange of CO2 of global terrestrial systems. International Journal of Applied Earth Observation and Geoinformation, 116, 103176. https://doi.org/10.1016/j.jag.2022.103176, 2023.

Liu, J., Bowman, K.W., Schimel, D.S., Parazoo, N.C., Jiang, Z., Lee, M., Bloom, A.A., Wunch, D., Frankenberg, C., Sun, Y., O'Dell, C.W., Gurney, K.R., Menemenlis, D., Gierach, M., Crisp, D., and Eldering, A.: Contrasting carbon cycle responses of the tropical continents to the 2015–2016 El Nino. ˜ Science 358 (6360). https://doi.org/ 10.1126/science.aam5690, 2017.

Loague, K., and Green, R. E.: Statistical and graphical methods for evaluating solute transport models: overview and application. Journal of contaminant hydrology, 7(1-2), 51-73. https://doi.org/10.1016/0169-7722(91)90038-3, 1991.

Mahadevan, P., Wofsy, S. C., Matross, D. M., Xiao, X., Dunn, A. L., Lin, J. C., and Gottlieb, E. W. : A satellite-based biosphere parameterization for net ecosystem CO2 exchange: Vegetation Photosynthesis and Respiration Model (VPRM). Global Biogeochemical Cycles, 22(2). https://doi.org/10.1029/2006GB002735, 2008.

Malhi, G. S., Kaur, M., and Kaushik, P.: Impact of climate change on agriculture and its mitigation strategies: A review. Sustainability, 13(3), 1318. https://doi.org/10.3390/su13031318, 2021.

Marthews, T. R., Quesada, C. A., Galbraith, D. R., Malhi, Y., Mullins, C. E., Hodnett, M. G., and Dharssi, I. : High-resolution hydraulic parameter maps for surface soils in tropical South America. Geoscientific Model Development, 7(3), 711-723. https://doi.org/10.5194/gmd-7-711-2014, 2014.

Meir, P., Metcalfe, D.B., Costa, A.C.L., and Fisher, R.A.,: The fate of assimilated carbon during drought: impacts on respiration in Amazon rainforests. Philos. Trans. R. Soc., B 363 (1498). https://doi.org/10.1098/rstb.2007.0021, 2008.

Moraes, R. M., Correa, S. B., Doria, C. R. C., Duponchelle, F., Miranda, G., Montoya, M., ... and ter Steege, H. Amazonian ecosystems and their ecological functions. Amazon assessment report 2021, 1, 2018.

Moreira, D. S., Freitas, S. R., Bonatti, J. P., Mercado, L. M., Rosário, N. E., Longo, K. M., & Gatti, L. V. : Coupling between the JULES land-surface scheme and the CCATT-BRAMS atmospheric chemistry model (JULES-CCATT-BRAMS1. 0): applications to numerical weather forecasting and the CO2 budget in South America. Geoscientific Model Development, 6(4), 1243-1259. https://doi:10.5194/gmd-6-1243-2013, 2013.

Moudrý, V., Gábor, L., Marselis, S., Pracná, P., Barták, V., Prošek, J., and Wild, J.: Comparison of three global canopy height maps and their applicability to biodiversity modeling: Accuracy issues revealed. Ecosphere, 15(10), e70026, 2024.

Nelder, J. A., and Mead, R.: A simplex method for function minimization. The computer journal, 7(4), 308-313. https://doi.org/10.1093/comjnl/7.4.308, 1965.

Nelson, J. A., Walther, S., Gans, F., Kraft, B., Weber, U., Novick, K., and Jung, M.: X-BASE: the first terrestrial carbon and water flux products from an extended data-driven scaling framework, FLUXCOM-X. Biogeosciences, 21(22), 5079-5115. https://doi.org/10.5194/bg-21-5079-2024, 2024.

Nelson, J. A., Walther, S., Gans, F., Kraft, B., Weber, U., Novick, K., Buchmann, N., Migliavacca, M., Wohlfahrt, G., Šigut, L., Ibrom, A., Papale, D., Göckede, M., Duveiller, G., Knohl, A., Hörtnagl, L., Scott, R. L., Zhang, W., Hamdi, Z. M., Reichstein, M., Aranda-Barranco, S., Ardö, J., Op de Beeck, M., Billesbach, D., Bowling, D., Bracho, R., Brümmer, C.,

Camps-Valls, G., Chen, S., Cleverly, J. R., Desai, A., Dong, G., El-Madany, T. S., Euskirchen, E. S., Feigenwinter, I., Galvagno, M., Gerosa, G. A., Gielen, B., Goded, I., Goslee, S., Gough, C. M., Heinesch, B., Ichii, K., Jackowicz-Korczynski, M. A., Klosterhalfen, A., Knox, S., Kobayashi, H., Kohonen, K.-M., Korkiakoski, M., Mammarella, I., Gharun, M., Marzuoli, R., Matamala, R., Metzger, S., Montagnani, L., Nicolini, G., O'Halloran, T., Ourcival, J.-M., Peichl, M., Pendall, E., Ruiz Reverter, B., Roland, M., Sabbatini, S., Sachs, T., Schmidt, M., Schwalm, C. R., Shekhar, A., Silberstein, R., Silveira, M. L., Spano, D., Tagesson, T., Tramontana, G., Trotta, C., Turco, F., Vesala, T., Vincke, C., Vitale, D., Vivoni, E. R., Wang, Y., Woodgate, W., Yepez, E. A., Zhang, J., Zona, D., and Jung, M.: X-BASE: the first terrestrial carbon and water flux products from an extended data-driven scaling framework, FLUXCOM-X. Biogeosciences, 21(22), 5079-5115. https://doi.org/10.5194/bg-21-5079-2024, 2024.

Ometto, J. P., Gorgens, E. B., de Souza Pereira, F. R., Sato, L., de Assis, M. L. R., Cantinho, R., and Keller, M.: A biomass map of the Brazilian Amazon from multisource remote sensing. Scientific Data, 10(1), 668. https://doi.org/10.1038/s41597-023-02575-4, 2023.

Osborne, T., Gornall, J., Hooker, J., Williams, K., Wiltshire, A., Betts, R., & Wheeler, T.: JULES-crop: a parametrisation of crops in the Joint UK Land Environment Simulator. Geoscientific Model Development Discussions, 7(5), 6773-6809. https://doi.org/10.5194/gmd-8-1139-2015, 2015.

Peel, M. C., Finlayson, B. L., and McMahon, T. A. (2007). Updated world map of the Köppen-Geiger climate classification. Hydrology and earth system sciences, 11(5), 1633-1644. https://doi.org/10.5194/hess-11-1633-2007, 2007

Prudente Junior, A. C., Vianna, M. S., Williams, K., Galdos, M. V., & Marin, F. R.: Calibration and evaluation of JULES-crop for maize in Brazil. Agronomy Journal, 114(3), 1680-1693.https://doi.org/10.1002/agj2.21066, 2022.

Raoult, N. M., Jupp, T. E., Cox, P. M., and Luke, C. M.: Land-surface parameter optimisation using data assimilation techniques: the adJULES system V1. 0. Geoscientific Model Development, 9(8), 2833-2852. https://doi.org/10.5194/gmd-9-2833-2016, 2016.

Reatto, A., Martins, É. D. S., Farias, M. F. R., Silva, A. V. D., & Carvalho Júnior, O. A. D.: Mapa pedológico digital-SIG atualizado do Distrito Federal escala 1: 100.000 e uma síntese do texto explicativo, 2004.

Restrepo-Coupe, N., da Rocha, H. R., Hutyra, L. R., da Araujo, A. C., Borma, L. S., Christoffersen, B., and Saleska, S. R.: What drives the seasonality of photosynthesis across the Amazon basin? A cross-site analysis of eddy flux tower measurements from the Brasil flux network. Agricultural and Forest Meteorology, 182, 128-144. https://doi.org/10.1016/j.agrformet.2013.04.031, 2013.

Restrepo-Coupe, N., da Rocha, H. R., Hutyra, L. R., de Araujo, A. C., Borma, L. S., Christoffersen, B., and Saleska, S.: LBA-ECO CD-32 Flux Tower Network Data Compilation, Brazilian Amazon: 1999-2006, V2. ORNL DAAC. https://doi.org/10.3334/ORNLDAAC/1842, 2021

Restrepo-Coupe, N., Levine, N. M., Christoffersen, B. O., Albert, L. P., Wu, J., Costa, M. H., and Saleska, S. R.: Do dynamic global vegetation models capture the seasonality of carbon fluxes in the Amazon basin? A data-model intercomparison. Global change biology, 23(1), 191-208. https://doi.org/10.1111/gcb.13442, 2017.

Rosan, T. M., Sitch, S., O'sullivan, M., Basso, L. S., Wilson, C., Silva, C., ... and Aragão, L. E.: Synthesis of the land carbon fluxes of the Amazon region between 2010 and 2020. Communications Earth & Environment, 5(1), 46. https://doi.org/10.5281/zenodo.10423522, 2024.

Saatchi, S.S., Harris, N.L., Brown, S., Lefsky, M., Mitchard, E.T.A., Salas, W., Zutta, B.R., Buermann, W., Lewis, S.L., Hagen, S., Petrova, S., White, L., Silman, M., Morel, A.: Benchmark map of forest carbon stocks in tropical regions across three continents. Proc. Natl. Acad. Sci. 108 (24), 9899–9904. https://doi.org/10.1073/ pnas.1019576108, 2011.

Shinozaki, K., Yoda, K., Hozumi, K., and Kira, T.: A quantitative analysis of plant form – the pipe model theory, I. Basic Analyses, Japanese Journal of Ecology, 14, 97–105, 1964

Silva, D. S., Blanco, C. J. C., dos Santos Junior, C. S., & Martins, W. L. D.: Modeling of the spatial and temporal dynamics of erosivity in the Amazon. Modeling Earth Systems and Environment, 6, 513-523.https://doi.org/10.1007/s40808-019-00697-6, 2020.

Simard, M., Pinto, N., Fisher, J. B., and Baccini, A.: Mapping forest canopy height globally with spaceborne lidar. Journal of Geophysical Research: Biogeosciences, 116(G4). https://doi.org/10.1029/2011JG001708, 2011

Sitch, S., O'sullivan, M., Robertson, E., Friedlingstein, P., Albergel, C., Anthoni, P., ... & Zaehle, S. (2024). Trends and drivers of terrestrial sources and sinks of carbon dioxide: An overview of the TRENDY project. Global Biogeochemical Cycles, 38(7). https://doi.org/10.1029/2024GB008102

Skillman, J. B.: Quantum yield variation across the three pathways of photosynthesis: not yet out of the dark. Journal of experimental botany, 59(7), 1647-1661. https://doi.org/10.1093/jxb/ern029, 2008.

Souza Jr, C. M., Z. Shimbo, J., Rosa, M. R., Parente, L. L., A. Alencar, A., Rudorff, B. F., and Azevedo, T. (2020). Reconstructing three decades of land use and land cover changes in brazilian biomes with landsat archive and earth engine. Remote Sensing, 12(17), 2735. https://doi.org/10.3390/rs12172735

Verbeeck, H., Peylin, P., Bacour, C., Bonal, D., Steppe, K., and Ciais, P.: Seasonal patterns of CO2 fluxes in Amazon forests: Fusion of eddy covariance data and the ORCHIDEE model. Journal of Geophysical Research: Biogeosciences, 116(G2). https://doi.org/10.1029/2010JG001544, 2011.

Virtanen, P., Gommers, R., Oliphant, T. E., Haberland, M., Reddy, T., Cournapeau, D., and Van Mulbregt, P.: SciPy 1.0: fundamental algorithms for scientific computing in Python. Nature methods, 17(3), 261-272,https://doi.org/10.1038/s41592-019-0686-2, 2020.

Wallach, D., Makowski, D., Jones, J. W., & Brun, F.: Working with dynamic crop models: Methods, tools and examples for agriculture and environment. Academic Press, 2018.

West, P. W.: Do increasing respiratory costs explain the decline with age of forest growth rate?. Journal of Forestry Research, 31(3), 693-712. https://doi.org/10.1007/s11676-019-01020-w, 2020.

Williams, K., Gornall, J., Harper, A., Wiltshire, A., Hemming, D., Quaife, T., and Scoby, D.: Evaluation of JULES-crop performance against site observations of irrigated maize from Mead, Nebraska. Geoscientific Model Development, 10(3), 1291-1320. https://doi.org/10.5194/gmd-10-1291-2017, 2017.

Willmott, C. J., Robeson, S. M., and Matsuura, K.: A refined index of model performance. International Journal of climatology, 32(13), 2088-2094. https://doi.org/10.1002/joc.2419, 2012.

Wiltshire, A. J., Burke, E. J., Chadburn, S. E., Jones, C. D., Cox, P. M., Davies-Barnard, T., and Zaehle, S.: JULES-CN: a coupled terrestrial carbon–nitrogen scheme (JULES vn5. 1). Geoscientific Model Development, 14(4), 2161-2186. https://doi.org/10.5194/gmd-14-2161-2021, 2021.

Wu, J., Albert, L. P., Lopes, A. P., Restrepo-Coupe, N., Hayek, M., Wiedemann, K. T., .and Saleska, S. R.: Leaf development and demography explain photosynthetic seasonality in Amazon evergreen forests. Science, 351(6276), 972-976. https//doi.org/10.1126/science.aad5068, 2016.

Wutzler, T., Antje, L M., Migliavacca M., Knauer, J., Sickel, K., Šigut, L., Menzer, O and Reichstein, M.: Basic and extensible post-processing of eddy covariance flux data with REddyProc. Biogeosciences, 15(16), 5015-5030. . https://doi.org/10.5194/bg-15-5015-2018, 2018.

Zhu, L., Ciais, P., Yao, Y., Goll, D., Luyssaert, S., Martínez Cano, I., Fendrich, A., Li, L., Yang, H., Saatchi, S., Dalagnol, R., and Li, W.: Spatially varying parameters improve carbon cycle modeling in the Amazon rainforest with ORCHIDEE r8849, Geosci. Model Dev., 18, 4915–4933, https://doi.org/10.5194/gmd-18-4915-2025, 2025.

Supplementary material

S.1 Model description

To calculate GPP and Respiration, JULES uses several equations based on the limitation factor of three potential photosynthesis rates (Collatz et al., 1991, 1992): Light limitation rate (W_l); Rubisco limited rate (W_c); and Transport of photosynthetic products for C3 and PEP Carboxylase limitation for C4 plants (W_e). One important aspect of calculating W_e and W_c is the dependence on the maximum rate of carboxylation of Rubisco (V_{cmax}) at 25° ~~C~~°C. To calculate V_{cmax} for any temperature, an optimal temperature range is required for each plant functional type (Tupp and Tlow), as described by Clark et al.~~,~~ (2011) (Equation 1):

$$~~Vc\ max~~V_{cmax} = \frac{~~VV_{cmax\ 25ft\ (Tc)}~~~~cmax,25ft(Tc)~~}{[1+e^{0.3(Tc-Tupp)}][1+e^{0.3(Tlow-Tc)}]} \quad (1)$$

where Tc is the canopy (leaf) temperature in Celsius degrees and *ft* is the standard Q_{10} temperature dependence (Equation 2):

$$ft(Tc) = Q_{10,leaf}^{0.1(Tc-25)} \quad (2)$$

where $Q_{10,\ leaf}$ is 2.0.

JULES calculates V_{cmax} in ~~25°C~~ 25 °C based on leaf nitrogen content (kg N kg C^{-1}) in each canopy layer (i) (Equation 3):

$$V_{cmax,25,i} = n_{eff} N_{10} e^{-kn(i-1)/10} \quad (3)$$

being, kn the extinction coefficient (kn = 0.78, based on Mercado et al., 2007); N_{10} is the top leaf nitrogen content (kg N kg C^{-1}) considering a 10-layer canopy and n_{eff} linearly relates to the concentration of N in leaves to V_{cmax}, 25.

Considering the V_{cmax} JULES can calculate the three potentially-limiting rates:

1-Rubisco-limited rate (W_c) (Equation 4)

$$Wc = \begin{cases} V_{c\,max}\left(\frac{c_i - \Gamma}{c_i + K_c\left(1+\frac{O_a}{K_o}\right)}\right), & for\ C3\ plants, \\ V_{cmax}, & for\ C4\ plants. \end{cases} \quad (4)$$

where V_{cmax} (mol CO_2 m^{-2} s^{-1}) is the maximum rate carboxylation of Rubisco, ci is the leaf internal carbon dioxide partial pressure (Pa), Γ is the CO_2 compensation point in the absence of mitochondrial respiration (Pa), Oa is the partial pressure of atmospheric oxygen, and K_c and K_o are the Michaelis-Menten parameters for CO_2 and O_2, respectively.

2- Light-limited rate (W_l) (Equation 5)

$$W_l = \begin{cases} \alpha(1-\omega) I_{PAR}\left(\frac{c_i - \Gamma}{c_i + 2\Gamma}\right), & for\ C3\ plants, \\ \alpha(1-\omega) I_{PAR}, & for\ C4\ plants. \end{cases} \quad (5)$$

where ω is the leaf scattering coefficient for PAR, I_{PAR} is the incident photosynthetically active radiation (PAR, mol m^{-2} s^{-1}), and α is the quantum efficiency for photosynthesis (mol CO_2 mol^{-1} PAR).

3- Rate of transport of photosynthetic products (in the case of C_3 plants) and PEPCarboxylase limitation (in the case of C_4 plants) (W_e) (Equation 6):

$$We = \begin{cases} 0.5 \cdot V_{cmax}, & for\ C3\ plants, \\ 2 \cdot \cancel{x}10^4 \cdot V_{cmax} \frac{c_i \cancel{ci}}{P*}, & for\ C4\ plants. \end{cases}$$

(6)

where P* is the surface air pressure.

The three potentially-limiting rates are essential to calculating the rate of gross photosynthesis (W) being the smoothed minimum of the three limited rates previously calculated (Equation 7):

$$\begin{cases} \beta_1 W_p^2 - W_p(W_c + W_l) + W_c W_l = 0, \\ \beta_2 W^2 - W(W_p + W_e) + W_p W_e = 0. \end{cases} \quad (7)$$

where β1 and β2 are co-limitation coefficients (0.83 and 0.9, respectively) and Wp is the smoothed minimum of W_c and W_l. The smaller root of each quadratic is selected.

The first step in calculating respiration is to define leaf dark respiration (Rd). Rd is based on a ~~proportional~~ proportion of V_{cmax}.(Equation 8)

$$R_d = f_d V_{cmax} \quad (8)$$

being f_d as the dark respiration coefficient.

After defining the leaf dark respiration, JULES can estimate the leaf photosynthesis (*Al*). *Al* estimation is based on the difference between gross photosynthesis rate and *Rd* with ~~and~~ a soil moisture stress factor based on Cox et al.~~,~~ 1998 (β) (Equation 9)~~. in~~ W~~wh~~i~~te~~h the stress factor is possible to ~~that can~~ represent how the photosynthesis rate falls due to the hydric stress (Equation 10):

$$Al = (W - Rd)\beta \quad (9)$$

$$\beta = \begin{cases} 1 for \Theta > \Theta_c, \\ \frac{\Theta - \Theta_w}{\Theta_c - \Theta_w} for \Theta_w < \Theta \leq \Theta_c, \\ 0 for \Theta \leq \Theta_w. \end{cases} \quad (10)$$

being, Θ the actual soil moisture; Θ_c is the soil moisture at the field capacity; Θ_w is the soil moisture at~~e~~ the wilting point.

Leaf photosynthesis is also important to define the stomatal conductance (gs). The estimate is, based on the approach of Jacobs (1984), which identified that the difference between internal and external CO_2 concentration at the leaf level can explain the stomatal opening and closure (Equation 11):

$$Al = \frac{gs(C_s - C_i)}{1.6} \quad (11)$$

where C_s is the leaf surface CO_2 concentration and C_i is the leaf internal CO_2 concentration.

The leaf CO_2 concentration on the surface or internal is defined based on the leaf humidity deficit estimated by the vapor deficit in the leaf surface (D) and in two parameters related to specific plant function types (f_0 and D*crit*) (Equation 12):

$$\frac{C_i - \Gamma}{C_s - \Gamma} = f_0\left(1 - \frac{D}{Dcrit}\right) \quad (12)$$

To calculate the total plant respiration, JULES considers the sum of two procedures: Growth and maintenance respiration (Rpm and Rpg, respectively, Equation 13 and 14, respectively)

$$R_{pm} = 0.012 \cdot R_d\left(\beta + \frac{N_r + N_s}{N_l}\right) \quad (13)$$

and

$$R_{pg} = r_g(GPP - R_{pm}) \quad (14)$$

where N_l, N_s, and N_r are the nitrogen contents of leaf, stem, and root, respectively, as described by Clark et al. (2011). R_g is the growth respiration coefficient set for 0.25 for all plant functional types (Clark et al., 2011, and Harper et al., 2016). GPP is based on the integration of *Al*, taking into account every leaf level adopted by Harper et al. (2016) in each used multi-layer canopy with sunlit and shaded leaves in each layer.

To calculate the nitrogen contents of leaves, ~~stem~~stems, and roots, leaf area index (LAI) and canopy height are important elements in the ~~estimative~~ estimation, as provided in ~~the~~ equations 15, 16, and 17:

$$N_l = n_m \sigma_l L \quad (15)$$

$$N_s = \mu_{sl} n_m S \quad (16)$$

$$N_r = \mu_{rl} n_m R \quad (17)$$

where n_m is the mean leaf nitrogen concentration (kg N (kg C)$^{-1}$), R and S are the quantity of carbon present in the root and respiring stem, L is the canopy leaf area index, and σl (kg C m^{-2} per unit of LAI) is the specific leaf density. The nitrogen contents of roots and ~~stem~~ stems are assumed to be fixed (functional type dependent) multiples, μ_{rl} and μ_{sl}, of the mean leaf nitrogen concentration: $\mu_{rl} = 1.0$ for all PFTs, $\mu_{sl} = 0.1$ for woody plants (trees and shrubs), and $\mu_{sl} = 1.0$ for grasses. To calculate the respiring stemwood, the pipe model of Shinozaki et al (1964) was utilized, taking into account canopy height, LAI (Equation 18):

$$S = n_{sl} h L \quad (18)$$

Where n_{sl} is a constant of proportionality from Friends et al (1993), and h is the canopy height.

JULES calculates t~~T~~he net ecosystem exchange (NEE) ~~is calculated by JULES~~ as the difference between GPP and total ecosystem respiration (plant and soil respiration, R_{eco}, Equation 19):

$$NEE = R_{eco} - \text{GPP} \quad (19)$$

S.2. ~~Sensivitivity~~ Sensitivity analysis

Table S1~~2.1~~: JULES parameters selected for sensitivity analysis in the Amazon region based on Li et al.~~,~~ (2016) for broadleaf tree forest. Maximum and minimum values for each parameter were based ~~in~~ on the literature

Parameters	Description	minimum value	maximum value
alnir	Leaf reflection coefficient for NIR.	0.225	0.675
alpar		0.05	0.15

	Leaf reflection coefficient for VIS (photosynthetically active radiation, PAR).		
alpha	Quantum efficiency (mol /mol^{-1}).	0.04	0.12
canht_ft	Canopy height (m).	19	50
catch0	Minimum canopy water capacity (kg /m^{-2}).	0.25	0.75
dcatch_dlai	Rate of change of canopy water capacity with LAI (kg /m^{-2}).	0	0.2
dgl_dt	Rate of change of leaf turnover rate with temperature (K^{-1}).	4.5	13.5
dqcrit	Critical humidity deficit (kgkg /kg^{-1}).	0.045	0.135
dz0v_dh	Rate of change of vegetation roughness length for momentum with height.	0.01	0.15
f0	Values of the maximum ratio of internal to external CO_2.	0.7	0.95
Fd	Scale factor for dark respiration.	0.005	0.025
g_leaf_0	Minimum turnover rate for leaves.	0.125	0.375

glmin	Minimum leaf conductance for H2O (mmol $m^{-2} s^{-1}$).	5.00E-07	1.50E-06
kext	Light extinction coefficient- used with Beer's Law for light absorption through tile canopies.	0.25	0.75
kpar	PAR Extinction coefficient ($m^2 m^{-2}$).	0.25	0.75
nl0	Top leaf nitrogen concentration (kg N kg C^{-1}).	0.023	0.069
r_grow	Growth respiration fraction.	0.125	0.375
rootd_ft	Root depth (m).	0.5	6
tleaf_of	Temperature below which leaves are dropped (K).	273.15	283.15
tlow	Lower temperature threshold for photosynthesis (°C).	-5	15
tupp	Upper temperature threshold for photosynthesis (°C).	20	50

Table S~~2.~~2: Relevance level of JULES parameters in the ATTO tower representing the Brazilian Amazon biome. The most sensitive parameters, highlighted in bold, were chosen based on the shared relevance in NEE simulations.

parameter	MAD (g C m^{-2} day^{-1})	parameter	var(%)
canht_ft_io	**16.5781**	**canht_ft**	**193.38**
fd	**12.3263**	**fd**	**141.81**
alpha	**4.1886**	**alpha**	**45.06**
tupp	**2.0199**	**f0**	**15.93**
f0	**1.6988**	**tupp**	**13.24**
dqcrit	0.8584	dqcrit	11.61
r_grow	0.7734	r_grow	5.79
dz0 max	0.4571	dz0v_dh	5.00
root	0.3521	root	4.66
tlow	0.1391	tlow	1.90
alpar	0.0896	dcatch	1.00
dcatch	0.0788	alpar	0.88
catch0	0.0238	catch0	0.32
kext	0.0046	kext	0.08
glmin	0.0007	glmin	0.02

alnir	0.0000	alnir	0.00
dgl_dt	0.0000	dgl_dt	0.00
kpar	0.0000	kpar	0.00
n10	0.0000	n10	0.00
tleaf	0.0000	tleaf	0.00
gleaf	0.0000	g_leaf	0.00

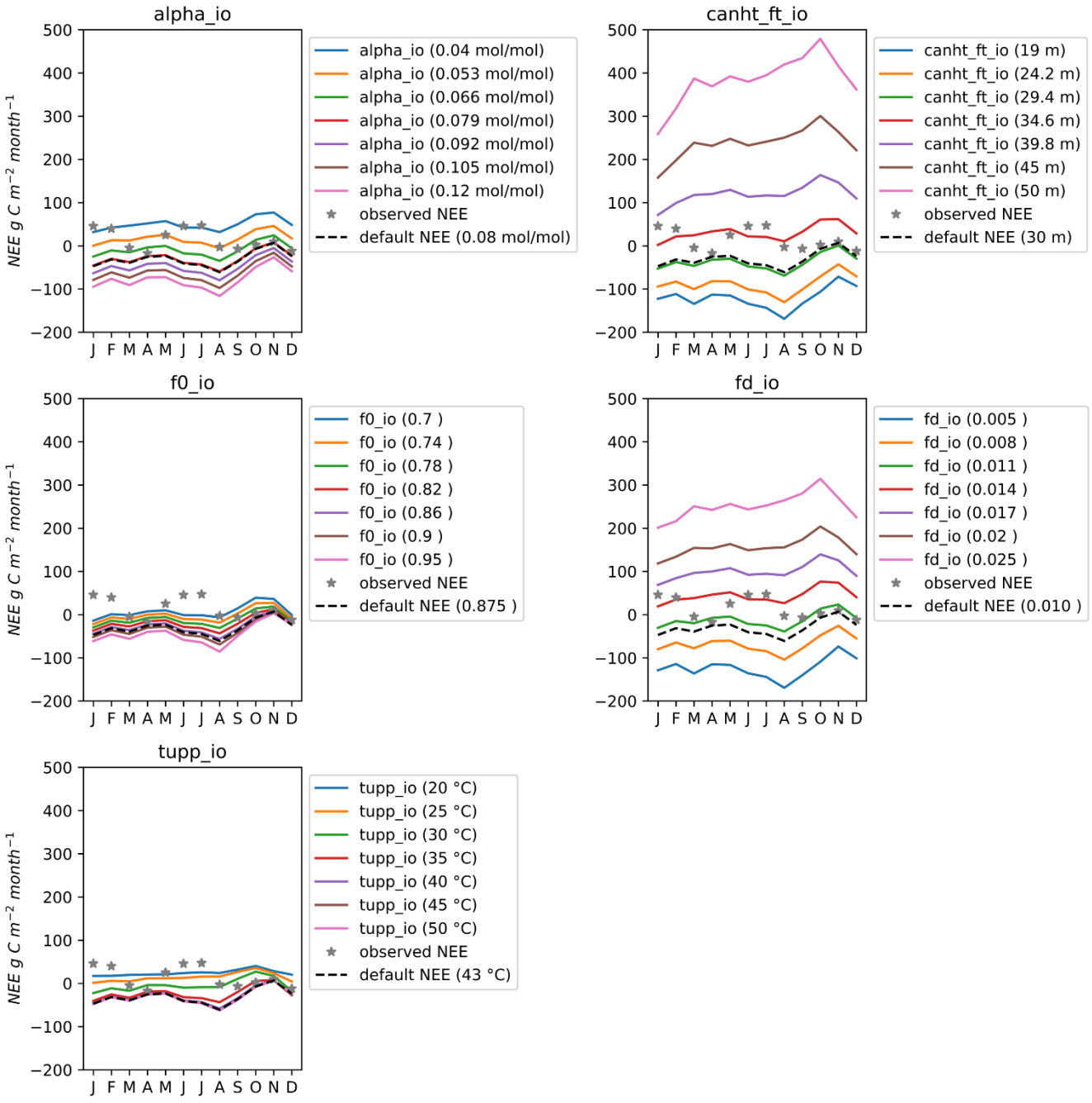

Figure S12.1: Sensitivity analysis of main parameters of JULES for NEE variable in the ATTO tower representing the Brazilian Amazon biome during the year of 2018.

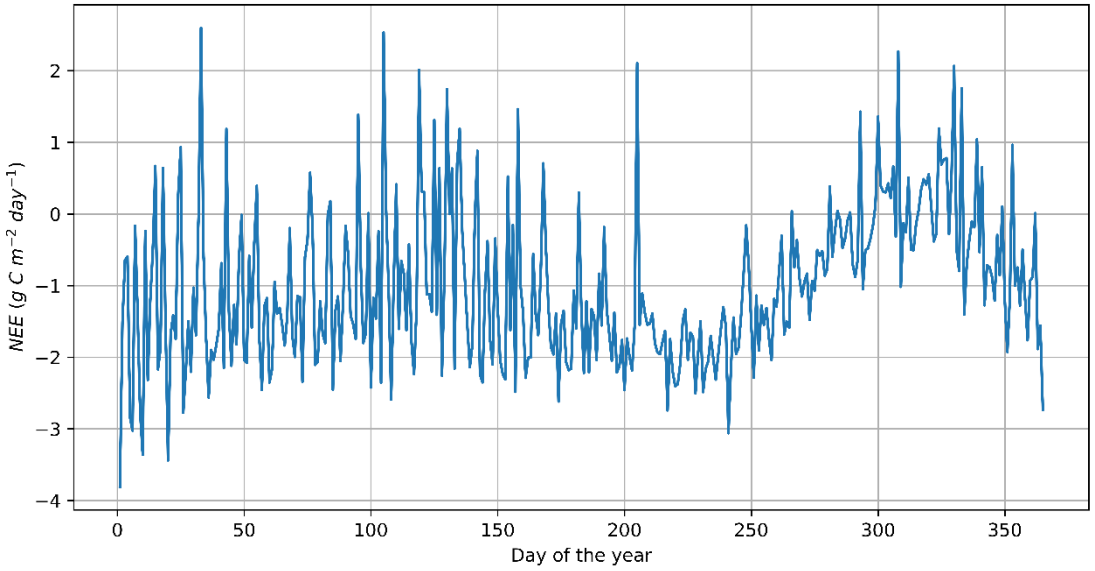

Figure S2.2: Daily NEE simulated by JULES in the ATTO tower based on Harper et al. (2016) parameters during the year of 2018

S.3 Spatialization of JULES parameters

S.3.1. Mapbiomas database adaptation for JULES

Table S3.1.1: Mapbiomas classes of vegetation and the respective land functional type from JULES applied to spatialize the Brazilian Amazon biome and land functional type (PFT) available in the JULES model.

Mapbiomas	JULES- PFT	Descrption
Forest Formation	BET-TR	Broadleaf Evergreen ~~tress~~ trees - tropical
Savannah Formation	ESH	Evergreen ~~schrubs~~shrubs
Mangrove	BET-TR	Broadleaf Evergreen ~~tress~~ trees - tropical
Floodable Forest	BET-TR	Broadleaf Evergreen ~~tress~~ trees - tropical
Wooded Sandbank Vegetation	ESH	Evergreen ~~schrubs~~shrubs
Grassland-Savannah	ESH	Evergreen ~~schrubs~~shrubs
Hypersaline Tidal Flat	ESH	Evergreen ~~schrubs~~shrubs
Herbaceous Sandbank Vegetation	ESH	Evergreen ~~schrubs~~shrubs
Pasture	C4	C4 grass
Soybean	C3	C3 grass and crops
Sugarcane	C4	C4 grass
Rice	C3	C3 grass and crops
Cooton	C3	C3 grass and crops
~~Perenial~~ Perennial crop	ESH	Evergreen ~~schrubs~~shrubs
Forest Plantation	BDT	Broadleaf ~~Decidious~~ Deciduous Trees
Beaches, ~~dune~~ dunes, and sand ~~spot~~spots	Bare soil	Bare soil
Urban Area	Urban	Urban

Mining	Bare soil	Bare soil
River, Lake, and Ocean	Water	Water
Aquaculture	Water	Water
Not observed	Bare soil	Bare soil

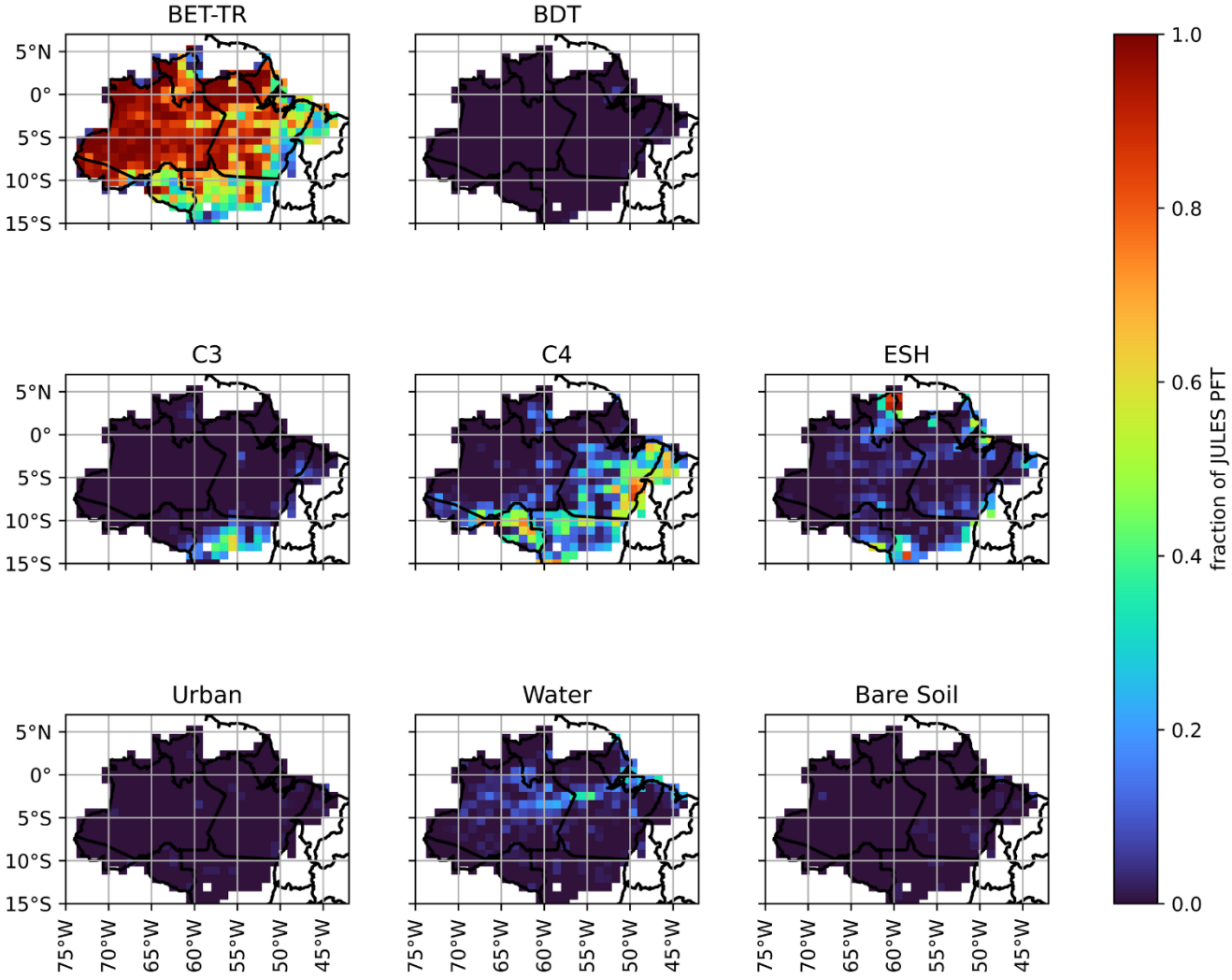

Figure S3.1.1: Distribution of each JULES plant and non-plant functional type in the S3.2.1 utilized for spatializing the carbon flux simulations.

S.3.2. Tupp, upper temperature threshold for photosynthesis

Two linear regression models were tested for the parameter tTupp, having the canopy height of the LAI as predictors. Tupp showed a directly proportional relationship with LAI and an inversely proportional relationship with the canopy height (Figure S53.2.1). Physically, it makes sense to have an inverse relationship between tTupp and canopy height, since low-canopy plants like C4 typically have higher temperature thresholds for photosynthesis. On the other hand, a positive relationship between tTupp and LAI is not physically consistent, since forest areas with higher LAI are expected to have lower temperature thresholds for photosynthesis Li et al.; (2016). Considering the arc of deforestation predominantly occupied by C4 grasses, the utilization of canopy height to spatialize tTupp resulted in higher values distributed in this zone. Obviously, since this is an inverse linear relationship, tTupp regression values were limited to 45ºC., Oetherwise, the regression model would deliver unrealistically high values. The 45ºC 45 °C limit was based in on Harper et al.; (2016), which defined a tTupp of 45ºC 45 °C for C4 grasses based on a field experiment in Tapajos. This is higher than the value used by Osborne et al (2015) for soybean (36 ºC) and near the tTupp value for Maize (45ºC45 °C). In the forest areas, the parameterization of tTupp using canopy height as a predictor results in a range of values from 37 ºC. In , in regions with high canopy height, such as in K67 and RJA towers (36 m and 35 m), to 42 ºC in the ATTO and K34 towers, with a lower canopy height (30 and 27 m, respectively) but a higher LAI (5,46 and 4,79 m^2 $m^{-2,}$ respectively).

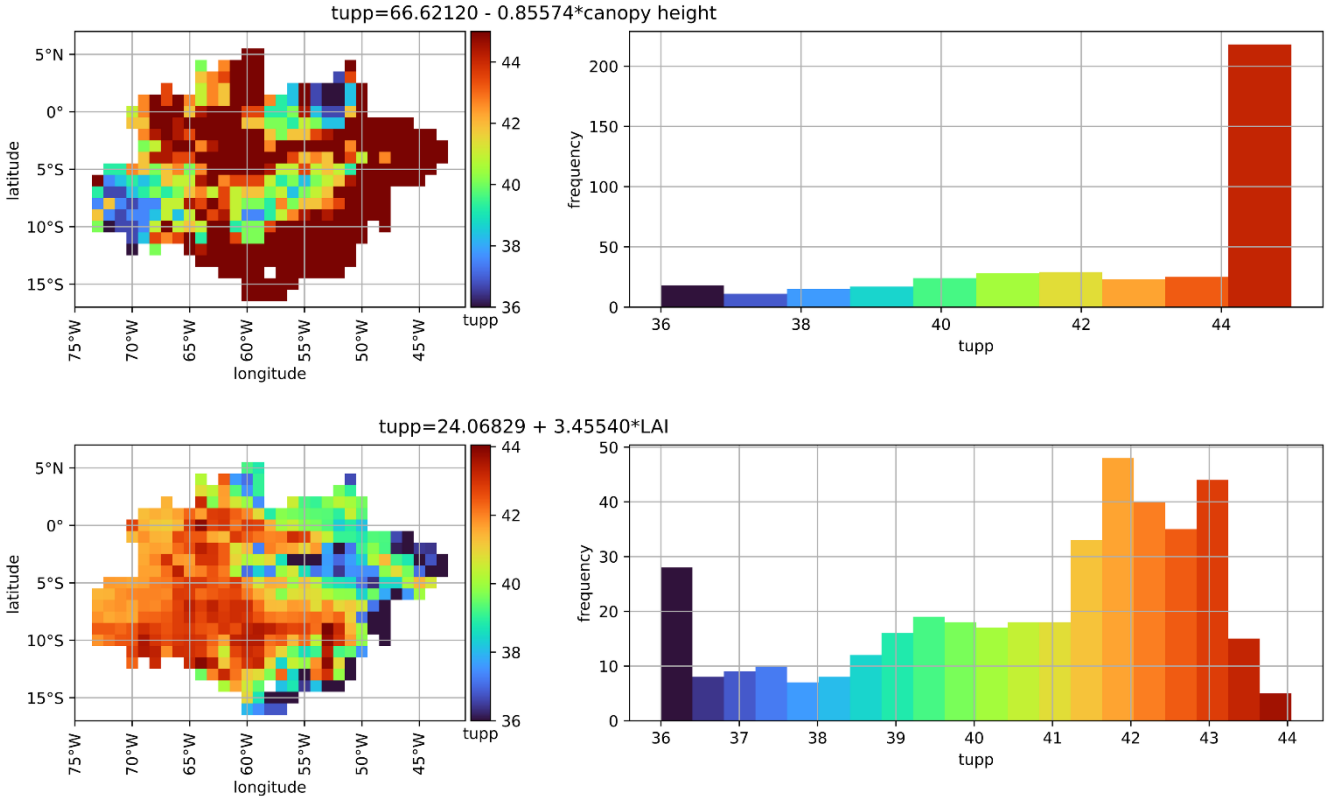

1305

Figure S~~43.2.1~~: Tupp spatialized for the Brazilian Amazon biome using two different predictors, canopy height and LAI.

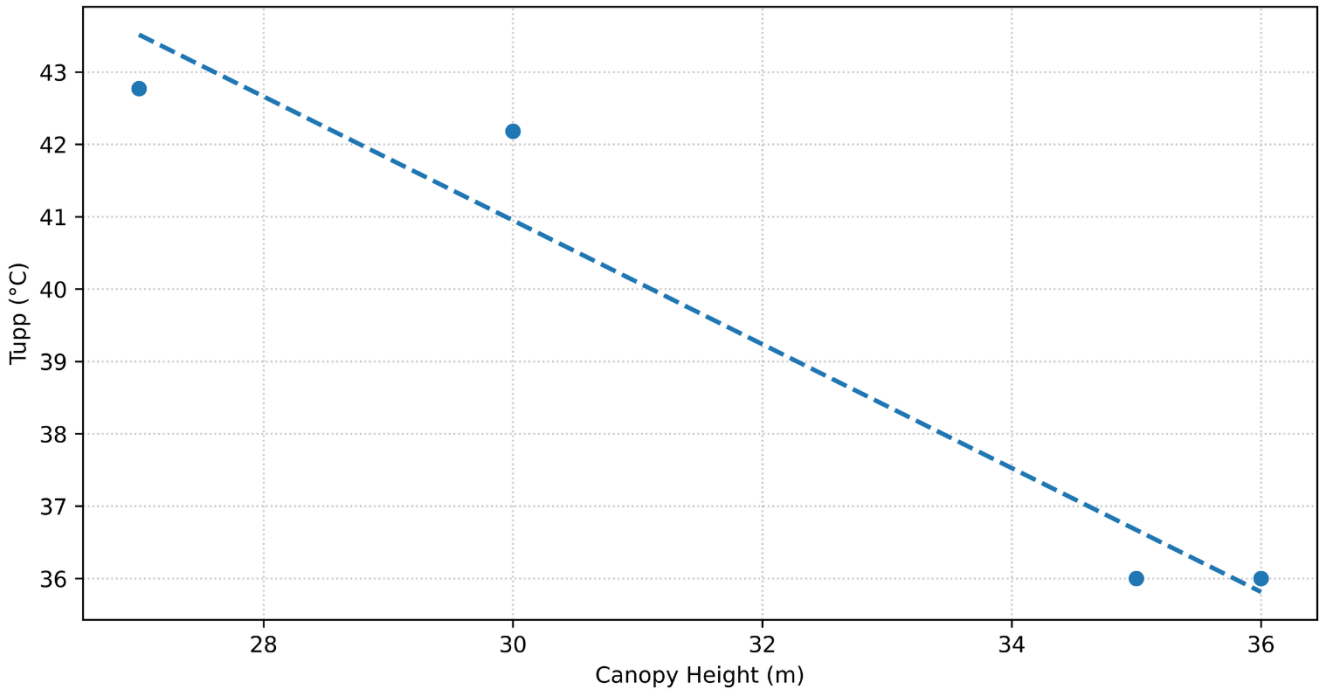

Figure S5~~3.2.2~~: Relationship between Canopy Height and Tupp (ºC) for different sites of the Brazilian Amazon biome.

S.3.3. alpha, quantum efficiency

Regarding the parameter alpha, the best alternative for spatialization is to use canopy height (Figure S6~~3.3.1~~), as demonstrated by Harper et al.~~,~~ (2016). Tropical forests are more ~~efficiency~~ efficient in converting PAR into carbon~~,~~ when compared to C4 plants (Harper et al., 2016). Using the canopy height as a predictor, the alpha values for forested regions were in the range 0.05 to 0.06 mol^{1} ~~/~~mol^{-1}, consistent with Skillman~~n~~ (2008), who evaluated different species of C3 plants.

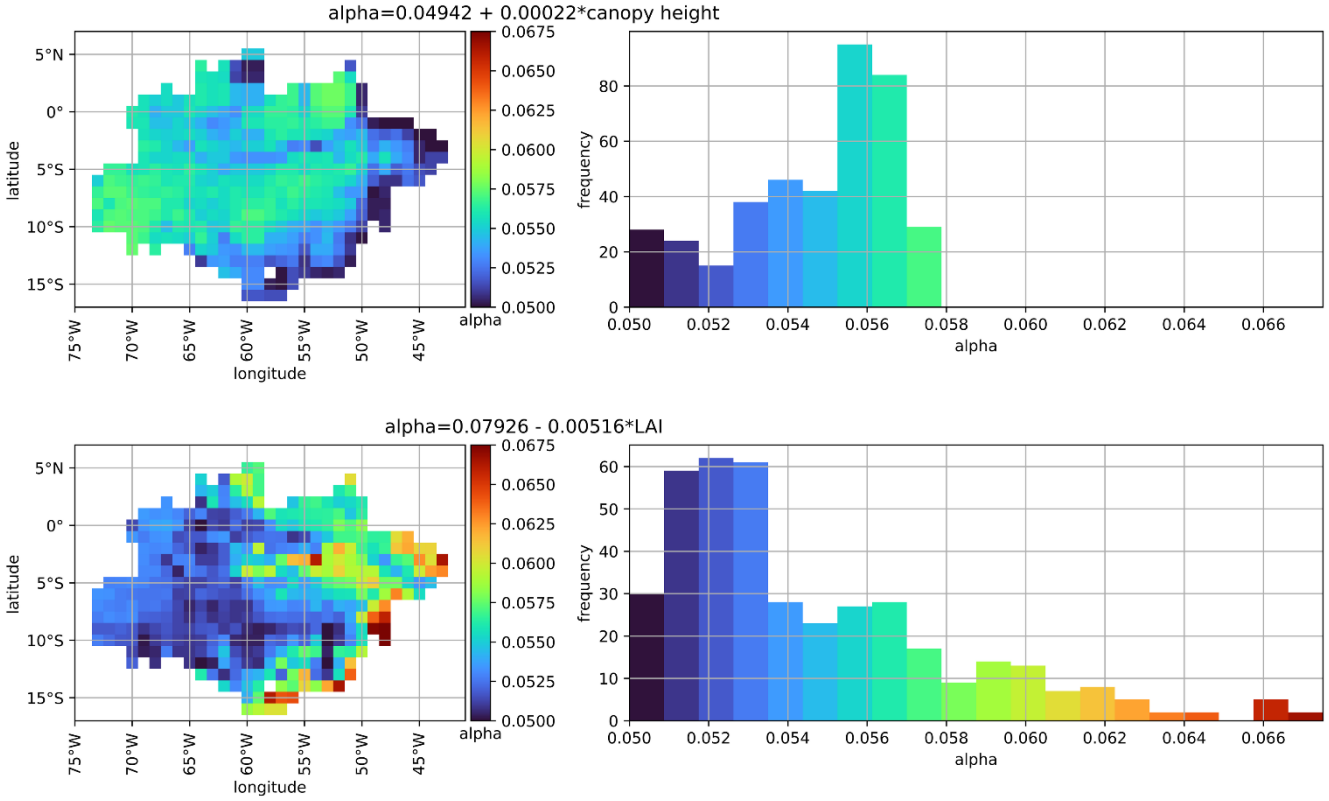

Figure S6~~3.3.1~~: Alpha spatialized for the Brazilian Amazon biome using two different methods, with canopy height and LAI.

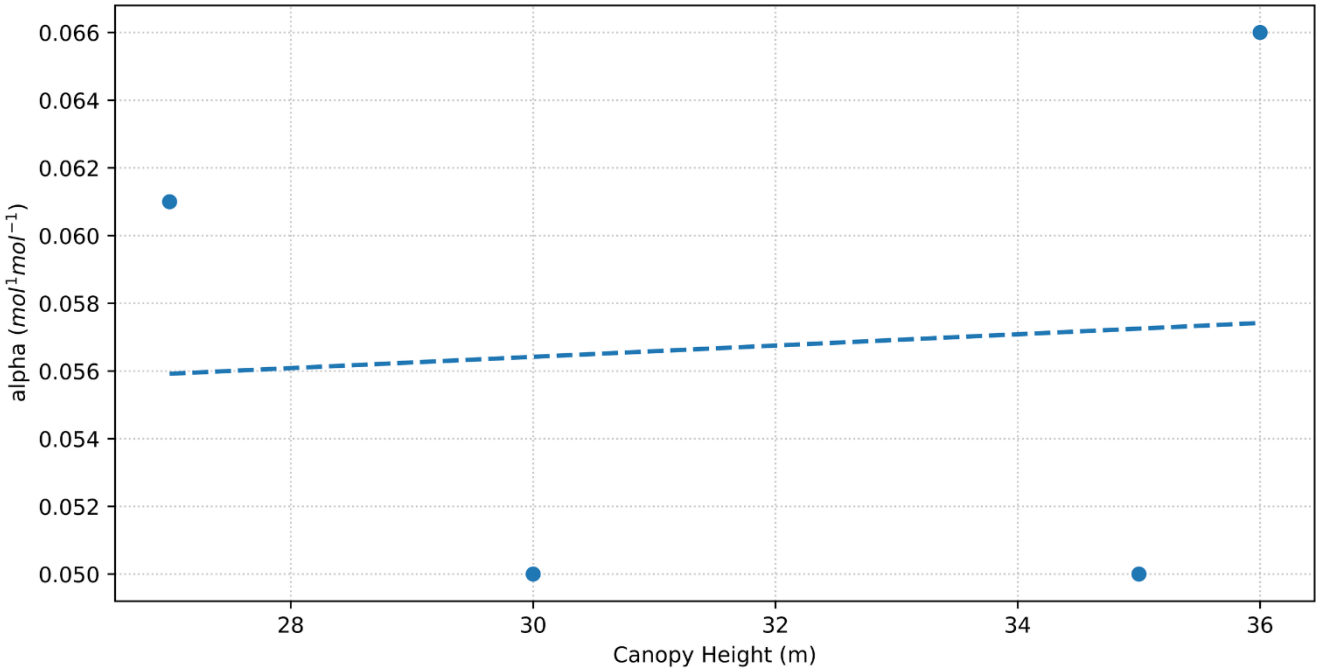

Figure S~~7~~~~3.3.2~~: Relationship between Canopy Height (m) and alpha (mol^{1} mol^{-1}) for different sites of the Brazilian Amazon biome.

S.3.4. f0, maximum ratio of internal to external CO_2

The parameter f0 controls the maximum values of leaf-level stomatal conductance. It is a dimensionless quantity ranging from 0 to 1, being associated with water use efficiency. As such, lower f0 values are expected for ~~in~~ plants that are more efficient in water use. Despite canopy height representing better t~~T~~upp and alpha spatialized, the best alternative for f0 is to use LAI (Figure S~~8~~3.4.1~~)~~). ~~This option using~~ LAI ~~is the only one that~~ can represent the expected reduction of this parameter in the arc of deforestation. C4 plants are more efficient in water use, using less water to produce biomass, due to ~~its~~ their metabolism. In a condition of high temperature and radiation, C4 plants reduce the ~~rubisco~~ Rubisco oxygenase activity and hence the photorespiration (Lambers et al., 2008). In Harper et al.~~,~~ (2016), f0 showed lower values for C4 plants than for tropical forests (0.8 and 0.875, respectively). The same concept can be applied in the center of the forest, ~~in which~~ where Santarem and Jaru have species more adaptable to longer dry seasons than ~~in~~the ATTO tower and Manaus. Accordingly, the parametrization of f0 based on LAI retrieved lower values in Santarem.

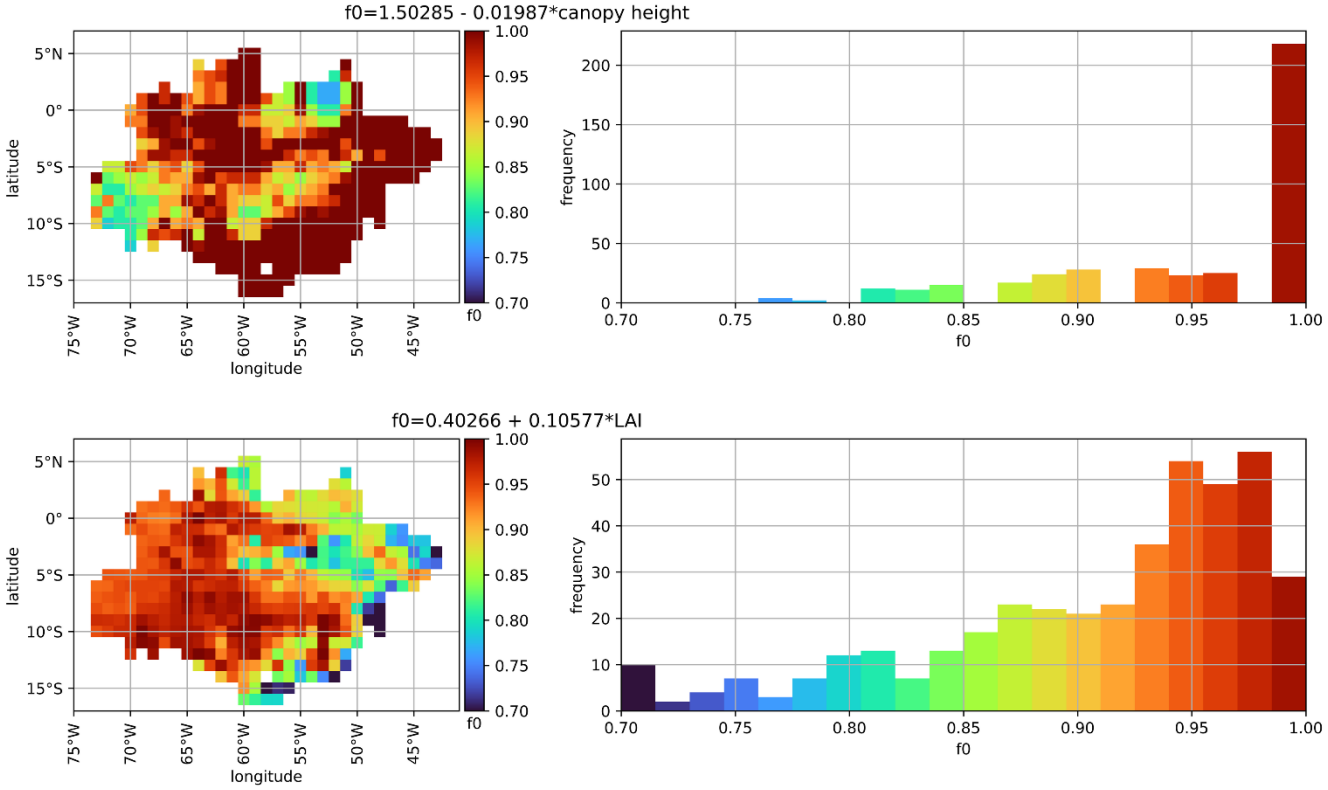

Figure S~~3.4.1~~8: f0 spatialized for the Brazilian Amazon biome using two different methods, with canopy height and LAI.

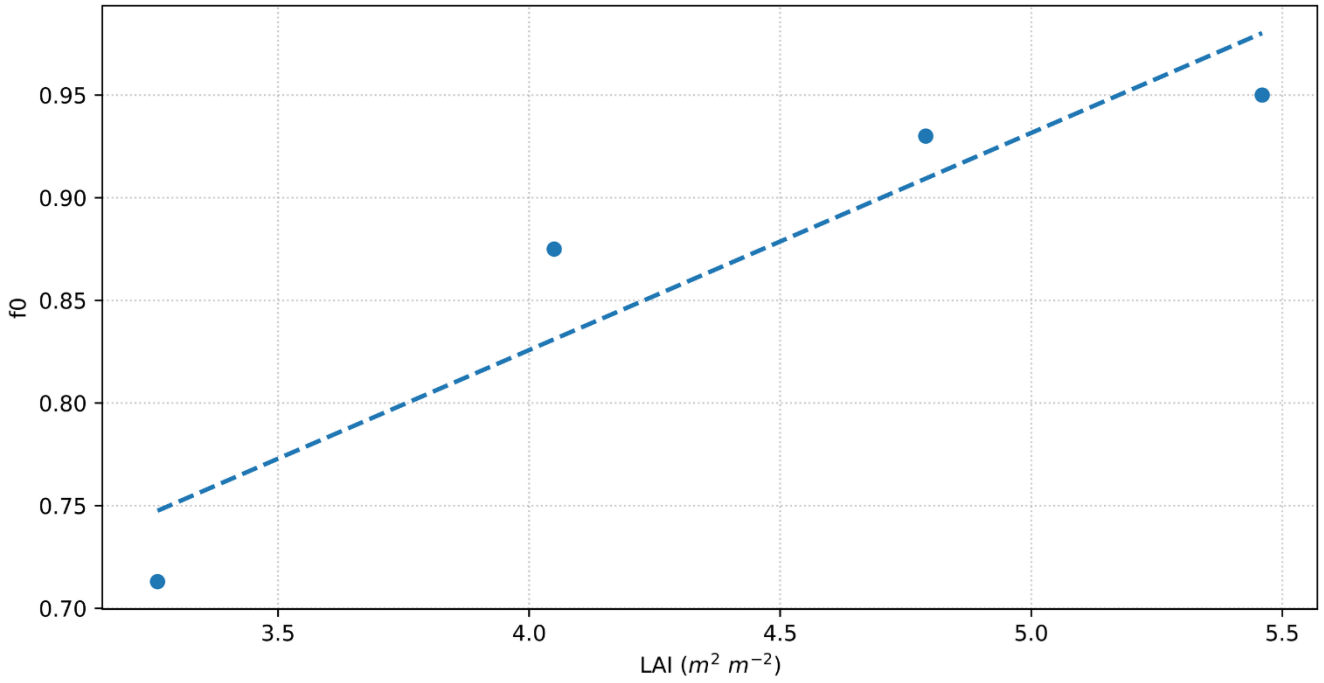

Figure S9~~3.4.2~~: Relationship between LAI and f0 for different sites of the Brazilian Amazon biome.

S.3.5. fd, scale factor for dark respiration

Similarly to~~Like~~ f0, the parameter fd was better represented in the Amazon Basin using LAI (Figure S11~~S3.5.1~~). C4 plants, as the tropical pastures widely used in Brazil, such as Marandu (*Urochloa brizantha* cv Marandu), are more efficient in the utilization of water. The high-water efficiency of C4 plants occurs due to the~~ due to the~~ metabolism that increases carbon concentration in the stomata, reducing ~~the~~ photorespiration. Thus, the parameter fd should be lower for this type of plant than for forest species. Using LAI to extrapolate fd for the Amazon Basin resulted in~~ fd~~ values ranging from 0.005 in the arc of deforestation to 0.015 in forested areas (Figure S10~~6~~). The resulting fd values are relatively small compared to references like: 0.019 for C4 grass (Harper et al., 2016), 0.0096 for maize (Williams et al., 2017), and 0.008 for maize (Leung et al., 2020). However, the same studies proposed reductions in the fd values compared to the default ones, indicating that the calibration of this parameter still need improvements in different PFTs.

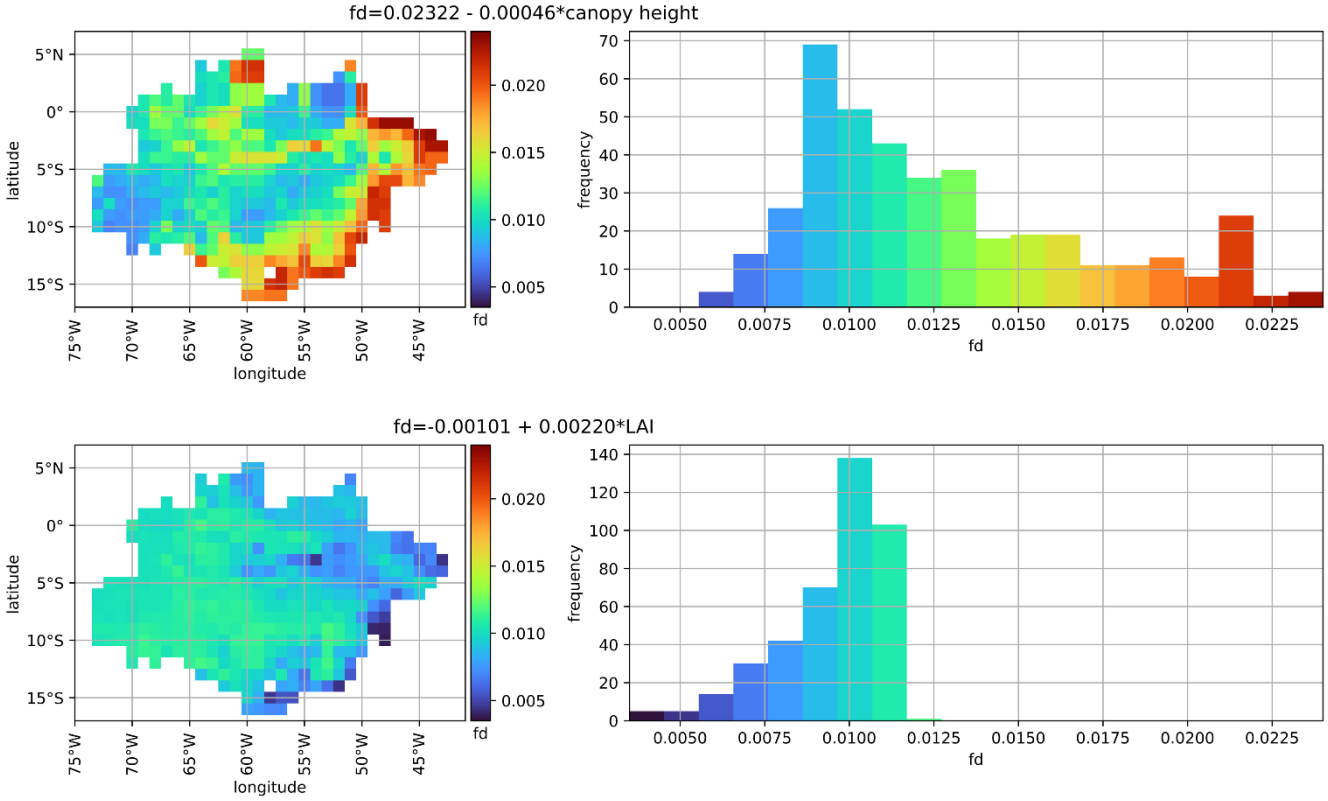

1360

Figure S10~~3.5.1~~: fd spatialized for the Brazilian Amazon biome using two different methods, with canopy height and LAI.

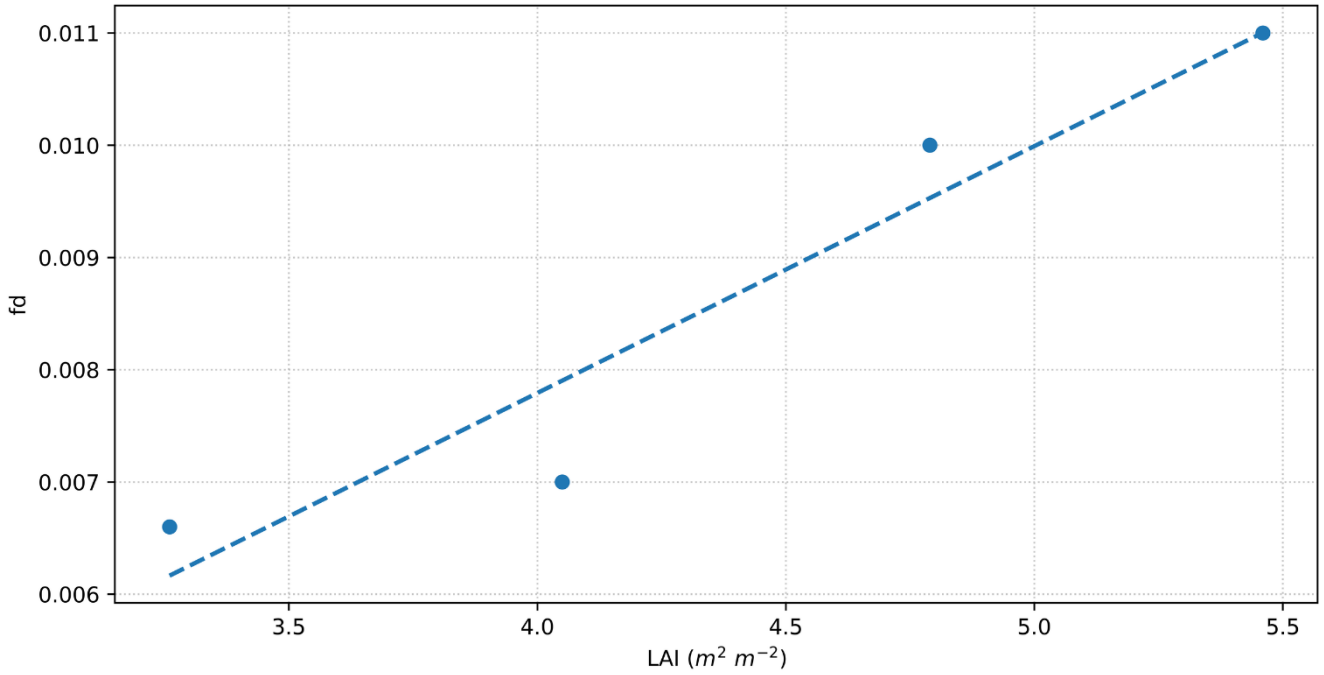

Figure S113.5.2: Relationship between LAI and f0 for different sites of the Brazilian Amazon biome.

S.4. Calibration and evaluation of JULES

Table S4.1: Physiological limits for JULES most sensitivities parameters for tropical forests applied for Nelder Mead optimization

Parameter	Physiological limit	unit	Minimum Reference	Maximum Reference
tupp_io	36 - 45	Celsius degree	Clark et al., 2012	Dreyer et al., 2001
alpha_io	0.05 - 0.011	mol CO_2 per mol PAR photons	Sklimmann 2008	Sklimmann 2008

fd_io	0.005 - 0.015	dimensionless	Clark et al., 2011	Harper et al., 2016
f0_io	0.7 - 0.95	dimensionless	Li et al., 2016	Li et al., 2016

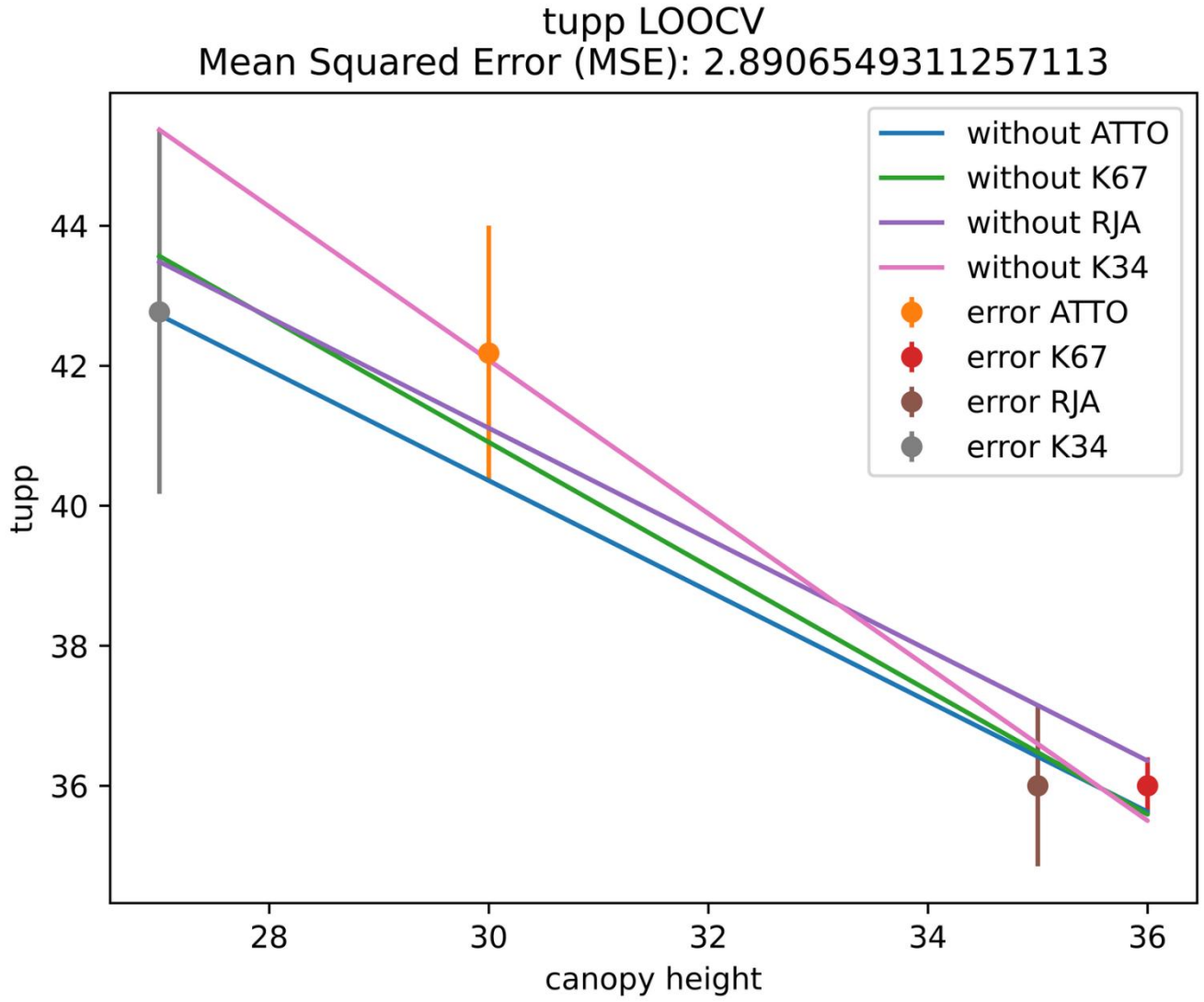

1375

Figure S124.1: Leave-one-out cross-validation (LOOCV) for Tupp in relation to canopy height for four different towers in the Brazilian Amazon biome.

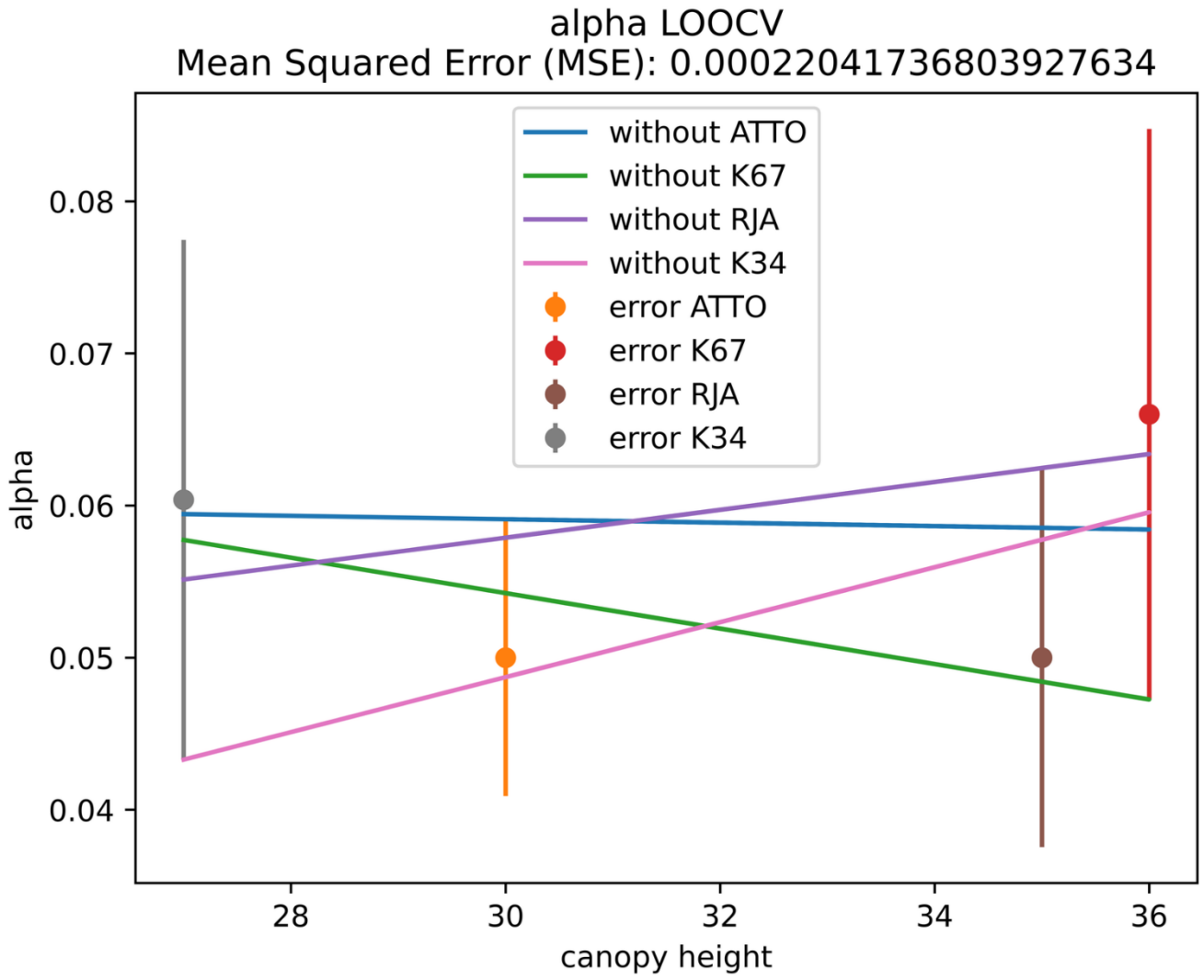

Figure S134.2: Leave-one-out cross-validation (LOOCV) for alpha in relation to canopy height for four different towers in the Brazilian Amazon biome.

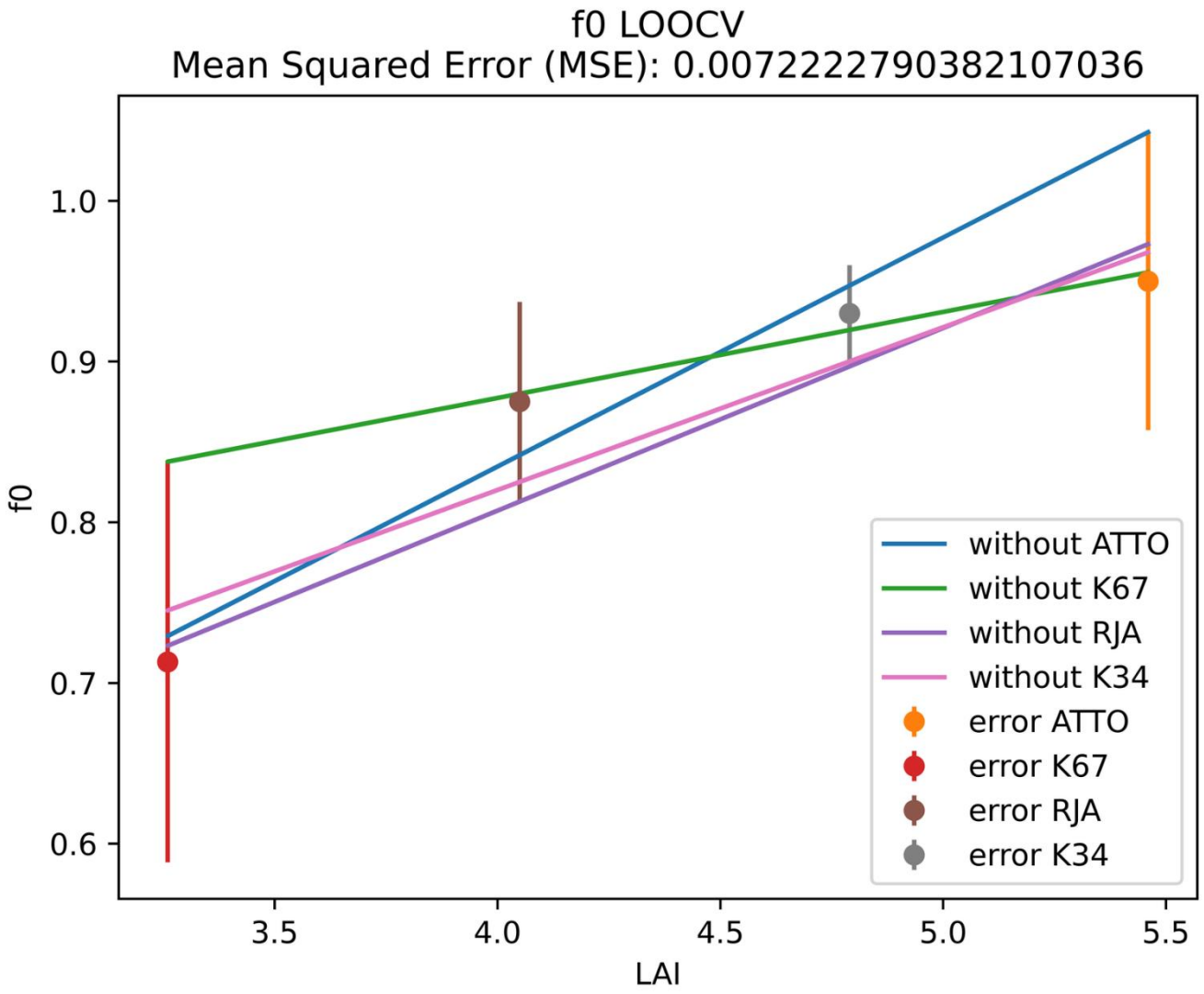

Figure S144.3: Leave-one-out cross-validation for f0 in relation to LAI for four different towers in the Brazilian Amazon biome.

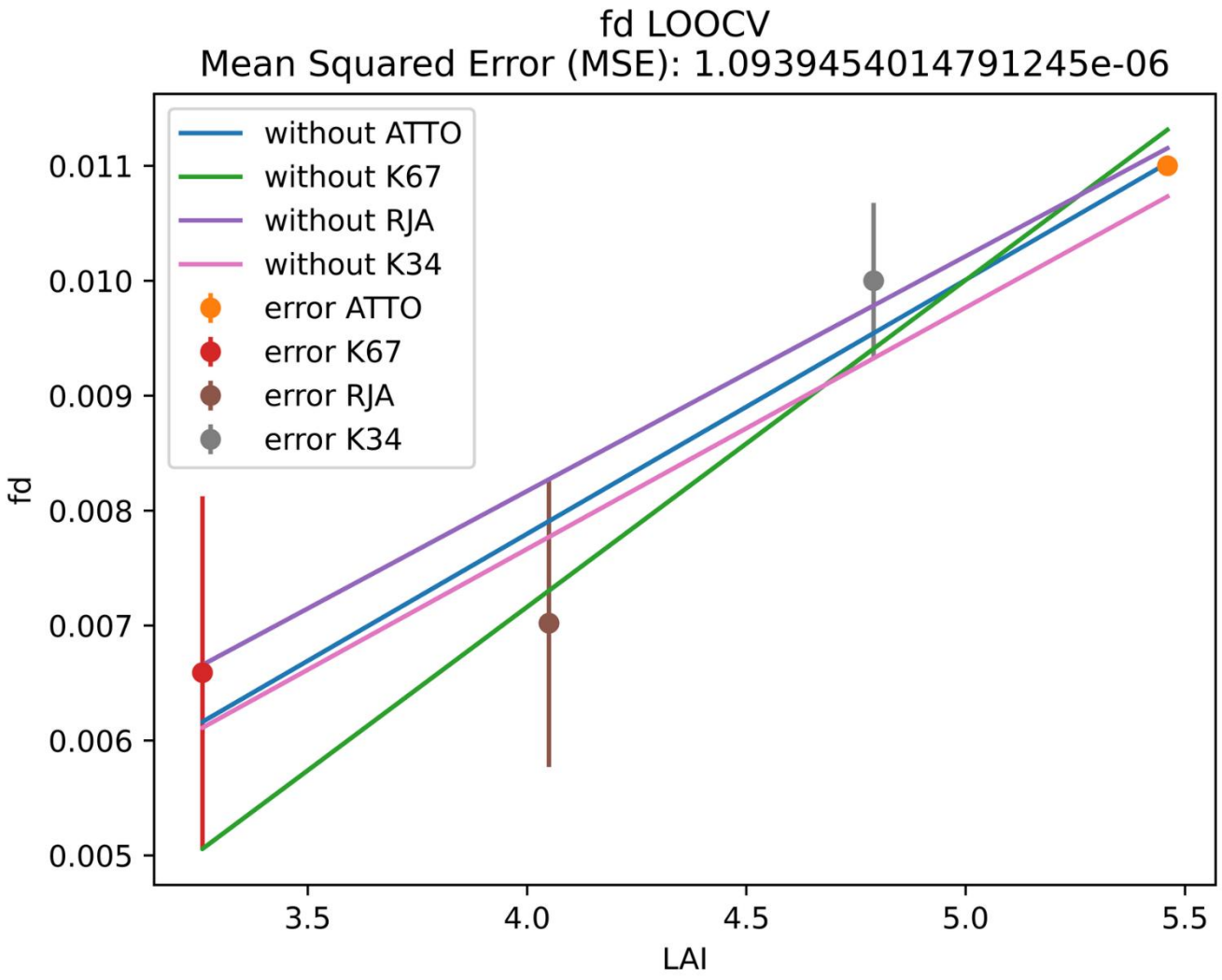

Figure S154.4: Leave-one-out cross-validation for fd in relation to LAI for four different towers in the Brazilian Amazon biome.

1390

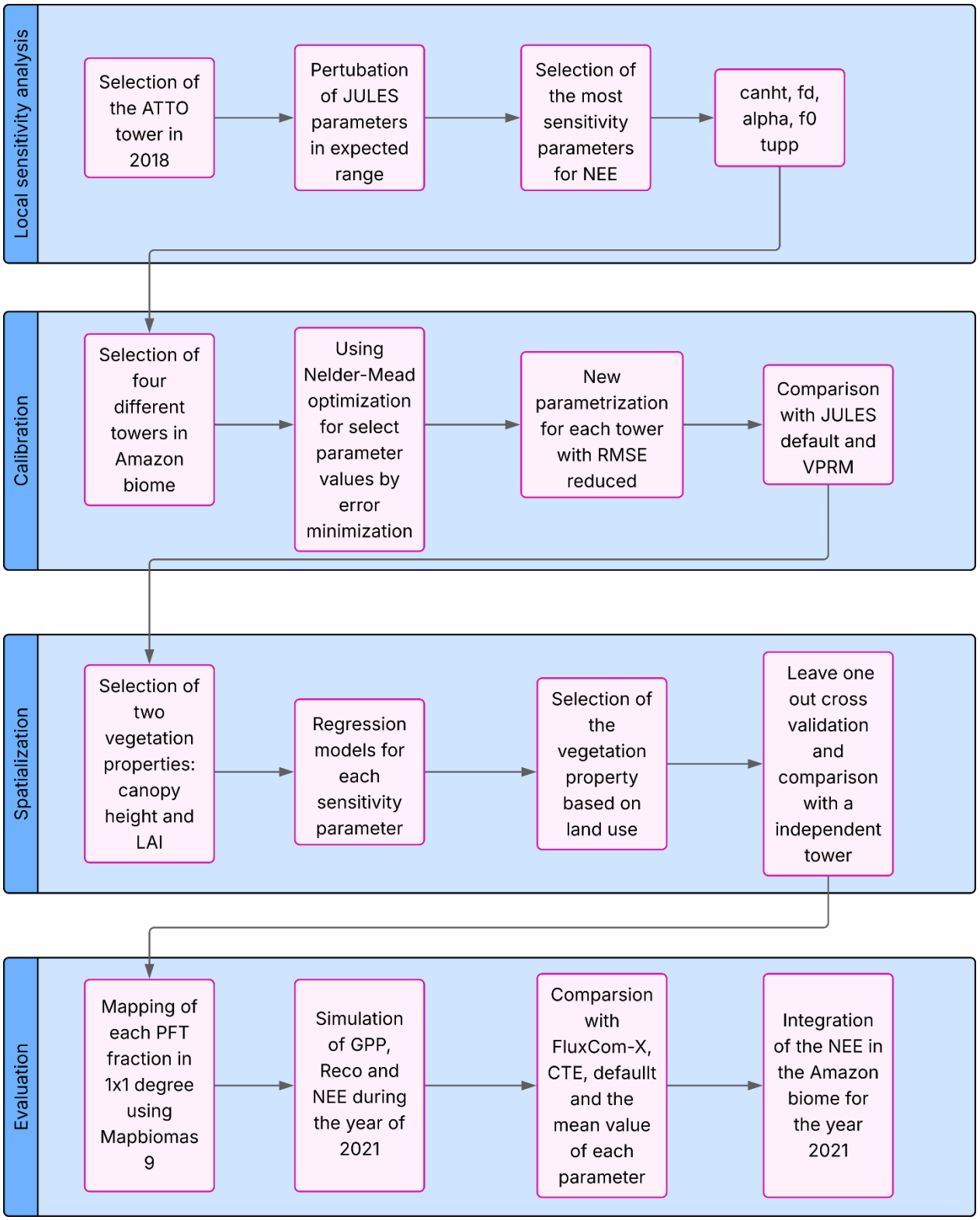
Local sensitivity analysis
Selection of the ATTO tower in 2018
Pertubation of JULES parameters in expected range
Selection of the most sensitivity parameters for NEE
canht, fd, alpha, f0 tupp
Calibration
Selection of four different towers in Amazon biome
Using Nelder-Mead optimization for select parameter values by error minimization
New parametrization for each tower with RMSE reduced
Comparison with JULES default and VPRM
Spatialization
Selection of two vegetation properties: canopy height and LAI
Regression models for each sensitivity parameter
Selection of the vegetation property based on land use
Leave one out cross validation and comparison with a independent tower
Evaluation
Mapping of each PFT fraction in 1x1 degree using Mapbiomas 9
Simulation of GPP, Reco and NEE during the year of 2021
Comparsion with FluxCom-X, CTE, defaullt and the mean value of each parameter
Integration of the NEE in the Amazon biome for the year 2021

Figure S16.4.5: Flowchart describing the procedures utilized to spatialize JULES and to obtain the NEE in the Brazilian Amazon biome.

S.5 Comparison with JULES versions

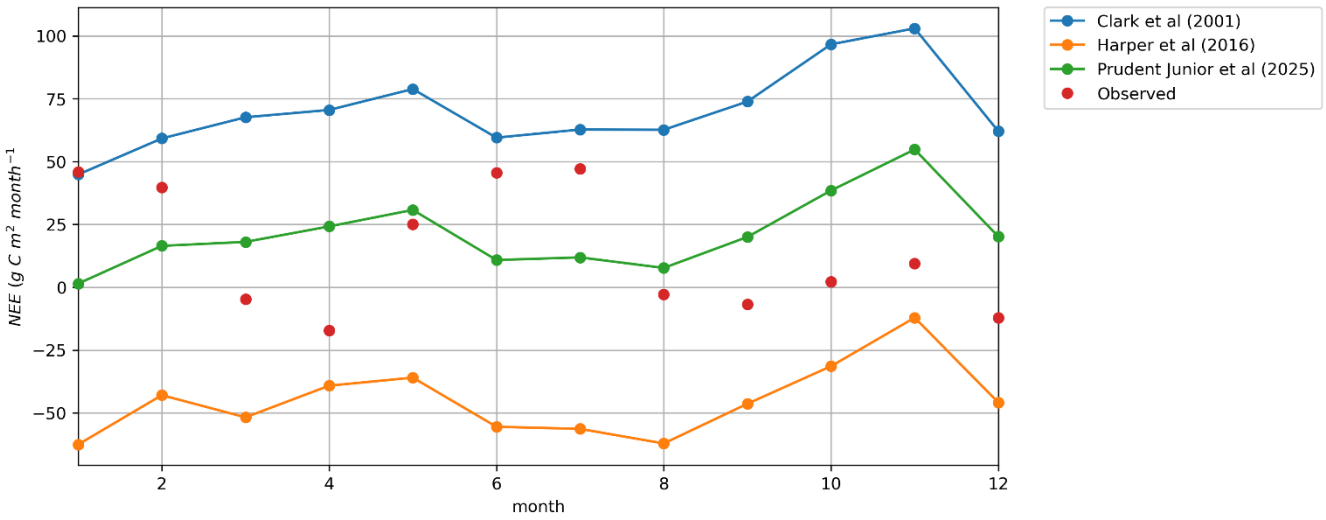

Figure S17:5.1 Comparison of NEE simulated in different JULES versions in the ATTO tower during the year of 2018.

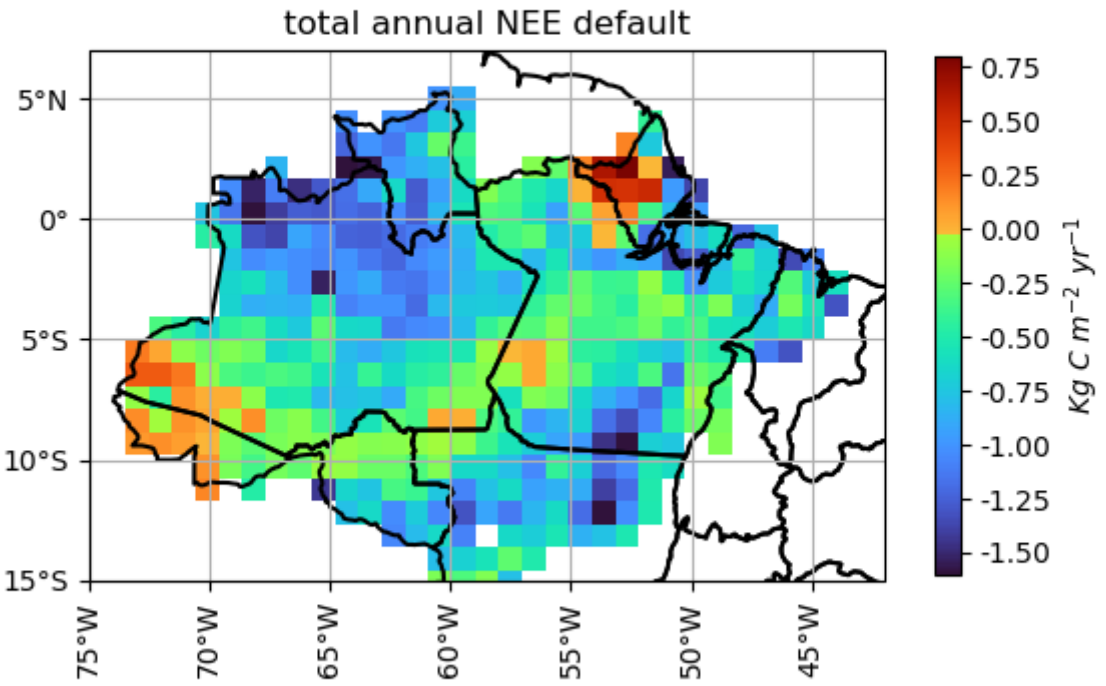

Figure S18~~5.2~~: NEE accumulated in Kg C m^{-2} during 2021 in the Brazilian Amazon biome in the default version of JULES (Harper et al., 2016).

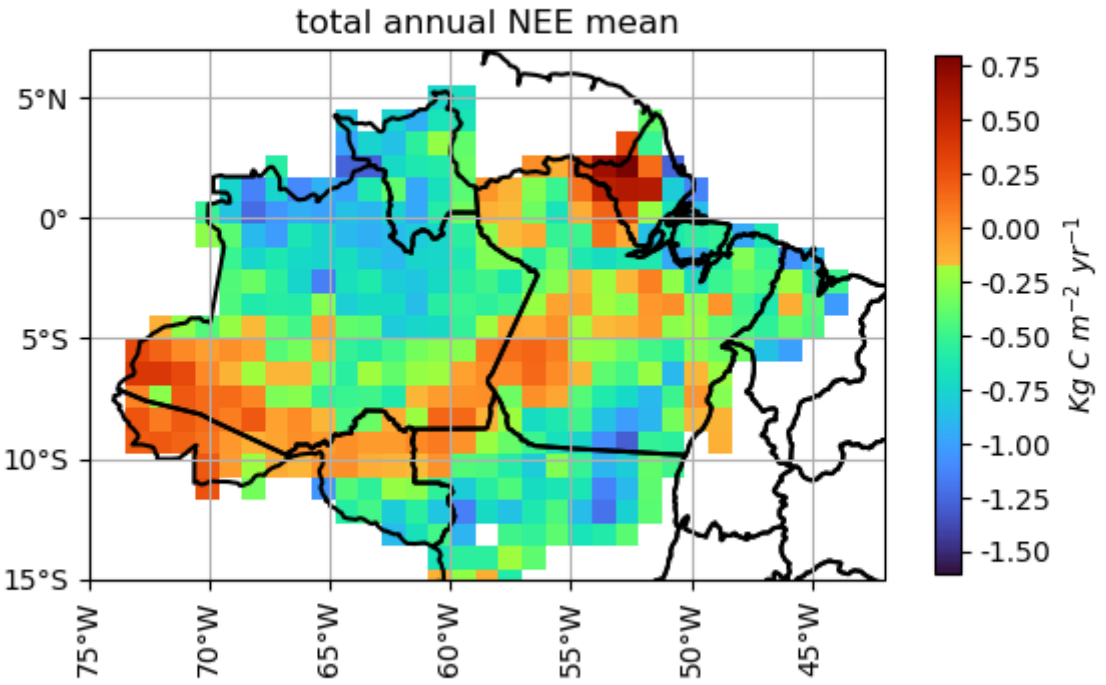

Figure S~~19~~5.~~3~~: NEE accumulated in Kg C m^{-2} during 2021 in the Brazilian Amazon biome with the mean value of the JULES ~~paramaters~~ parameters optimized.

References

Clark, D. B., Mercado, L. M., Sitch, S., Jones, C. D., Gedney, N., Best, M. J., Pryor, M., Rooney, G. G., Essery, R. L. H., Blyth, E., Boucher, O., Harding, R. J., Huntingford, C., and Cox, P. M.: The Joint UK Land Environment Simulator (JULES), model description – Part 2: Carbon fluxes and vegetation dynamics, Geosci. Model Dev., 4, 701–722, https://doi.org/10.5194/gmd-4-701-2011, 2011.

Collatz, G. J., Ball, J. T., Grivet, C., & Berry, J. A. (1991). Physiological and environmental regulation of stomatal conductance, photosynthesis and transpiration: a model that includes a laminar boundary layer. Agricultural and Forest meteorology, 54(2-4), 107-136. https://doi.org/10.1016/0168-1923(91)90002-8

Collatz, G. J., Ribas-Carbo, M., and Berry, J. A.: Coupled photosynthesis-stomatal conductance model for leaves of C4 plants. Functional Plant Biology, 19(5), 519-538. https://doi.org/10.1071/PP9920519, 1992.

Cox, P. M., Huntingford, C., and Harding, R. J.: A canopy conductance and photosynthesis model for use in a GCM land surface scheme. Journal of Hydrology, 212, 79-94. https://doi.org/10.1016/S0022-1694(98)00203-0, 1998.

Dreyer, E., Le Roux, X., Montpied, P., Daudet, F. A., and Masson, F.: Temperature response of leaf photosynthetic capacity in seedlings from seven temperate tree species. Tree physiology, 21(4), 223-232, 2001.

Harper, A. B., Cox, P. M., Friedlingstein, P., Wiltshire, A. J., Jones, C. D., Sitch, S., and Bodegom, P. V. .: Improved representation of plant functional types and physiology in the Joint UK Land Environment Simulator (JULES v4. 2) using plant trait information. Geoscientific Model Development, 9(7), 2415-2440. https://doi.org/10.5194/gmd-9-2415-2016, 2016.

Jacobs, C. M. J.: Direct impact of atmopsheric CO2 enrichment on regional transpiration, Ph.D. thesis, Wageningen Agricultural University, 1994.

Lambers, H., Chapin III, F. S., and Pons, T. L.: Plant physiological ecology. Springer Science & Business Media. https://doi.org/10.1007/978-0-387-78341-3, 2008.

Leung, F., Williams, K., Sitch, S., Tai, A. P., Wiltshire, A., Gornall, J., and Scoby, D.: Calibrating soybean parameters in JULES5. 0 from the US-Ne2/3 FLUXNET sites and the SoyFACE-O 3 experiment. Geoscientific Model Development Discussions, 2020, 1-29.https://doi.org/10.5194/gmd-13-6201-2020, 2020.

Li, J., Wang, Y. P., Duan, Q., Lu, X., Pak, B., Wiltshire, A., and Ziehn, T.: Quantification and attribution of errors in the simulated annual gross primary production and latent heat fluxes by two global land surface models. Journal of Advances in Modeling Earth Systems, 8(3), 1270-1288. https://doi.org/10.1002/2015MS000583, 2016.

Osborne, T., Gornall, J., Hooker, J., Williams, K., Wiltshire, A., Betts, R., & Wheeler, T.: JULES-crop: a parametrisation of crops in the Joint UK Land Environment Simulator. Geoscientific Model Development Discussions, 7(5), 6773-6809. https://doi.org/10.5194/gmd-8-1139-2015, 2015.

Shinozaki, K., Yoda, K., Hozumi, K., and Kira, T.: A quantitative analysis of plant form – the pipe model theory, I. Basic Analyses, Japanese Journal of Ecology, 14, 97–105, 1964

Skillman, J. B.: Quantum yield variation across the three pathways of photosynthesis: not yet out of the dark. Journal of experimental botany, 59(7), 1647-1661. https://doi.org/10.1093/jxb/ern029, 2008.

1450